

***In vitro* characterization of the novel
solubility enhancing excipient Soluplus®**



UNIVERSITÄT
DES
SAARLANDES

DISSERTATION

zur Erlangung des Grades

des Doktors der Naturwissenschaften der

Naturwissenschaftlich-Technischen Fakultät III

Chemie, Pharmazie, Bio- und Werkstoffwissenschaften

der Universität des Saarlandes

von

Michael Linn

Saarbrücken

2011

Tag des Kolloquiums: 19. Dezember 2011
Dekan: Prof. Dr. Wilhelm F. Maier
Berichterstatter: Prof. Dr. Claus-Michael Lehr
Prof. Dr. Rolf Hartmann
Vorsitz: Prof. Dr. Ingolf Bernhardt
Akad. Mitarbeiter: Dr. Matthias Engel

To my offspring

*The important thing is not to stop questioning.
Curiosity has its own reason for existing.*
Albert Einstein

Table of Contents

1. Short summary	V
2. Kurzzusammenfassung	VII
3. General Introduction	1
3.1. Liberation and absorption of drugs after oral application	1
3.1.1. Drug solubility and dissolution	2
3.1.2. Principles of drug absorption across the intestinal mucosa	4
3.2. Formulation of poorly aqueous soluble drugs by micellar solubilization . .	10
3.3. Solid dispersions and hot melt extrusion	14
3.3.1. Solid dispersions for pharmaceutical applications	14
3.3.2. Hot melt extrusion	15
3.4. The novel solubility enhancer Soluplus [®]	18
3.5. The Caco-2 cell culture model	19
3.6. Aims of this thesis	21
3.6.1. The Caco-2 model as predictive tool for Soluplus [®] formulations . .	22
3.6.2. Potential inhibition of P-glycoprotein and/or trypsin by Soluplus [®] .	23
3.6.3. Optimization of Soluplus [®] formulations	23
4. Soluplus[®] as an effective absorption enhancer of poorly soluble drugs <i>in vitro</i> and <i>in vivo</i>	25
4.1. Introduction	26
4.2. Materials and Methods	29
4.2.1. Chemicals	29
4.2.2. Solid Solutions	29
4.2.3. Caco-2 cell culture	30
4.2.4. Caco-2 transport experiments	30
4.2.5. Sample preparation & HPLC analysis	31
4.2.6. Animal studies	32
4.2.7. Equilibrium dialysis	33
4.3. Results	34
4.3.1. Danazol	34
4.3.2. Fenofibrate	34
4.3.3. Itraconazole	37
4.3.4. Dialysis	39
4.4. Discussion	40
4.5. Conclusion	45

5. Inhibition of P-glycoprotein and/or trypsin by Soluplus®	47
5.1. Introduction	48
5.2. Materials and Methods	50
5.2.1. Chemicals	50
5.2.2. Cell culture	50
5.2.3. Bi-directional transport experiments	51
5.2.4. Dialysis	52
5.2.5. MDCK II uptake assay	53
5.2.6. Trypsin inhibition assay	53
5.3. Results	54
5.3.1. Caco-2 transport assay	54
5.3.2. Dialysis	57
5.3.3. Uptake into MDCK II cells	58
5.3.4. Trypsin inhibition	59
5.4. Discussion	59
5.5. Conclusion	63
6. Optimization of Soluplus® formulations	65
6.1. Introduction	66
6.2. Materials and Methods	68
6.2.1. Chemicals	68
6.2.2. Extrudates	68
6.2.3. Caco-2 cell culture	68
6.2.4. Caco-2 transport experiments	69
6.2.5. HPLC analysis	73
6.2.6. Equilibrium dialysis	74
6.2.7. Differential scanning calorimetry (DSC)	74
6.3. Results	75
6.3.1. Fluorescein sodium (control)	75
6.3.2. Danazol	76
6.3.3. Fenofibrate	78
6.3.4. Itraconazole	80
6.4. Discussion	83
6.5. Conclusion and Outlook	87
7. Summary and Outlook	89
8. Zusammenfassung und Ausblick	93
9. Bibliography	99
A. Characterization of Soluplus® micelles	113
B. TEER measurements throughout transport experiments	119
C. HPLC and LC/MS analytics	121

D. Abbreviations	127
E. Curriculum vitae	129
F. Publications	131
G. Danksagung	133

1. Short summary

Although the oral route is preferred for drug administration due to its convenience for the patient, many new chemical entities suffer from low oral bioavailability due to poor aqueous solubility. Especially for BCS class II drugs, overcoming the limited solubility is crucial for a successful therapy. A relatively new technique in this context is the use of hot melt extrusion for the production of fast dissolving solid solutions.

This thesis focuses on the novel excipient Soluplus[®], combining solubilization and the ability to form solid solutions by hot melt extrusion in one molecule. The potency of different formulations to improve the bioavailability of BCS class II drugs was evaluated in the Caco-2 cell culture model. An excellent correlation between *in vitro* transport across cells and *in vivo* studies in dogs was found.

As many solubilizers can modulate active transporters, Soluplus[®] was tested in Caco-2 cells for a possible interaction with the P-glycoprotein efflux system. An efflux inhibition by Soluplus[®] at comparably high effective concentrations was found. Uptake studies in MDCK II cells validated these results.

Furthermore, the mechanism of interaction between Soluplus[®] and model drugs was studied, allowing the optimization of formulations with regards to drug/excipient ratios. There is a window of ratios with maximal transport rates across Caco-2 cells, as result of an interplay between solubilization, binding of drug to Soluplus[®] and the amorphous state of the drugs.

2. Kurzzusammenfassung

Die beliebtesten Arzneiformen sind die zur oralen Gabe. Viele neue Arzneistoffe besitzen allerdings eine geringe orale Bioverfügbarkeit auf Grund ihrer schlechten Wasserlöslichkeit. Insbesondere für BCS Klasse II Substanzen ist die geringe Löslichkeit die entscheidende Hürde für eine erfolgreiche Therapie. Eine neue Technik zur Überwindung dieser Hürde ist die Schmelzextrusion zur Herstellung schnellauflösender fester Lösungen.

In dieser Arbeit wurde der neuartige Hilfsstoff Soluplus[®] untersucht, welcher Löslichkeitsverbesserung und die Möglichkeit zur Herstellung fester Lösungen durch Schmelzextrusion in einem Molekül vereinigt. Die Wirksamkeit von Formulierungen mit Soluplus[®] wurde im Caco-2 Zellkulturmodell beurteilt. Eine sehr gute Korrelation ergab sich zwischen dem Arzneistofftransport über Caco-2-Zellen und *in vivo* Studien an Beaglen.

Da viele Solubilizer den Effluxtransporter P-Glykoprotein modulieren, wurde Soluplus[®] auf eine solche Interaktion getestet. An Caco-2 und MDCK-II Zellen konnte eine P-gp-Hemmung bei hoher Soluplus[®]-Konzentration gezeigt werden.

Zusätzlich wurde die Interaktion zwischen Soluplus[®] und Modellarzneistoffen untersucht. Hierbei wurden Formulierungen hinsichtlich des Verhältnisses zwischen Arzneistoff und Hilfsstoff optimiert. Ein Optimum für maximalen Arzneistofftransport konnte an Caco-2-Zellen gezeigt werden, welches sich aus dem Zusammenspiel von Solubilisierung, Bindung des Arzneistoffs zu Soluplus[®] und der Amorphizität des Arzneistoffs ergibt.

3. General Introduction

3.1. Liberation and absorption of drugs after oral application

The action of drugs is steered by the two partners pharmacokinetics and pharmacodynamics. While pharmacodynamics is mainly dependent on the active pharmaceutical ingredient (API), for pharmacokinetics the dosage form also plays an important role. Pharmacokinetics is often described by the LADME scheme which summarizes the processes of pharmacokinetics:

- Liberation from the dosage form
- Absorption into the blood circulation
- Distribution of the drug in fluids and tissues
- Metabolism of the compound
- Excretion or elimination of the drug from the body

For oral application, the steps of liberation and absorption of a drug are essential for a successful therapy. Oral dosage forms are the most frequently used and favored formulations: At least 40 % of all APIs are applied as tablets [1]. Therefore, the development and optimization of these dosage forms is one of the main aspects of pharmaceutical technology.

The liberation of the API from its formulation is a complex process, including a number of simultaneous subprocesses such as wetting, disintegration, swelling, diffusion and dissolution [2]. All of these subprocesses may be targeted and controlled in formulation of an API, resulting in diverse coatings, sustained release formulations, rapidly disintegrating dosage forms and so on. However, the solubility of an API itself in the intestinal fluids

is the limiting factor for the liberation of many drugs. Especially for lipophilic APIs, their characteristically poor aqueous solubility is the biggest hurdle for a successful oral application.

3.1.1. Drug solubility and dissolution

The aqueous solubility of an API is mainly dependent on its chemical structure. Hydrophilic, polar APIs provide a good solubility, while lipophilic, nonpolar substances show a poor aqueous solubility. Therefore it is clear, that drug solubility may be improved in an early state of drug development by the synthesis of water-soluble salt forms or prodrugs. Drug dissolution is generally described by the equation of Noyes and Whitney [3]:

$$\frac{dc}{dt} = \frac{A \times D \times (c_s - c_t)}{V \times h} \quad (3.1)$$

whereas $\frac{dc}{dt}$ represents the rate of dissolution, A the surface area, D the diffusion coefficient, c_s the saturation solubility of the compound in the dissolution medium, c_t the concentration of the compound at time t , V the volume of the dissolution medium and h the thickness of the diffusion layer around the surface of the solid compound. Following this equation, one main possibility to increase the dissolution rate is an increase of the surface A . Obviously, the surface area of a drug powder is strictly dependent on the size of each particle. Size reduction (and hence an increased surface area) may be realized by micronization through milling processes. Micronized particles provide a large surface area and therefore also a better wettability, which may also be enhanced by addition of surfactants. A maximal surface area of the solid compound may be realized if it is applied in amorphous state or molecularly dispersed in a solid form (see Chapter 3.3). Another approach to increase the dissolution rate is the increase of the apparent solubility c_s by addition of solubility enhancers (e.g. micelle forming surfactants; see Chapter 3.2).

Furthermore the temperature of the solvent triggers the aqueous solubility, depending on the enthalpy change of a solution. If the dissolution process is exothermic, the solubility decreases by increasing temperature and vice versa for an endothermic process [1]. As for

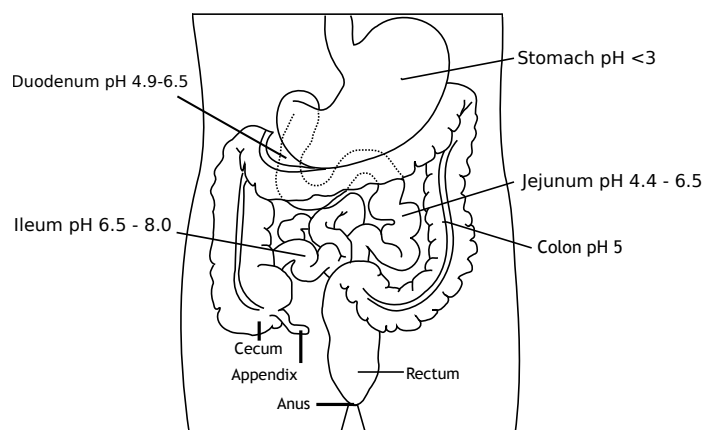


Figure 3.1.: The gastrointestinal tract and corresponding pH values (according to [4]; Picture: public domain)

all mammals the body temperature is equilibrated to about 37 °C, this fact does not play an important role in the formulation of oral dosage forms.

Even more important regarding API solubility is the composition of the gastro-intestinal fluids. First, the pH of the solvent is crucial for the solubility of APIs, which are present as salts, weak bases or acids. Such compounds undergo protonation and deprotonation and therefore changes in their polarity. The pH of the intestinal fluids is mainly dependent on the section of the GI-tract (Figure 3.1). The stomach provides acidic conditions, through the secretion of hydrochloric acid [5]. The intestinal pH gradually increases, caused by secretion of bicarbonate from the pancreas. Through GI-passage the pH rises from around 5 in the duodenum up to 7–8 in the terminal ileum [4]. Finally, in the colon the pH slightly decreases, as undigested carbohydrates are metabolized to short chain fatty acids [6]. Furthermore, the pH is dependent on food intake. In fed state the gastric pH rises to values between 3 and 7, while intestinal pH stays approximately constant [4].

Second, the intestinal fluids contain bile salts and lecithin. These two components are able to form mixed micelles, which may solubilize APIs. The amount of bile salts is strongly increased within thirty minutes after ingestion and decreases 120–150 minutes reverting back to the pre-prandial level. However, also at fasted state mixed micelles are present in

Class I	Class II
High solubility High permeability	Low solubility High permeability
Class III	Class IV
High solubility Low permeability	Low solubility Low permeability

Table 3.1.: The Biopharmaceutics Classification System (BCS), according to [7]

the intestine [4].

Gordon Amidon et al. introduced the Biopharmaceutics Classification System (BCS), which classifies APIs upon their solubility and their intestinal permeability ([7], Table 3.1). This system is established and accepted by the US Food and Drug Administration (FDA) as guide for the prediction of drug absorption after oral intake. The FDA considers a drug as *highly soluble* when the highest dose strength is soluble in 250 ml or less of aqueous media over the pH range of 1–7.5 [8]. A drug is considered as *highly permeable* if 90 % or more of an orally applied dose is absorbed in humans [8]. This usually correlates to an apparent permeability of 10×10^{-6} cm/s in Caco-2 transport experiments. According to this system, the intestinal absorption of lipophilic drugs with a high intestinal permeability (BCS class II) can be predicted by *in vitro* dissolution experiments [9]. Although the standard pharmacopoeia dissolution methods provide good *in-vitro-in-vivo* correlations (IVIVC), an even better correlation between *in vitro* and *in vivo* data for BCS class II substance can be reached by the use of more biorelevant dissolution media such as simulated intestinal fluids. Since for BCS class II substances the drug dissolution is the most important step for successful intestinal absorption, the use of solubilizing agents is accordingly a promising way to increase the oral bioavailability of poorly aqueous soluble drugs.

3.1.2. Principles of drug absorption across the intestinal mucosa

The intestinal mucosa is the most important barrier for drug absorption after oral application. As the small intestine provides a large area of 180 m², it is the main organ for the absorption of nutrients and also xenobiotics [5]. As described by the BCS, the per-

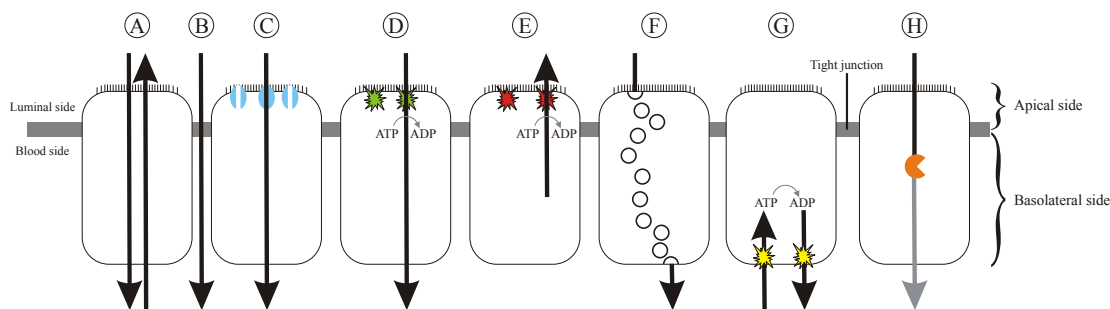


Figure 3.2.: Pathways for transport across the intestinal epithelium: (A) Transcellular passive diffusion (B) Paracellular passive diffusion (C) Facilitated transport (D) Active influx under ATP consumption (E) Active efflux under ATP consumption (F) Vesicular transport after apical endocytosis (transcytosis) (G) Basolateral active transport (efflux or influx) (H) Passive diffusion with additional enzymatic metabolism

meability of a certain drug through the intestinal barrier is as well important for its oral bioavailability. There are several ways for a drug to pass the intestinal epithelium as described in Figure 3.2. The transcellular and the paracellular pathway (Figure 3.2 (A) & (B)) are passive processes, following a concentration gradient. Both ways are dependent on the physicochemical parameters of the API. The limitations of transcellular diffusion are described by “Lipinski’s Rule of 5” [10]. According to this, a high permeability is likely for molecules that provide at least three of the criteria:

1. Maximal 5 H-bond donors
2. Maximal 10 H-bond acceptors
3. A molecular mass less than 500 Da
4. A logP lower than 5

Paracellular transport is described as diffusion in between the cells, passing the interconnecting tight junctions through pores. These pores were found to have a diameter of 0.5–5 nm. Therefore, the size of molecules transported by this way should not exceed 300 Da [11]. Furthermore, paracellular diffusion is preferred by hydrophilic compounds, since these compounds hardly diffuse into the lipophilic cell membrane, which is essential for transcellular transport.

Besides passive diffusion through or between the cells, transporter proteins may affect the intestinal absorption. These proteins permit the absorption of compounds, which are excluded from transcellular or paracellular diffusion, e.g. due to their physicochemical parameters. Facilitated transport (Figure 3.2 ©) enables the diffusion of a certain substrate, but is still driven by a concentration gradient. Facilitated transport is described for very polar molecules, such as amino acids or glucose. In contrast, active transport can take place against a concentration gradient under consumption of energy. It is described for both possible directions (Figure 3.2 ④ & ⑤): from the blood to the luminal side (efflux) and from the luminal side to the blood (influx).

Active efflux in the intestinal mucosa generally leads to a reduced bioavailability of substrates of such active transporter proteins. Additionally, efflux transporters are a possible site of drug-drug or drug-excipient interactions. Inhibition or induction of those proteins may lead to a changed relative bioavailability and hence results either in increased toxicity and side effects or in a reduced activity of a certain drug [12].

The big majority of human efflux transporters belong to the ATP binding cassette (ABC) superfamily, a class of proteins that is ubiquitarily expressed [13]. This large group of proteins is characterized by the sequence and organization of their ATP binding sites. This so called nucleotide binding folds (NBFs) consist of specific motifs: Walker A and B, which are separated by 90–120 amino acids and a signature C motif, upstream of the Walker B motif [14]. To establish an efflux, also against a concentration gradient, energy is needed. As for many biological processes the hydrolysis of ATP to ADP is used as energy source, releasing around 30 kJ/mol of free energy. The physiological function of these efflux transporters is mainly to protect the human body from potentially toxic substances, including xenobiotics and also physiological metabolites [15, 13]. ATP transporters are the main cause for the phenomenon of multidrug resistance in cancer therapy [16, 17]. Especially the transporter proteins P-glycoprotein, multidrug resistance associated proteins (MRPs) and the breast cancer resistance protein (BCRP) were identified to be overexpressed in tumor cells and to efflux cytostatic drugs from tumors [16, 18].

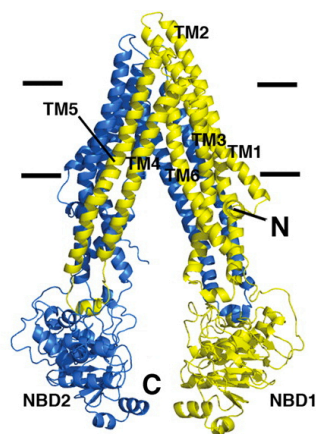


Figure 3.3.: X-ray structure of P-gp. Yellow: N-terminal half of the protein. Blue: C-terminal half of the protein. Transmembraneous (TM) and nucleotide binding domains (NBD) are labeled. The horizontal bars represent the position of the cell membrane. Adopted from [21]

Active efflux by human P-glycoprotein

P-glycoprotein is often considered as the most important human efflux protein. The existence of this protein was firstly proven in mutant chinese hamster ovary (CHO) cells, showing a resistance towards colchicine [19]. Human P-glycoprotein is coded by the gene MDR1 on chromosome 21 which is also known as ATP-binding cassette sub-family B member 1 gene (ABCB1). However, P-gp, MDR1 or ABCB1 are often used as synonyms for the transporter protein. It is a transmembraneous protein of 170 kDa with two halves of six transmembraneous domains each [13, 20]. Each half wears an intracellular ATP-binding site (nucleotide binding domain (NBD)). The active transport is established by the energy from the enzymatic hydrolysis of ATP. The transport is commonly explained by the so-called *hydrophobic vacuum cleaner* hypothesis. According to this model, the substrate partitions into the lipid bilayer and enters the drug binding site of the protein through an open portal [21]. When ATP then binds to the NBDs, a conformational change of the protein is performed and the substrate is presented to the extracellular space (Figure 3.4).

Apart from overexpression of P-gp in multidrug resistant tumors, P-gp plays an important physiological role at several barriers of the human body [22]. In general, P-gp transport is

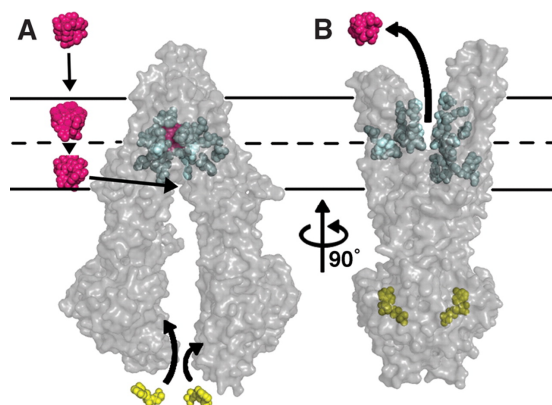


Figure 3.4.: Substrate efflux by P-gp: Substrate (magenta) diffuses into the lipid bilayer and enters P-gp to the drug binding site (cyan). After binding of ATP to the NBDs, conformational changes lead to the unidirectional substrate efflux. Adopted from [21]

directed towards the elimination routes from the human body. For example, it mediates the transport from the intestinal mucosa cells into the lumen, in the kidneys into the urinary system or at the blood-brain barrier in direction of the blood [23, 24]. Accordingly, P-glycoprotein activity may reduce the oral bioavailability of certain drugs [25]. Inhibition or induction of P-gp therefore may lead to increased or reduced bioavailability, respectively. The group of drugs and natural products which are known to affect the function of P-gp is not much smaller than the group of substrates. An overview of substances known to be substrate, inhibitor or inducer of P-gp is given in Table 3.2. Substrates of P-gp are usually of hydrophobic nature and do not exceed the size of 2000 Da.

As a result of this broad range of substrates, P-gp is prone to drug-drug and also drug-excipient interactions [27, 28]. Especially the combination of P-gp inhibitors with drugs providing a low therapeutic index is known to result in increased toxicity, e.g. azol-fungicides + digoxin. A reduced bioavailability of drugs is described for the interactions between P-gp inducers, such as St. John's wort flavonoids and P-gp substrates, for example oral contraceptives or anticoagulants [26]. P-gp inhibition has not only been described for drugs and herbal products, but also for many excipients. Especially for non-ionic surfactants, P-gp inhibition could be shown but also for other natural and synthetic polymers

Substrates	Inducers	Inhibitors
β-blockers: carvedilol, celiprolol, talinolol Calcium channel blockers: diltiazem, nifedipine, verapamil H₁-blockers: fexofenadine, terfenadine HIV protease inhibitors: indinavir, nelfinavir, ritonavir, Steroids: endogenous steroid hormones, dexamethasone Immunosuppressants: cyclosporine, sirolimus, tacrolimus Cytostatics: doxorubicin, etoposid, mitomycin, mitoxantron, paclitaxel, teniposid, vinca alkaloids Other: chlorpromazine, colchicine, digoxin, furosemide, loperamid, methadon, midazolam, phenytoin, quetiapin, rifampicin, simvastatin	Dexamethasone doxorubicin flavonoids (quercetin, kaempferol) St. John's wort phenobarbital phenytoin rifampicin vinblastine	Antiarrhythmics: amiodaron, chinidin, lidocain Antimycotics itraconazole, ketoconazole Calcium channel blockers: diltiazem, felodipine, nifedipine, nifedipine, nitrendipine, verapamil HIV protease inhibitors: indinavir, nelfinavir, ritonavir, saquinavir Steroids: ethinylestradiol, norgestrel, progesterone, testosterone Immunosuppressants: cyclosporine, tacrolimus Antibiotics: clarithromycin, erythromycin Other: mifepriston, paroxetine, talinolol, vincristine

Table 3.2.: Substrates, inducers and inhibitors of P-glycoprotein. Adopted from [26]

[29, 30, 31]. A summary of excipients which are known to have a P-gp inhibitory potential is given in Table 3.3. Besides unwanted interactions between P-gp inhibitors and substrates, the interaction may also be desired in the case of poorly bioavailable drugs. The combination of the inhibitor (& solubilizer) Vitamin E TPGS 1000 and the HIV-1 protease inhibitor amprenavir was commercialized under the trade name Agenerase[®] oral solution [32]. However, this drug was replaced by the pro-drug fosamprenavir calcium salt (Telzir[®]/Lexiva[®]) which provides a higher aqueous solubility [33]. Also in cancer therapy the combination of drug and P-gp inhibiting excipient was used to circumvent the multidrug resistance phenomenon, for example by the use of Cremophor EL [34, 35]. Due to this high potential of possible wanted or unwanted interactions it is clear that a novel solubilizing non-ionic excipient, such as Soluplus[®], is suspected to be a potential inhibitor of P-gp.

Excipient	Effective concentration [%]
Xanthan gum	0.05
Gellan gum	0.05
Flavicam	0.05
Dextran	0.05–0.1
PEG 300	20
PEG 400, 2000, 20000	0.1–20
TPGS 1000	0.0038
TPGS 200–6000	0.005
Tween 80	<0.13
Myrj 52	0.5
Pluronic P85	0.001–1

Table 3.3.: Excipients known for P-glycoprotein inhibition, assembled from [31]

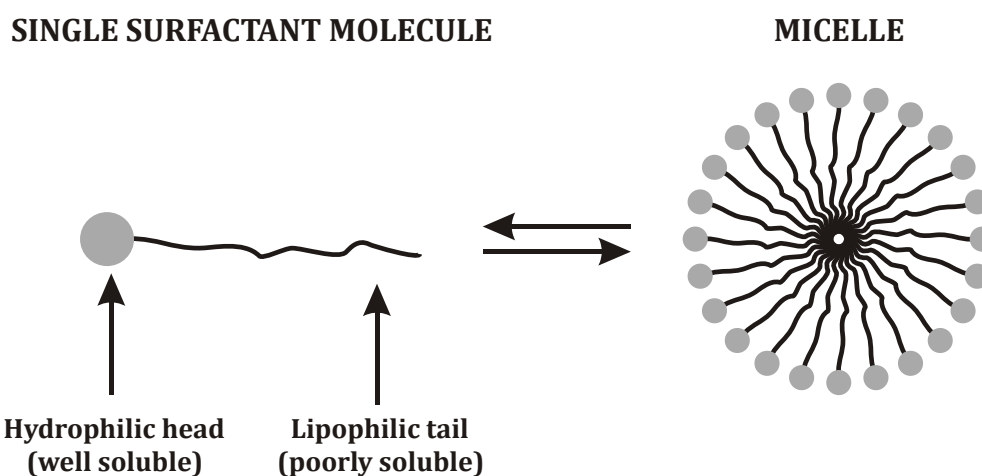


Figure 3.5.: Principle structure and formation of micelles.

3.2. Formulation of poorly aqueous soluble drugs by micellar solubilization

Strategies to increase the aqueous solubility of an API are the use of surfactants, co-solvents, complexing agents, micronization, or special drug delivery technologies such as nanocrystals or nanoparticles. In solution, surfactants aggregate to micelles in concentrations above the critical micelle concentration (CMC) forming a colloidal solution. In an aqueous solutions the surfactant molecules in a micelle are orientated, such that their nonpolar tails form the core and their polar heads the shell of the structure (Figure 3.5). In surfactant concentrations below the CMC the solubility of an API is equal to its solu-

bility in the pure solvent, e.g. an intestinal fluid. Above the CMC the solubility increases linearly with the surfactant concentration, described by the general equation for micellar solubilization:

$$S_{TOT} = s_w + \kappa \times c_{MIC} \quad (3.2)$$

where S_{TOT} is the total molar solubility of the solute, s_w is the water solubility of the solute, κ is the molar solubilization capacity of the surfactant and c_{MIC} is the molar concentration of the micellar surfactant (i.e., the total surfactant concentration minus the CMC) [36]. Throughout solubilization the lipophilic solubilize (the API) is incorporated in the core structure of the micelle, formed by its lipophilic tails [37]. The localization of an API molecule inside a micelle is dependent on its lipophilicity: While hydrophilic molecules are located in the outer shell formed by the hydrophilic heads, lipophilic molecules are most likely to stay in the lipophilic core region [38]. As micelles formed by small-molecular surfactants are thermodynamically unstable and also provide comparably high CMCs [38], polymeric micelles formed by amphiphilic co-polymers are as well candidates for pharmaceutical applications. These polymers usually have low CMCs compared to small-molecular surfactants which consequently leads to a higher stability upon dilution in the biological fluids. The micellar structure of such polymeric micelles is dependent on the polymer. The mechanism of micelle formation from amphiphilic di-block, tri-block, and graft co-polymers (such as Soluplus[®]) is illustrated in Figure 3.6.

Due to their size and hydrophilicity micelles are not likely to pass the intestinal barrier. However, the uptake of intact micelles by pinocytosis (Figure 3.2 F) could be shown [39]. The uptake of intact micelles seems not to be the main criteria for increased bioavailability through polymeric micelles. In the case of Vitamin K, it was shown that the API is released by bile salts from the micelles and subsequently uptaken [40]. Although micelles may pass the intestinal membrane, the most common way of intestinal absorption of micellar solubilized APIs is the release from the micelle, leading to an equilibrium between free drug molecules and those entrapped in micelles [41]. Therefore, polymeric micelles formed by pH-dependent polymers were designed to improve the release of drugs through the in-

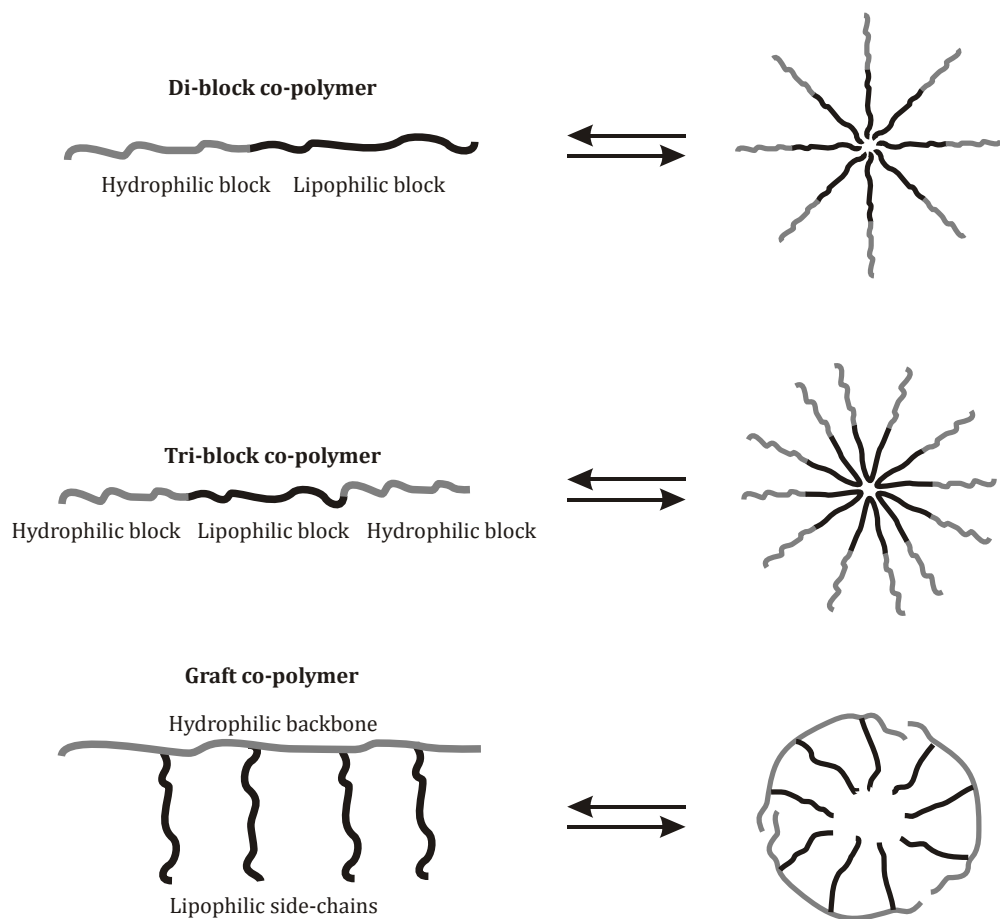


Figure 3.6.: Formation of micelles from amphiphilic co-polymers, according to [38]. The novel excipient Soluplus[®] is a graft co-polymer, providing a PEG backbone and vinylcaprolactam/vinyl acetate sidechains (Figure 3.9).

Polymer	API	Trade name	Formulation
Cremophor EL	Cyclosporine A	Gengraf	Soft capsules, oral solution
Cremophor EL	Lopinavir (+ ritonavir)	Kaletra (Norvir)	Soft gelatin capsule
Cremophor RH 40	Lopinavir + ritonavir	Kaletra	Oral solution
Gelucire 44/14	Fenofibrate	Cil, Lipirex	Capsules
Labrasol	Piroxicam	Piroflam	Tablets
Vitamin E TPGS	Amprenavir	Agenerase	Oral solution
Labrafils	Cyclosporine A	Gengraf, Sandimmune	Soft capsules, oral solution

Table 3.4.: Commercialized micellar drugs, derived from [43], Rote Liste & rxlist.com

testinal pH gradient [42]. Independent from the uptake mechanism, polymeric micelles are an excellent option for solubilization and therefore enhanced bioavailability of poorly soluble drugs. A broad variety of drug/excipient combinations forming polymeric micelles have so far been commercialized.

Among others, the following micelle-forming non-ionic surfactants were commercially used for oral drug delivery: polyoxyl 35 castor oil (Cremophor EL), polyoxyl 40 hydrogenated castor oil (Cremophor RH 40), polysorbate 20 (Tween 20), polysorbate 80 (Tween 80), d- α -tocopherol polyethylene glycol 1000 succinate (TPGS), Solutol HS-15, sorbitan mono-oleate (Span 80), polyoxyl 40 stearate, various polyglycolized glycerides (Labrafils), Labrasol, Gelucire 44/14, and Softigen 767 [43]. A short overview of commercialized products using the formation of micelles is given in Table 3.4. In most of these products, the API is presolubilized either in an oral solution or as solution in soft capsules, due to the low effectiveness of the incorporation of drugs into micelles is not effective by a simple equilibration in water [44]. The step of solubilizing and incorporation of non-dissolved drug by a potent solubilizer might also be too slow to be realized throughout the intestinal passage. Therefore, drug loading in liquid dosage forms can be facilitated by techniques such as dialysis against water or evaporation from an organic solvent [44]. The novel solubilizing agent Soluplus[®] offers the possibility of a good solubility enhancement in combination with a fast dissolution to drug loaded micelles if applied in form of a solid solution [45].

	glassy solid solution	solid solution	glass suspension		eutectic	amorphous precipita- tion
phases	1	1	2	2	2	2
drug	molecularly dispersed	molecularly dispersed	amorphous	crystalline	crystalline	amorphous
carrier	amorphous	crystalline	amorphous	amorphous	crystalline	crystalline

Table 3.5.: Classification for solid dispersions upon amorphous or crystalline state of drug and carrier, according to [47]

3.3. Solid dispersions and hot melt extrusion

3.3.1. Solid dispersions for pharmaceutical applications

Solid dispersions offer a novel way for the formulation of poorly aqueous soluble drugs. By definition a solid dispersion is the dispersion of an API in a solid matrix [46]. Based upon the amorphous or crystalline state of the used drug and the carrier, solid dispersions may be classified as described in Table 3.5. A *solid solution* is therefore present if the drug is molecularly dispersed in the solid matrix. As for a usual liquid solution, those systems consist of a single phase. Contrarily, a *glass suspension* is a biphasic system whereas the crystalline or amorphous API is dispersed in an amorphous matrix. Since pharmaceutical polymers are usually of amorphous nature, only three of the solid dispersions described in Table 3.5 may occur: glassy solid solutions and both glass suspension types.

These types show differences in their stability: While a dispersion of a crystalline drug in the polymer is almost stable, a dispersion of an amorphous API in the polymer matrix may be affected by crystallization during storage and processing (e.g. milling, tableting). The most desired form for the formulation of poorly soluble drugs is the glassy solid solution, whereas the drug is molecularly dissolved in the polymer. In this case, the concentration of the drug in the solid solution must be below its saturation solubility in the respective polymer. Therefore, this type of solid solution is thermodynamically stable, just as a common liquid solution. As the drug is molecularly dissolved, the absolute minimum of its particle size is reached (= the molecular diameter) [48]. Thereby, the dissolution rate is determined by the dissolution of the polymeric carrier [48]. Such a rapid dissolution of

the solid solution leads to a supersaturation of the drug in the dissolution media. If no stabilizing agents are present, a supersaturation is very unstable. A supersaturated solution of an API may be stabilized by solubilizing agents as described above (see Chapter 3.2). Also the carrier itself may act as stabilizer for the so formed supersaturated solution [48]. The novel excipient Soluplus[®] provides both: The capability to form solid solutions and the formation of micelles in aqueous solution as result of its amphiphilic structure.

The preparation of solid dispersions may be realized either by the solvent method or by the hot melt method. The solvent method was introduced by Tachibani and Nakamura [49]. In this method, the solid solution is produced by cosolvation of both drug and carrier in a liquid solvent, followed by an evaporation of the solvent under vacuum. The evaporation of the solvent may also be realized by other common methods, such as freeze-drying or spray-drying [50, 51]. As organic solvents are often used for this method, the solvent must be evaporated completely due to toxicity reasons. Another problem of this method may be that by evaporating a solvent, small variations in the setup lead to high variations in the product [48]. The main advantage of this method compared to hot melt methods is its applicability on heat-sensitive drugs, especially in combination with carriers providing a high melting point.

3.3.2. Hot melt extrusion

The hot melt method was introduced by Sekiguchi and Obi in 1961 for an eutectic mixture of sulfathiazole and urea [52]. In this simple approach both substances were molten together and cooled in an ice bath. The cooling step establishes a supersaturation of the drug which is then stabilized by the solid matrix. It depends on the miscibility of drug and matrix in the molten form if the product appears as a molecularly dispersed system [48]. The stability of the thereby reached supersaturation during the cooling process is also dependent on the process itself. This led to improvements in the cooling rate, such as snap-cooling on stainless steel [53, 54] or by spraying the melt on a cool plate [55]. The

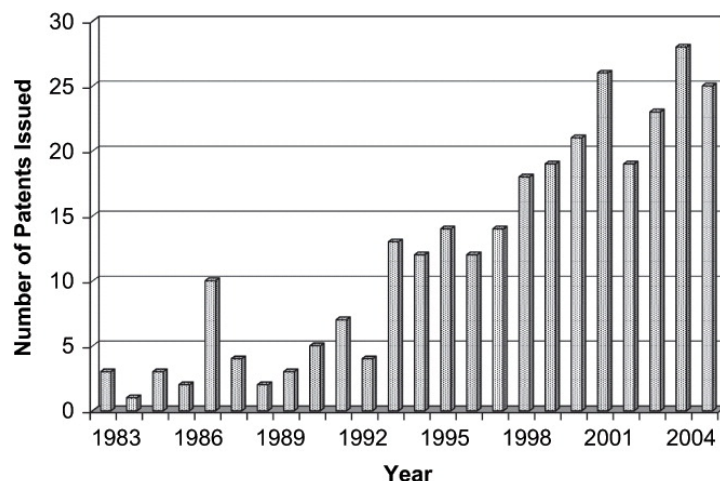


Figure 3.7.: The number of patents for hot melt extrusion for pharmaceutical applications strongly increased from 1982–2006. Adopted from [58]

main limitation of the melting process is the application to thermolabile drugs. However, the introduction of hot melt extrusion to pharmaceutical applications led to fast processing times, reducing the stress the APIs to a minimum. Also the addition of plasticizers improved the applicability of melt processes to thermosensitive drugs, as the process temperatures could be reduced [56, 57].

Hot-melt extrusion is defined as *the process of pumping raw materials with a rotating screw under elevated temperature through a die into a product of uniform shape* [58]. This process is originated in plastics industry and was first used for the production of plastic insulations for wires in the mid-19th century [58]. Nowadays, hot melt extrusion is still an important process for plastics industry, but also gains more and more interest for pharmaceutical applications (Figure 3.7). After the first use of this technique for delayed release dosage forms in the 1970s [59], hot melt extrusion is today an attractive process for the production of diverse drug delivery systems [58, 60, 61]. The advantages of hot melt extrusion compared to other production techniques for solid dispersions are numerous: it's a fast and continuous process, which is also easy to scale-up. Furthermore, the product of the extrusion is ready for further steps as milling or pelletizing without any preceding drying step.

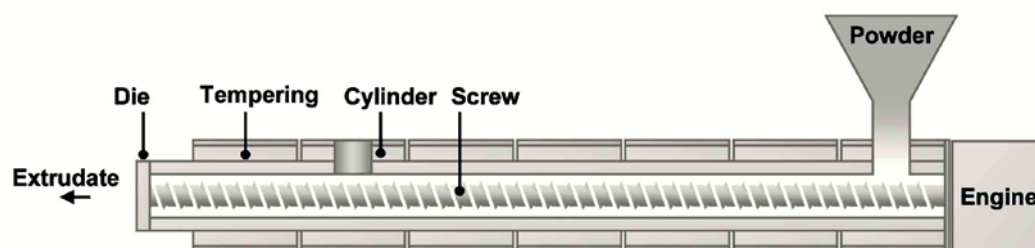


Figure 3.8.: General setup of an extruder, adopted from [62]

Extruders for pharmaceutical applications are similar to those for other industries, but with adaption to regulatory requirements. Hence, these extruders are generally made of an inert material such as stainless steel and constructed to meet the cleaning standards for drug manufacturing [62]. Generally, an extruder consists of one or two transport screws which rotate enclosed in a cylinder (Figure 3.8). During the extrusion process the product is molten, mixed and finally shaped by the passage through a die. Mixing and kneading of the material is usually established by the application of conveying and mixing elements, applied on the extruder screw [61, 62].

Polymers used for hot melt extrusion have to meet several requirements for a successful formation of a solid dispersion. It has to be thermoplastic, has to provide an appropriate glass transition temperature (T_g) and has to be stable at the applied temperatures (50–180 °C). Furthermore, it has to be non-toxic for pharmaceutical applications. The solubilization capacity of the used polymer is most important for the production of a molecularly disperse extrudate. The solubility parameters for a polymer are similar to those of a liquid solvent, including H-bond donors & acceptors, amide groups and a sufficient lipophilicity for poorly soluble drugs [63, 64]. The alchemist rule *similia similibus solvuntur* (lat.: *like dissolves like*) is valid for solid solvents as well as for liquid solvents.

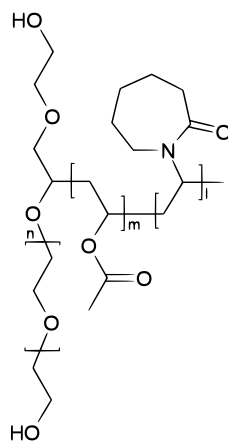


Figure 3.9.: Chemical structure of Soluplus[®]. PEG 6000/vinylcaprolactam/vinyl acetate are polymerized in a ratio of 13/57/30, according to [62]

Molecular weight	~ 118000 g/mol
Glass transition temperature (T_g)	~ 70 °C
CMC	7.6 mg/l = 7.6 ppm
K-value (1 % ethanol)	31-41
Lower crystalline solution temperature (LCST)	~ 40 °C
Solubility	
water	soluble
acetone	up to 50 %
methanol	up to 45 %
ethanol	up to 25 %
DMF	up to 50 %

Table 3.6.: Physico-chemical properties of Soluplus[®]

3.4. The novel solubility enhancer Soluplus[®]

Soluplus[®] is an amphiphilic polymer with the chemical formula: poly(vinyl caprolactam)-poly(vinyl acetate)-poly(ethylene glycol) graft copolymer (Figure 3.9). This graft copolymer provides a poly(ethylene glycol) backbone as hydrophilic part and vinylcaprolactam/vinyl acetate side chains as lipophilic structure. Therefore, it forms micelles in aqueous solution above the CMC of 7.6 mg/l. This polymeric excipient was designed for (micellar) solubilization of poorly aqueous soluble compounds and for the feasibility of forming solid solution through hot melt extrusion. The main physico-chemical parameters of Soluplus[®] are summarized in Table 3.6. Especially the comparably low T_g qualifies Soluplus[®] as well

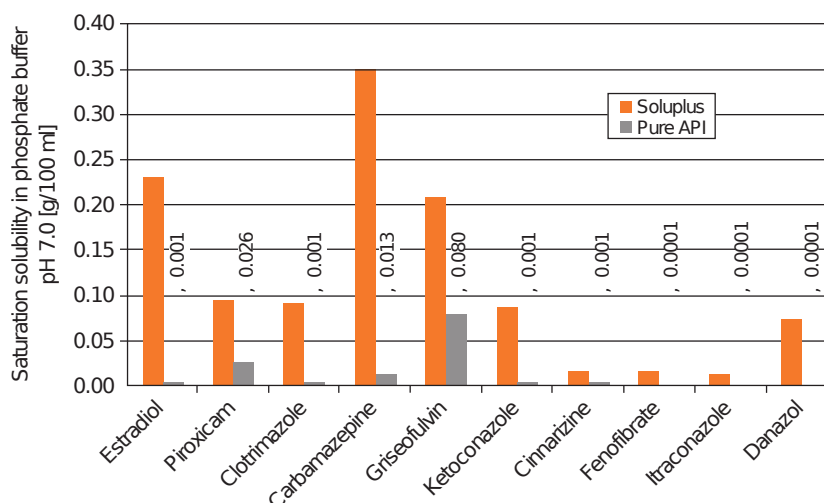


Figure 3.10.: Solubility of several drugs with and without Soluplus[®] (10 % w/w), adopted from [45]

suitable for hot melt extrusion, since the process temperatures can be reduced. Furthermore, Soluplus[®] can easily be used in tablets as it is a solid powder, that also can act as binder [45].

Due to its amphiphilic structure Soluplus[®] forms micelles in aqueous solution which can solubilize poorly soluble APIs. It was shown that Soluplus[®] enables a many fold supersaturation for several drugs (Figure 3.10). In form of a solid solution, manufactured by hot melt extrusion the dissolution rate of poorly soluble APIs was strongly increased [84]. Furthermore, the oral bioavailability of the model drugs danazol, fenofibrate and itraconazole (Figure 3.12) was strongly increased if applied as solid solution [84, 45]. This result stands in strong agreement with Amidon's biopharmaceutics classification system (BCS) which predicts a high oral bioavailability for BCS class II substance if their characteristic solubility problems are circumvented.

3.5. The Caco-2 cell culture model

Caco-2 cells were isolated from a human colon adenocarcinoma of a 77 year-old male caucasian. Caco-2 monolayers are a well established and characterized model for the small

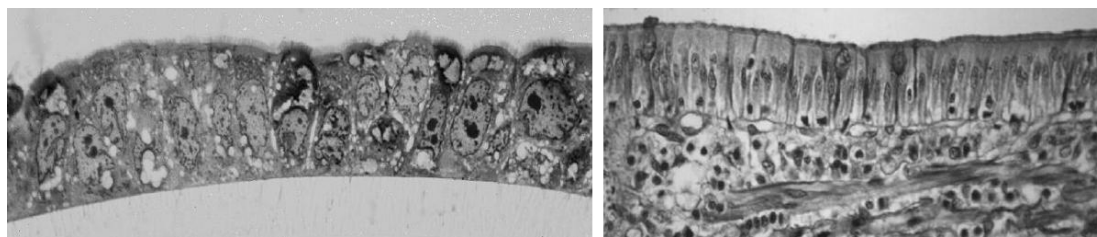


Figure 3.11.: Left: Cross section of Caco-2 monolayer. Right: Cross section of porcine intestinal mucosa

intestine [65, 66]. Permeability assays using Caco-2 cells are routinely used in pharmaceutical research and development [67, 68]. Additionally Caco-2 cells are used for investigations in drug-transporter interactions as well as in intestinal drug metabolism [69, 70]. The usability of this cell line as model for the intestinal barrier can be explained by its behavior under cell culture conditions. Caco-2 cells differentiate to cells, phenotypically similar to human small intestine enterocytes (Figure 3.11). Accordingly, Caco-2 cells provide microvilli, tight junctions, transporter proteins (e.g. P-glycoprotein) and also a wide range of metabolic enzymes [71, 72]. Furthermore, Caco-2 cells differentiate to polarized monolayers, forming an apical and a basolateral side [73]. Growing Caco-2 cells on permeable filters establishes the possibility to investigate drug transport across cell monolayers [66, 65]. Good *in-vitro-in-vivo* correlations (IVIVC) were found between drug permeability across Caco-2 monolayers and the intestinal absorption [11, 72, 74]. The expression of active transporters (influx & efflux) such as MCT1, OATP-B, MDR1, MRP2 and BCRP in Caco-2 cells underlines the potential of this cell line as an excellent predictive tool for intestinal drug absorption [75]. Although expression of these proteins can be observed in Caco-2 cells, their expression levels differ from those in the human body [76]. Especially the metabolic active enzyme CYP3A4 is only poorly expressed in Caco-2 cells. However, there are approaches to avoid these limitations for example by the use of CYP3A4 induced [77] or transfected [78] cell lines.

General differences between Caco-2 cells and the intestinal membrane lead to further limitations of this model. The human intestinal membrane not only consists of enterocytes

but also of goblet cells. Goblet cells produce mucus, forming a thin layer on the luminal side of the intestinal barrier. This mucus layer might influence the intestinal drug absorption: Firstly, it is gel-like and may hinder drug diffusion by its high viscosity. Secondly, the mucus layer provides a pH gradient which may influence the solubility of basic or acidic drugs [79]. Furthermore, this mucus layer might be the aim of gastroretentive dosage forms, using mucoadhesive excipients [80]. To reduce this gap between Caco-2 monolayers and the intestinal membrane co-cultures of Caco-2 cells and goblet like cell lines (e.g. HT29 cells) were developed [81, 82, 83]. Although these co-cultures provide an *in-vivo-like* mucus layer, they couldn't replace Caco-2 monocultures as they didn't show much superior *in-vitro-in-vivo* correlations, justifying higher costs and efforts. Another difference between Caco-2 cultures and the real intestine is the specifically higher tightness of the cell culture model [66]. This is also expressed in a higher transepithelial electrical resistance (TEER value) of Caco-2 monolayers compared to the original membranes [11]. The TEER value is an accepted measure for the tightness of cell monolayers, grown on permeable filters. Therefore, the electrical resistance between the apical and basolateral compartment of such a system (e.g. Transwell) is measured by an electrical Volt-Ohm meter (EVOM). As result of their higher tightness, the paracellular transport route (Figure 3.2 B) is hindered. Accordingly the transport of hydrophilic drugs, which are mainly transported via this route, is often underestimated in the Caco-2 model [72]. Therefore, Caco-2 monolayers show better predictions of intestinal absorption for highly permeable substances (BCS class I,II), which are generally more lipophilic and transported via the transcellular pathway (Figure 3.2).

3.6. Aims of this thesis

In this work Soluplus[®], a novel solubilizing agent was characterized for its interaction with poorly soluble drugs and the intestinal mucosa. Caco-2 cell monolayers were used as *in vitro* model for the intestine. Formulations of Soluplus[®] with poorly soluble drugs were investigated for their transport behavior and their potential to increase the oral bioavail-

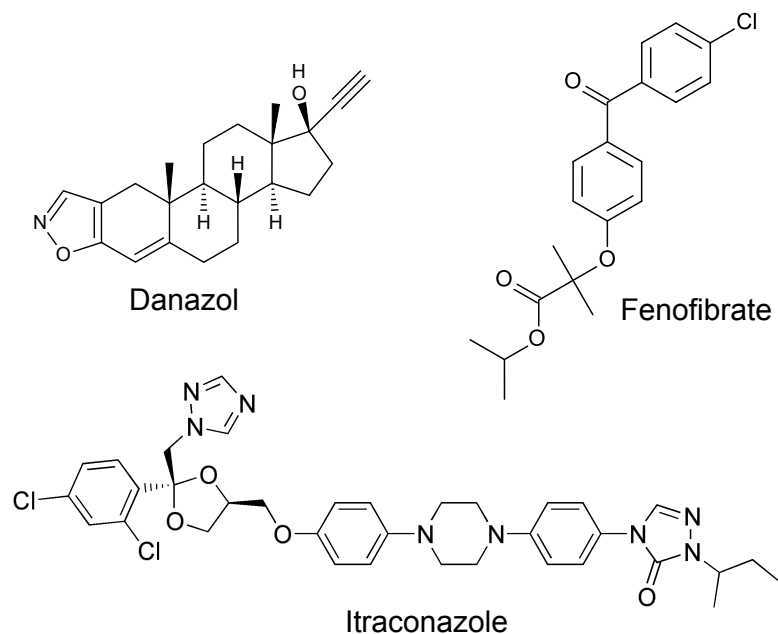


Figure 3.12.: Chemical structure of the used model drugs danazol, fenofibrate and itraconazole

ability of these drugs. Additionally, this work furthered the understanding of the interplay between a solubilizing excipient, the drug and the mucosa. These interactions play an important role for the liberation and absorption part of the LADME scheme. Additionally, the interaction between Soluplus[®] and bioactive proteins (P-glycoprotein, trypsin) was investigated which might also interact with the absorption of poorly soluble drugs.

The aims of this thesis may be summarized as:

1. Evaluation of the Caco-2 model as surrogate for *in vivo* behavior of Soluplus[®] formulations
2. Testing Soluplus[®] for a possible inhibition of human P-glycoprotein
3. Optimization of Soluplus[®] formulations, using the Caco-2 model

3.6.1. The Caco-2 model as predictive tool for Soluplus[®] formulations

In this work the Caco-2 monolayer model was evaluated for its predictive value for formulations with Soluplus[®]. While the Caco-2 monolayer model is widely accepted as sur-

rogate for pure drugs, the application of more complex excipient/drug is not well established. Therefore, this work might help to fulfil the aim of reducing, refining and replacing (3R-rule) animal experiments.

The starting point of this thesis were *in vivo* pharmacokinetic studies of Soluplus[®] formulations with danazol, fenofibrate and itraconazole. This data was collected in animal experiments in beagle dogs. According to this animal experiments, the solid solution of Soluplus[®] and the respective drugs showed a many fold increase in AUC and C_{max} values compared to the pure drug. Furthermore, a physical mixture of Soluplus[®] and the respective API was administered to the animals which was only effective in the case of fenofibrate. As first aim of this thesis, the possibility of predicting *in vivo* data of Soluplus[®] formulations by the Caco-2 model should be proven.

3.6.2. Potential inhibition of P-glycoprotein and/or trypsin by Soluplus[®]

As many non-ionic surfactants were shown to inhibit P-glycoprotein or other active proteins, Soluplus[®] was tested for its inhibitory potential on a) P-glycoprotein as transmembraneous active transporter and b) trypsin as soluble enzyme, present in the GI.

3.6.3. Optimization of Soluplus[®] formulations

After establishment of the methods to use Caco-2 cells as a surrogate for *in vivo* data of Soluplus[®] formulations, the Caco-2 tool was used for optimization of such formulations. Especially the effect of the ratio between excipient and drug in hot melt extrudates was investigated. The aim of this part was to discover an optimal Soluplus[®]/drug ratio, as result of the interactions in binding, solubilization and crystallinity of drug and excipient.

4. Soluplus[®] as an effective absorption enhancer of poorly soluble drugs *in vitro* and *in vivo*

Parts of this chapter have been published as journal article:

Soluplus[®] as an effective absorption enhancer of poorly soluble drugs *in vitro* and *in vivo* Michael Linn, Eva-Maria Collnot, Dejan Djuric, Katja Hempel, Eric Fabian, Karl Kolter, Claus-Michael Lehr

European Journal of Pharmaceutical Sciences **Article in press**

Abstract

As many new active pharmaceutical ingredients are poorly water soluble, solubility enhancers are one possibility to overcome the hurdles of drug dissolution and absorption in oral drug delivery. In the present work a novel solubility enhancing excipient (Soluplus[®]) was tested for its capability to improve intestinal drug absorption. BCS class II compounds danazol, fenofibrate and itraconazole were tested both *in vivo* in beagle dogs and *in vitro* in transport experiments across Caco-2 cell monolayers. Each drug was applied as pure crystalline substance, in a physical mixture with Soluplus[®], and as solid solution of the drug in the excipient. In the animal studies a many fold increase in plasma AUC was observed for the solid solutions of drug in Soluplus[®] compared to the respective pure drug. An effect of Soluplus[®] in a physical mixture with the drug could be detected for fenofibrate. *In vitro* transport studies confirm the strong effect of Soluplus[®] on the absorption

behavior of the three tested drugs. Furthermore, the increase of drug flux across Caco-2 monolayer is correlating to the increase in plasma AUC and C_{\max} *in vivo*. For these poorly soluble substances Soluplus[®] has a strong potential to improve oral bioavailability. The applicability of Caco-2 monolayers as tool for predicting the *in vivo* transport behavior of the model drugs in combination with a solubility enhancing excipient was shown. Moreover, the improvement of a solid dispersion compared to physical mixtures of the drugs and the excipient was correctly reflected by Caco-2 experiments. In the case of fenofibrate the possible improvement by a physical mixture was demonstrated, underscoring the value of the used tool as alternative to animal studies.

4.1. Introduction

According to the biopharmaceutical classification system (BCS), the dissolution of poorly water-soluble drugs in gastrointestinal media is the limiting step for its permeation and absorption through the intestinal system [7, 9]. Thus, the aim of many formulation attempts is to increase drug solubility in physiological fluids by means of surface-active excipients which can act as wetting agents and solubilizers. Other methods for improving oral drug solubility include nanosizing or the use of cyclodextrin complexes [85, 48, 86]. In recent years, the emergence of the hot melt extrusion technique has enabled the formulation of solid solutions of poorly soluble drugs in polymer matrixes such as polyethyleneglycol, polyvinylpyrrolidone or cellulose derivatives (e.g. hydroxypropylmethylcellulose). In a solid solution the drug is molecularly dispersed in the solid matrix. After fast dissolution, a supersaturated solution is formed, allowing high drug fluxes. [48].

In the present study, polyvinyl caprolactam-polyvinyl acetate-polyethylene glycol graft copolymer (Soluplus[®]), a new polymer with amphiphilic properties was used. Soluplus[®] shows excellent solubilizing properties for BCS class II substances and offers the possibility of producing solid solutions by hot-melt extrusion. The dissolution of poorly soluble drugs in aqueous media can be highly improved by the use of solid solutions with Soluplus[®] [84]. The ability of Soluplus[®] to improve oral bioavailability of poorly soluble

CHAPTER 4. SOLUPLUS[®] AS AN EFFECTIVE ABSORPTION ENHANCER OF POORLY SOLUBLE DRUGS *IN VITRO* AND *IN VIVO*

	Molecular weight [g/mol]	Melting point [°C]	logP	pKa	Solubility (water) [µg/ml]	Solubility (10 % Soluplus [®] ; phosphate buffer) [µg/ml]	Solubility in used physical mixture formulation [µg/ml]
Danazol	337.46	224.4–226.8	4.5[9]	-	~ 1[9]	730[45]	4.8
Fenofibrate	360.831	80.5	5.2[87]	-	0.1[88]	170[45]	5.2
Fenofibric acid	318.76	179–183	3.99	3.09	70	n.d.	n.d.
Itraconazole	705.64	166.2	5.7[89]	3.7[89]	~ 0.001[90]	130[45]	2.7

Table 4.1.: Physico-chemical parameters of model drugs

drugs was investigated using three different BCS class II drugs, danazol, fenofibrate and itraconazole, their physico-chemical parameters are shown in Table 4.1.

Danazol, a testosterone derivative suppressing luteinizing and follicle stimulating hormone used for the treatment of endometriosis [91], shows a low relative bioavailability of $5.1 \pm 1.9\%$ as determined in beagle dogs, due to its poor aqueous solubility ($10 \mu\text{g/ml}$) [92]. Its oral bioavailability could be raised by different formulation techniques using nanoparticles or cyclodextrin complexes up to $82.3 \pm 10.1\%$ and $106.7 \pm 12.3\%$, respectively [92]. Furthermore, danazol formulations with polyvinylpyrrolidone obtained by ultra-rapid freezing or spray freezing processes showed enhanced dissolution rates *in vitro* [93, 94].

The lipid modifying drug fenofibrate with an aqueous solubility of $0.1 \mu\text{g/ml}$ is less soluble than danazol. Sant et al. discovered polymeric micelles of poly(ethylene glycol)-block-poly(alkyl acrylate-co-methacrylic acid) as an efficient solubility enhancer [95]. Fenofibrate dissolution can also be improved by nanosizing, spray-drying or cogrinding of the drug [96]. Buch et al. showed the effectiveness of a melt-extruded solid solution, lipid microparticles, micronized and nanosized fenofibrate on intestinal drug absorption versus fenofibrate bulk ware *in vivo* as well as in a combined dissolution/permeation system *in vitro* [97].

The antifungal drug itraconazole is practically insoluble in water and has the highest logP of the drugs used in this study. It is a weak base with a pKa of 3.7 and appears ionized in gastric fluids with a pH lower than 3 resulting in pH dependent intestinal absorption [98]. Itraconazole is commercialized as Sporanox[®] capsules, where it is applied as a drug/polymer layer with HPMC on neutral pellets. Six et al. developed a fast dissolving,

but not homogenous solid solution of itraconazole and HPMC [99]. Other solid solutions of itraconazole were introduced by Miller et al. who generated a ternary solid solution, obtained by hot-melt extrusion of itraconazole in a matrix formed by Carbopol[®] 974P and Eudragit[®] L100-55 [100]. Buchanan et al. showed an increased oral bioavailability applying itraconazole as a formulation with hydroxypropyl- β -cyclodextrin (HP β CD) HP β CD is as well used as solubilizer for itraconazole in the commercialized Sporanox[®] for injection [101].

Solid solutions are usually characterized by their crystallinity and their dissolution behavior. However, as permeation across the intestinal epithelium is missing, merely performing *in vitro* solubility will not always afford an *in vivo* prediction. In particular, the interplay between drug, excipient and epithelial cells cannot be investigated in a cell free setup.

Caco-2 monolayers are a widely used *in vitro* tool to predict permeation behavior of drugs over the intestine [66, 74, 102]. In general, drugs are applied as solutions to the apical side of the *in vitro* model and drug permeation rate to the basolateral side is correlated to the *in vivo* absorbed fraction of the drug or directly to the AUC. The Caco-2 model has also been successfully applied to study the influence of pharmaceutical excipients on drug permeation not only via solubility enhancement but also via modulation of tight junction functionality and active transport systems [103, 30, 104]. Hence, the Caco-2 monolayer assay has been successfully used to evaluate complex formulations such as nanoparticulate formulations and self-emulsifying systems. Nevertheless, there is still need for further evaluation in particular with regards to experimental design and to acceptor and donor media chosen [105].

In the present study, we used the Caco-2 *in vitro* model to predict the effect of Soluplus[®] on oral bioavailability of three BCS class II compounds. Drug permeation from the pure crystalline substance and from the physical mixtures of drug and excipient were compared to the respective aqueous dispersed solid solutions. Drug affinity to Soluplus[®] was studied by equilibrium dialysis to allow interpretation of possible differences in Soluplus[®] effi-

	% API [w/w]	Temperature [°C]	Powder feed rate [kg/h]	rpm
Danazol	15	140	0.9	200
Fenofibrate	20	95	0.7	200
Itraconazole	15	150	1	200

Table 4.2.: Melt extrusion parameters for production of the used solid solutions

cacy. Data obtained in the transport experiments was compared to data from *in vivo* studies in beagle dogs, validating the findings from the cell culture setup and demonstrating its strengths and weaknesses for the testing of complex formulations.

4.2. Materials and Methods

4.2.1. Chemicals

The solubility enhancer Soluplus[®] was provided by BASF SE (Ludwigshafen, Germany). Danazol and itraconazole were donated by Selectchemie AG (Zurich, Switzerland). Dulbecco's modified Eagle's medium (DMEM) and non-essential amino acids were obtained from PAA Laboratories GmbH (Pasching, Austria). Fetal bovine serum (FBS) was purchased from PAN-Biotech GmbH (Aidenbach, Germany). Vitamin E TPGS 1000 was supplied by Eastman Chemical Company (Kingsport, TN, USA). Transwell permeable membrane inserts (type 3460, 0.4 µm pore size, polycarbonate) were from Corning Incorporated Life Science (Lowell, MA, USA). Fenofibrate and all other chemicals were from Sigma-Aldrich (St. Louis, MO, USA).

4.2.2. Solid Solutions

Solid solutions were prepared by hot melt extrusion in a ThermoFisher PolyLab twin-screw extruder (ThermoFisher Scientific Inc., Waltham, MA, USA). Extrusion parameters were adjusted for each drug and are summarized in Table 4.2. The solid solutions employed in this study contained 15 % API for danazol and itraconazole and 20 % for fenofibrate, respectively.

4.2.3. Caco-2 cell culture

Caco-2 cells of clone C2BBE1 were obtained from American Type Culture Collection (Manassas, CA, USA). Cells were grown in an incubator at 37 °C with an atmosphere of 5 % CO₂ and 80 % relative humidity. Cell culture medium was DMEM, containing 10 % FBS and 1% NEAA and was changed every 2-3 days. Every 7 days cells were passaged at a confluence of about 90 %. Cell passages 65–75 were used for transport experiments. For transport experiments cells were seeded on Transwell permeable membrane inserts (0.4 μm pore size, 1.12 cm² membrane area) at a density of 60000 cells per well. Fully differentiated cells were used for transport experiments after 21–23 days in culture. Only monolayers with a transepithelial electrical resistance (TEER) higher than 500 Ohm x cm² were qualified for transport assay.

4.2.4. Caco-2 transport experiments

Transport medium was Krebs Ringer buffer (KRB) containing 114.2 mM NaCl, 3.0 mM KCl, 4.0 mM d-glucose, 1.4 mM CaCl₂, 2.6 mM MgCl₂, and 10.0 mM HEPES. pH was adjusted by NaOH to a final value of 7.4. 0.2 % Vitamin E TPGS 1000 was added to the buffer to maintain sufficient drug solubility in the receiver compartment, as described by Mellaerts et al [106]. For itraconazole, a known substrate of the P-gp efflux system, transport studies were conducted using KRB + 1 % HPβCD as acceptor medium, since Vitamin E TPGS is known to inhibit P-gp and thus might interfere with the transport experiment.

The following formulations of each drug were used for transport experiments: I) the pure crystalline drug, II) a physical mixture of the drug and Soluplus[®] in the same ratio as in the respective solid solution and III) the solid solution of the drug in Soluplus[®]. All formulations were suspended in KRB and diluted to a final drug concentration of 0.5 mg/ml for danazol and itraconazole and of 1.0 mg/ml for fenofibrate. The suspensions were stirred for 1.0 h on a magnetic stirrer to simulate gastrointestinal dissolution. Throughout this timescale the solid solutions dissolve and enable a micellar-stabilized supersaturation of the respective drug. Cells were washed twice and pre-incubated with KRB for 1.0 h. 500 μl

of each drug suspension was applied on the apical side, while 1500 µl of the respective acceptor medium was placed on the basolateral side. Transport experiments were conducted in a cell culture incubator at 37 °C, 80 % rH, 5 % CO₂ and the system was agitated on an orbital shaker at 100 ± 20 rpm. Samples of 200 µl volume were taken at 30, 60, 90, 120 and 180 minutes from the basolateral side. The lost volume was replaced by fresh tempered buffer. TEER measurements as control for membrane integrity took place at the beginning and after the experiment.

Drug flux was calculated over the linear range of the permeation curve for each well, using the formula:

$$Flux = \frac{dc}{dt} \times \frac{1}{A} \quad (4.1)$$

whereas dc/dt indicates the slope of the permeation curve and A the surface of the monolayer.

4.2.5. Sample preparation & HPLC analysis

Samples, as drawn from the basolateral compartment, were diluted in a 1:1 ratio either with acetonitrile (fenofibrate, itraconazole) or with methanol (danazol). For danazol a methanol:water:phosphate buffer pH 6.8 [80:17:3 (v/v/v)] mixture was used as mobile phase. 50 µl of the samples were injected on a reversed phase column [LiChroCART[®] 125-4 LiChrospher[®] 100 RP18 (5 µm) by Merck KGaA (Darmstadt, Germany)] and detected by UV-VIS absorption at 288 nm.

Fenofibrate samples were injected at a volume of 50 µl on a reversed phase column [RP 18 (5 µm) as above] using a mixture of 30 volumes water acidified to pH 2.5 by phosphoric acid and 70 volumes acetonitrile. Due to enzymatic hydrolysis, fenofibrate was detected as the mother compound and as its metabolite fenofibric acid by UV-Vis absorption at 286 nm with retention times of 6.4 and 2.3 minutes respectively.

The mobile phase for itraconazole consisted of a mixture of acetonitrile, water and pH 6.8 phosphate buffer (70:27:3 [v/v/v]). A volume of 80 µl was injected on a reversed phase column (RP 18 (5 µm) as above) and detected at a wavelength of 263 nm (see Appendix C for further details).

4.2.6. Animal studies

The investigated formulations were administered as oral application via capsule to female fasted beagle stock dogs (n=5/per test substance preparation). Purebred Beagle dogs (7–8 months; danazol; 20–22 months for itraconazole and fenofibrate) were selected, as this non-rodent species is recommended by the guidelines and there is extensive laboratory experience with this strain of dogs. Dogs were housed in animal rooms with forced ventilation system and additional heating in winter. The animals had free access to inner and outer kennels of at least 6 m². Dog diet was offered in the mornings for a period of two hours. The animals had free access to water by and automatic watering device.

Before drug administration, food was withdrawn for at least 22 hours, but access to water was maintained. On experiment days, the dogs were fed about 2 hours after administration of the test substances (following the blood sampling after 2 h). Appropriate amounts of drug preparations, adjusted on the basis of each individual animals weight, were weighed and placed in gelatin capsules, size 11 (Torpac Inc., Fairfield, NJ 07004, USA) and administered to the dogs in the morning: I) Crystalline API, II) a physical mixture of API and Soluplus® and, III) a solid solution of API and excipient (as described in 4.2.2). The administered doses were 10 mg/kg bodyweight for itraconazole and fenofibrate and 30 mg/kg bodyweight for danazol, respectively. Dose levels were selected based on literature data: [107, 108] (fenofibrate), [101] (itraconazole), [92] (danazol). Experiments were performed according to German Animal Welfare legislation under the license number 1.577-07/873-50. The laboratory is AAALAC (Association for Assessment and Accreditation of Laboratory Animal Care) certified.

Blood samples for kinetic investigations (approx. 3 ml each) were taken prior to administration and after 0.5, 1, 2, 4, 6, 8 and 24 h from the *Vena cephalica antebrachii* and collected into lithium heparin blood collection tubes. After centrifugation, plasma was divided into two equal parts and transferred into plastic tubes and placed on dry ice until storage at -20 ± 5 °C. One aliquot of each sample was subsequently transferred frozen to the analytical laboratory of BASF for analysis. The remaining aliquot was stored as contingency sample.

Plasma samples were diluted by addition of acetonitrile [1:9 (v/v)]. After centrifugation at 5,000 rpm, the received supernatant was analyzed by appropriate LC-MS-, LC-MS/MS-analyses in the linear range of the quantification method. The linear range was assessed by standard solutions of the test compounds in the same matrix. See Appendix C for further details on the used LC-MS methods.

AUC levels were determined based on analyzed plasma concentrations by application of the linear trapezoid calculation method using a BASF internal Microsoft Excel based kinetic assessment tool. For the performed experiments single animal plasma values at the different time points were transferred into the program and single animal AUC values were calculated. Mean AUC values and standard deviations were used in the results section.

4.2.7. Equilibrium dialysis

Dialysis experiments were performed to investigate binding behavior of the investigated drugs to Soluplus[®]. Studies were performed in a DIANORM apparatus (identical to DI-ALYZER by Harvard Apparatus, Holliston, MA, USA) with a working volume of 2 ml per dialysis chamber. For our experiments, suspensions of a physical mixture of 0.5 % Soluplus[®] and 0.5 mg/ml (danazol and itraconazole) or 1.0 mg/ml (fenofibrate and fenofibric acid) respectively were prepared in KRB by stirring on a magnetic stirrer for 24 h. The dispersions were centrifuged to eliminate non-dissolved drug, resulting in saturated drug-excipient solutions. The donor chambers of the dialysis cell were filled with 2 ml of these suspensions. The acceptor sides, separated by a cellulose membrane with a cutoff of 10 kDa (Harvard Apparatus, Holliston, MA, USA), were filled either with KRB + 1 % BSA or KRB + 0.2 % Vitamin E TPGS 1000 at the same volume. Dialysis was performed over four hours at a rotation speed of 20 rpm at 37 °C. A control experiment using fluorescein sodium as model substance showed that equilibrium was reached throughout this time scale (data not shown). Samples from donor and acceptor were analyzed by HPLC as described above. Results are expressed as donor/acceptor ratio (D/A ratio) serving as an indicator for drug binding to Soluplus[®].

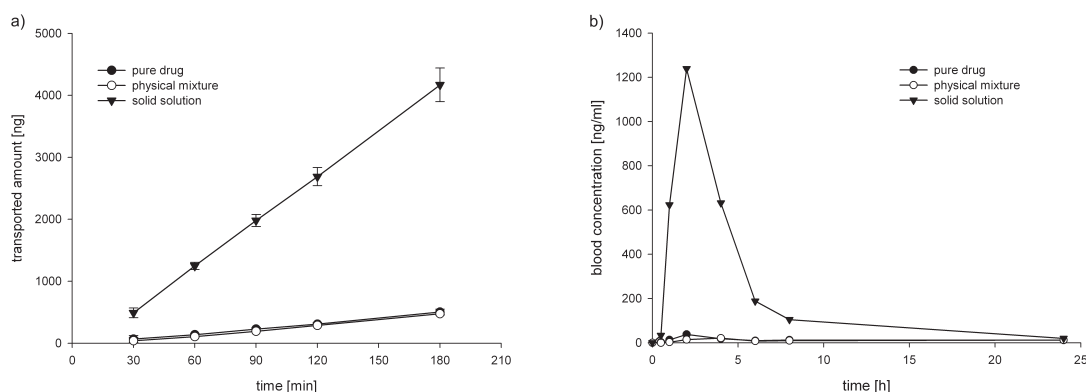


Figure 4.1.: a) Danazol transport across Caco-2 monolayers (n=3-6; mean \pm SD) b) *In vivo* blood levels of danazol applied to beagle dogs (n=5; mean values)

4.3. Results

4.3.1. Danazol

Danazol transport across Caco-2 monolayers was demonstrated for all three formulations. As shown in Figure 4.1a, the highest transport rate *in vitro* was reached from the solid solution of Soluplus[®] and the danazol. The pure crystalline substance and the physical mixture showed no significant difference in transport rate. The solid solution enabled a drug flux of $20.61 \text{ ng} \times \text{min}^{-1} \times \text{cm}^{-2}$, a 8-fold increase (Figure 4.2) compared to the pure drug which afforded a flux of $2.67 \text{ ng} \times \text{min}^{-1} \times \text{cm}^{-2}$. *In vivo* experiments in beagle dogs showed a 15-fold increase in plasma AUC from $329 \text{ ng} \times \text{h} \times \text{ml}^{-1}$ for the pure drug up to $5081 \text{ ng} \times \text{h} \times \text{ml}^{-1}$ for the solid solution after oral administration. For the physical mixture no significant effect of Soluplus[®] was determined compared to the pure drug (Figure 4.1b). Besides increased AUC, an increased C_{max} was shown for the solid solution compared to the pure drug. C_{max} and T_{max} values are summarized in Table 4.3.

4.3.2. Fenofibrate

Since fenofibrate is mostly hydrolyzed to fenofibric acid either by a first pass effect in the animal or by hydrolytic enzymes present in Caco-2 cells, all results refer to fenofibric acid.

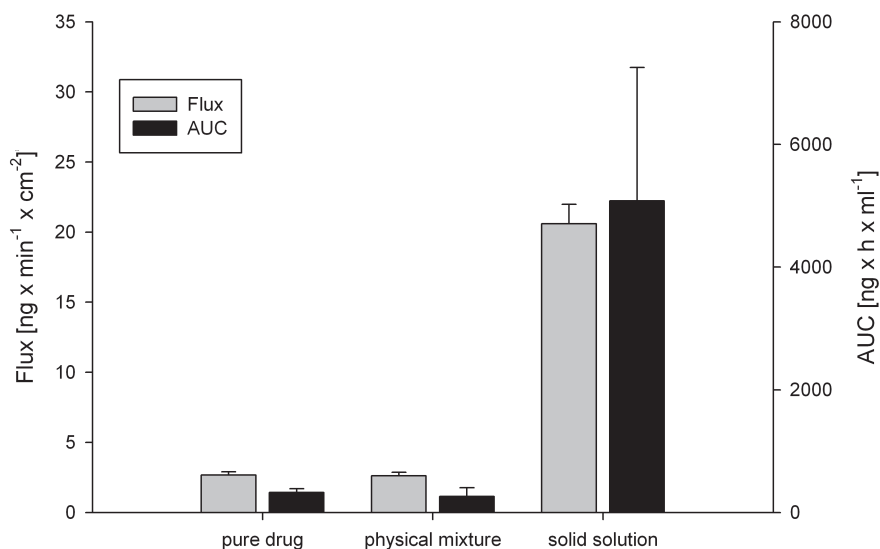


Figure 4.2.: Effect of Soluplus[®] on danazol flux across Caco-2 monolayers and on AUC in beagle dog animal study (n=3–6 for *in vitro* data, n=5 for *in vivo* data. Mean \pm SD)

With a drug flux of $99.33 \text{ ng} \times \text{min}^{-1} \times \text{cm}^{-2}$ the solid solution of fenofibrate showed the highest transport rate, followed by the physical mixture at $53.91 \text{ ng} \times \text{min}^{-1} \times \text{cm}^{-2}$ and the pure drug at $34.46 \text{ ng} \times \text{min}^{-1} \times \text{cm}^{-2}$ (Figure 4.3a).

In animal experiments increased absorption of the drug was detected when fenofibrate was formulated with Soluplus[®] (Figure 4.3b). Both formulations containing Soluplus[®] showed a strong increase in plasma AUC as well as in C_{max} values (Table 4.3). No significant difference was detected between the solid solution and the physical mixture of drug and excipient, both showing an AUC of about $60,000 \text{ ng} \times \text{h} \times \text{ml}^{-1}$, an almost 5-fold increase compared to the unformulated crystalline drug.

Comparing *in vitro* and *in vivo* results (Figure 4.4), drug flux was highest for the solid solution and the AUC of solid solution and physical mixture were on the same high level. The physical mixture therefore showed a stronger effect on drug absorption *in vivo* than *in vitro*.

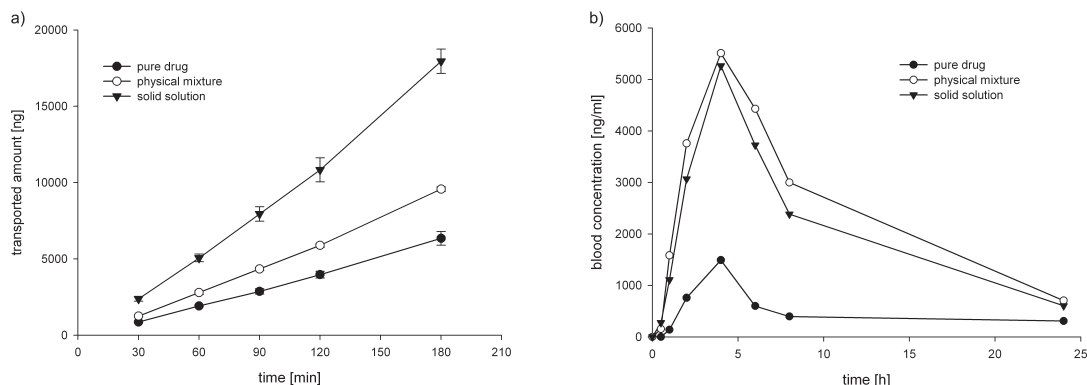


Figure 4.3.: a) Fenofibrate transport across Caco-2 monolayers. Transported amount expressed as fenofibric acid (n=3-6; mean \pm SD) b) Fenofibric acid in blood samples of *in vivo* study in beagle dogs (n=5; mean values)

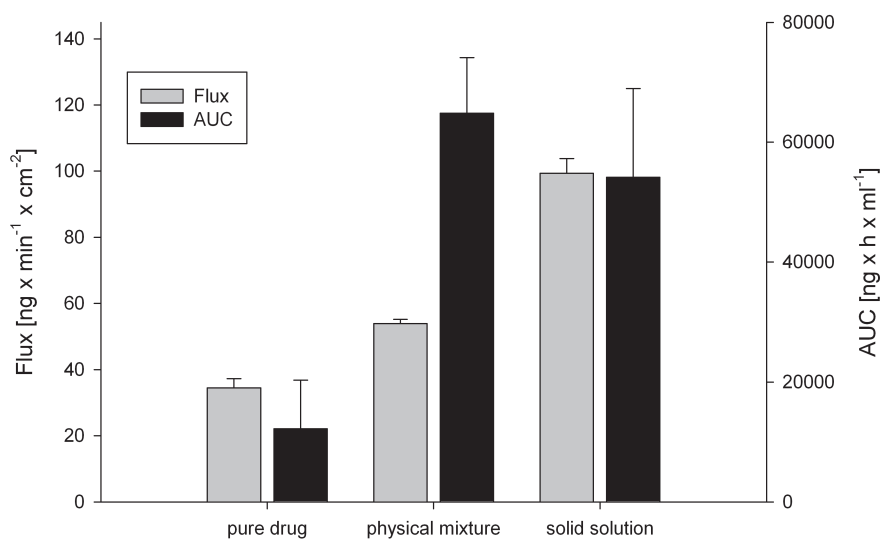


Figure 4.4.: Effect of Soluplus® on fenofibrate flux across Caco-2 monolayer and on AUC in animal study (n=3-6 for *in vitro* data, n=5 for *in vivo* data. Mean \pm SD)

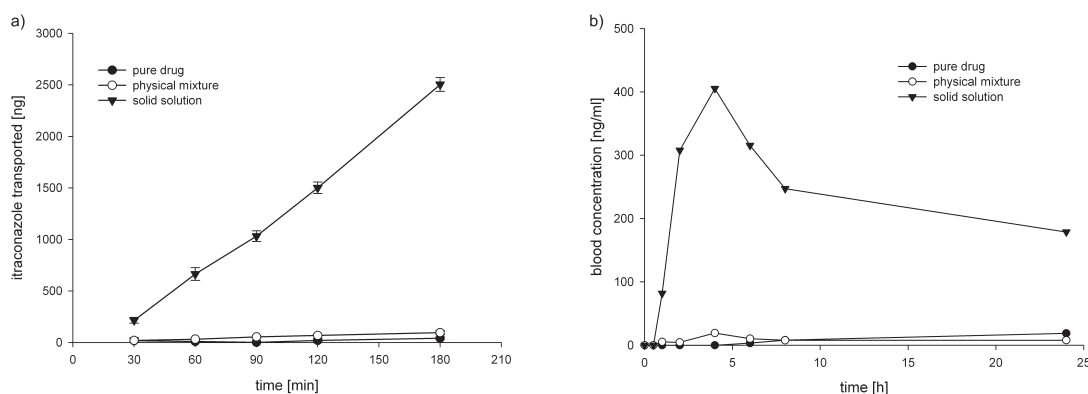


Figure 4.5.: a) Itraconazole transport across Caco-2 monolayers (n=3; mean \pm SD) b) Itraconazole bioavailability study in beagle dogs (n=5; mean values)

4.3.3. Itraconazole

Itraconazole is characterized by a very poor aqueous solubility below 0.1 $\mu\text{g/ml}$, resulting in a low donor concentration. Thus, from the pure crystalline substance and from the physical mixture only very low transport rates just at the analytic limits were detected (Figure 4.5a). For the pure drug the transported amount of itraconazole was below the limit of quantification, therefore no calculation of a flux value was possible. The physical mixture showed a flux of $0.458 \text{ ng} \times \text{min}^{-1} \times \text{cm}^{-2}$. In contrast, the solid solution of itraconazole in Soluplus[®] showed a high transport rate across Caco-2 cells, resulting in a drug flux of $14.51 \text{ ng} \times \text{min}^{-1} \times \text{cm}^{-2}$ an about 30 times increase compared to the physical mixture.

In vivo, the solid solution showed a plasma AUC of $2212 \text{ ng} \times \text{h} \times \text{ml}^{-1}$. For the physical mixture the AUC was $77 \text{ ng} \times \text{h} \times \text{ml}^{-1}$, while no AUC could be determined for the crystalline substance, since no or only low drug amounts reached the blood (Figure 4.5b & Figure 4.6). The more than 30-fold increase in AUC is in line with strong *in vitro* effect of the solid solution of itraconazole in Soluplus[®].

Drug	Formulation	AUC (<i>in vivo</i>) [ng × h × ml ⁻¹]	C _{max} (<i>in vivo</i>) [ng/ml]	T _{max} (<i>in vivo</i>) [h]	Rel. AUC	Flux (<i>in vitro</i>) [ng × min ⁻¹ × cm ⁻²]	Rel. Flux (<i>in vitro</i>)
Danazol	Crystalline	329 ± 58	37.6	2	1	2.67 ± 0.23	1
	Physical mixture	261 ± 143	20.6	4	0.8	2.63 ± 0.25	0.98
Fenofibrate	Solid solution	5081 ± 2174	1238.6	2	15.4	20.61 ± 1.37	7.7
	Crystalline	12201 ± 8080	1492.2	4	1	34.46 ± 2.76	1
	Physical mixture	64830 ± 9299	5509.0	4	5.3	53.91 ± 1.33	1.56
	Solid solution	54167 ± 14775	5262.0	4	4.4	99.33 ± 4.48	2.88
Itraconazole	Crystalline	-	-	-	-	-	-
	Physical mixture	77 ± 52	19	4	-	0.46 ± 0.01	-
	Solid solution	2212 ± 662	405	4	>29 (estimated)	14.51 ± 0.29	>30 (estimated)

Table 4.3.: Enhanced bioavailability and drug flux of Soluplus®/drug formulations (*in vivo* n=5; mean ± SD; *in vitro* n=3–6; mean ± SD)

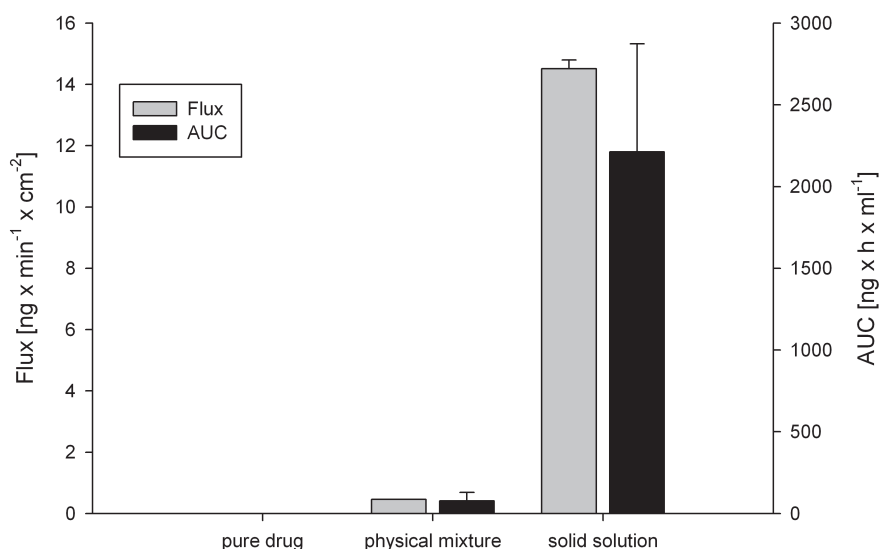


Figure 4.6.: Effect of Soluplus[®] on itraconazole flux across Caco-2 monolayer and on AUC in animal study ($n=3$ for *in vitro* data, $n=5$ for *in vivo* data; mean \pm SD)

4.3.4. Dialysis

Equilibrium dialysis experiments were conducted to evaluate drug interactions with Soluplus[®]. As indicated by donor/acceptor ratios > 1 (Table 4.4) danazol, fenofibrate and itraconazole were retained on the donor side of the dialysis system, i.e. the side to which Soluplus[®] was applied, indicating complex formation or binding of drug to Soluplus[®]. In contrast, for fenofibric acid, a donor/acceptor ratio nearby 1 was reached for 0.2 % TPGS as acceptor medium. This equal distribution to both sides of the system proves that no stable complex is formed with fenofibric acid. Mass balance of drug amounts on both sides of the dialysis system afforded recovery rates of nearby 100 % (data not shown). The donor/acceptor ratios were highest for itraconazole, followed by danazol and lowest for fenofibrate. An influence of the acceptor medium used was only detectable for fenofibrate and danazol which significantly increased when Vitamin E TPGS (0.2 % as used in the transport experiments) was replaced by 1 % bovine serum albumine (BSA) to solubilize the drug in the acceptor compartment. In case of fenofibric acid, the equilibrium shifted to the acceptor side when BSA was added, probably by a bigger binding strength

	donor/acceptor (KRB + 1 % BSA)	donor/acceptor (KRB + 0.2 % TPGS)
Danazol	9.88 ± 0.39	3.68 ± 0.34
Fenofibrate	4.91 ± 0.16	1.43 ± 0.17
Fenofibric acid	0.43 ± 0.01	1.01 ± 0.02
Itraconazole	16.35 ± 0.67	21.02 ± 5.9

Table 4.4.: Results from dialysis experiments of a physical mixture of 0.5 % Soluplus[®] and the respective drug. Data given as donor/acceptor ratio (n=5; mean ± SD)

of fenofibric acid to the protein than to Soluplus[®]. However, the order of the strength of binding remained the same for both acceptor media (itraconazole > danazol > fenofibrate > fenofibric acid).

4.4. Discussion

As shown in many studies, the Caco-2 monolayer model is an useful tool to predict drug permeation in the human intestine [66, 74, 102]. As such, the model has not only been used to investigate the permeability of pure drugs in solution, but also of more complex systems studying the effect of solubility enhancers and other excipients on drug transport rates or even studying novel formulations such as nanoparticles or solid solutions [109, 102]. In the present study we looked at the effect of Soluplus[®] on intestinal absorption of the poorly soluble, highly permeable BCS class II compounds itraconazole, fenofibrate and danazol. The novel excipient Soluplus[®] not only provides solubility enhancement by its amphiphilic structure but also offers the feasibility of forming solid solutions with poorly soluble drugs. Thus, both physical mixtures of drug and Soluplus[®] and solid solutions with respective drug/excipient ratios were investigated. As a validation of the *in vitro* experiments, the different formulations were also orally applied to beagle dogs for *in vivo* monitoring of drug bioavailability via plasma levels.

For all three drugs the highest permeation over the Caco-2 monolayer was, for fenofibrate besides the physical mixture, realized by the solid solution. For danazol and itraconazole no or only limited effectiveness of a physical mixture of drug and excipient on drug permeation was detected. Although the drug solubility was increased in presence of Soluplus[®]

(Table 4.1), drug permeation remained on a low level, comparable to the pure drug. The superior bioavailability from the solid solution and the poor effect of the physical mixture predicted in the Caco-2 model was confirmed in the *in vivo* experiments. In particular, the magnitude of absorption change correlated in both setups when drug flux was compared with AUC. The failure of Soluplus[®] as a mere solubility enhancer in the physical mixture suggests that the amorphous state of the drug in the solid solution plays a crucial role for drug dissolution and permeation. Supersaturated drug solutions are only realized from the solid solutions allowing for steeper concentration gradient and higher drug flux across the epithelial barrier. Tight junction integrity and epithelial barrier properties are not affected by Soluplus[®] as TEER values stayed constant throughout the course of the experiments (see Appendix B for additional data) and no increase in transport of paracellularly transported marker dye fluorescein sodium could be observed in control experiments (see Chapter 6 for fluorescein transport experiments). Furthermore, both danazol and itraconazole showed strong binding to Soluplus[®] in equilibrium dialysis experiments, indicating that increased solubility in the presence of Soluplus[®] is compensated by high affinity complex formation to the non-permeable excipient.

In contrast, for fenofibrate, Soluplus[®] in a physical mixture was as effective as the solid solution (in animal) and also significantly superior to the pure drug in increasing *in vitro* transport. Thus, for some drugs already a physical mixture could be an alternative for a solid solution, reducing production costs and avoiding stability issues as might be faced with heat-sensitive and polymorphous drugs. The mechanistic basis for the observed differences between danazol and itraconazole on one hand and fenofibrate on the other hand are not completely understood yet but might be connected to the low melting point of fenofibrate compared to the other tested drugs (Table 4.1, [110]). Chu and Yalkowsky introduced a melting point based absorption potential (MPbAP) which correlates the melting point to the absorbed fraction of BCS class II/IV drugs. Based on the MPbAP, a lower melting point leads to a higher absorption. Accordingly, fenofibrate shows higher *in vitro* and *in vivo* absorption than danazol and itraconazole, especially in case of the physical mixture.

A discrepancy exists between fenofibrate *in vitro* and *in vivo* data with regards to the physical mixture: in animal studies the physical mixture performed equal to the solid solution, while in the *in vitro* experiments the observed drug flux was in between the solid solution and the pure drug, the observed increase in drug permeation rate being about 2-fold lower than the *in vivo* impact. This may be attributed to *in vivo* interaction of the drug and/or Soluplus[®] with the intestinal fluids which contain bile salts and phospholipids leading to the formation of mixed micelles [111, 112]. The impact of dissolution and transport media composition for fenofibrate was previously confirmed by *in vitro* dissolution and permeation experiments using fasted or fed state simulated intestinal fluids (FaSSIF; FeSSIF). It was shown that dissolution and permeation rate is improved by these media [97]. Therefore, it is probable that for the physical mixture of fenofibrate, Soluplus[®] and the micelles present in the intestine show a synergistic effect on drug absorption *in vivo*. Although food effects are also reported for danazol and itraconazole [113, 114, 115], in our study no effect of the physical mixture was shown *in vitro* and *in vivo*. We suggest that danazol and itraconazole are already well solubilized by Soluplus[®] micelles and show strong binding to the excipient. Thus, the mixed micelles present *in vivo* do not have an additional effect. The differences in binding affinity between the three compounds are not yet mechanistically understood, although it seems that higher lipophilicity is associated with stronger binding to the excipient structures. Furthermore, the pH may play a role in the differences between *in vivo* and *in vitro* absorption. While cell culture experiments were performed at a constant pH of 7.4, *in vivo* the formulations occur a pH gradient which will especially affect the ionizable drugs itraconazole and fenofibric acid.

Additionally, it was shown that fenofibrate mainly appears as fenofibric acid on basolateral side. Samples drawn from the apical side of the Transwell system also show a significant amount of fenofibric acid. It is therefore probable, that solubilized fenofibrate is hydrolyzed by enzymes located on apical side of the Caco-2 cells and that mainly the metabolite fenofibric acid diffuses across the cell monolayer. As fenofibric acid is less lipophilic than fenofibrate and provides a much higher aqueous solubility, it provides a

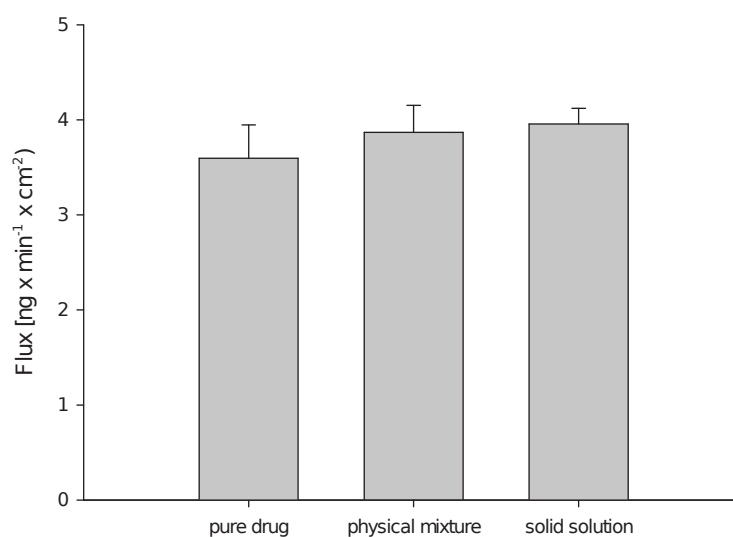


Figure 4.7.: Fenofibrate flux across Caco-2 monolayers at 4 °C. Results expressed as fenofibric acid (n=3; mean ± SD)

reduced binding to Soluplus[®] as proven by equilibrium dialysis (Table 4.4). Also the effectiveness of the physical mixture might be explained by that fact: an extensive supersaturation of the drug provided by a solid solution is not necessary, since the transport is controlled by the hydrolysis to fenofibric acid and its diffusion. Further experiments conducted at 4 °C (reduced enzyme activity) confirmed this hypothesis. The drug flux and also the amount of fenofibric acid on apical side were many fold lower under these conditions (Figure 4.7).

The same mechanism is as well suitable for the *in vivo* situation as the intestinal membrane also provides a high variety of hydrolyzing enzymes and the bioavailable form of fenofibrate detected in blood is also fenofibric acid [116].

For itraconazole, HP β CD was added in a concentration of 1 % (w/w) to the acceptor medium. Although Mellaerts et al. considered an addition of 0.2 % Vitamin E TPGS (as used for danazol and fenofibrate) with Caco-2 monolayers as equivalent to rat plasma as acceptor medium for itraconazole transport experiments [106], we changed the constitution of the acceptor medium as Vitamin E TPGS 1000 is known to inhibit the P-gp efflux

system [117, 30]. Since itraconazole is a substrate of P-gp, efflux inhibition would likely have altered drug transport in our experiments [118]. In contrast HP β CD, has no effect on P-gp efflux, drug permeability and monolayer integrity in Caco-2 transport experiments [119, 120]. However, an intrinsic P-gp inhibition afforded by Soluplus[®] cannot be excluded neither *in vivo* nor *in vitro* and may account for some of the observed increase in itraconazole absorption. Besides Vitamin E TPGS, P-gp inhibition was already reported for a number of non-ionic surface-active excipients such as Tween 80, Cremophor EL and several Pluronic block copolymers [121, 30]. A possible P-gp modulating effect of Soluplus[®] is still under investigation.

This study clearly proves the potential of Soluplus[®] to improve oral bioavailability. For danazol the observed bioavailability enhancement (15-fold increased AUC) was slightly lower compared to a 16-fold or 20-fold increased AUC (compared to the pure drug) in beagle dogs which was reached using nanoparticulate or cyclodextrin formulations, respectively [92]. However, these formulation approaches never reached the market. Also conventional hard capsules of crystalline danazol (Danacrine[®]) are mostly off-market as Gonadotropin-releasing hormone agonists offer a better benefit-to-risk profile for the treatment of endometriosis. In the case of fenofibrate, the marketed nanoparticulate formulation TriCor[®]/Lipidil[®] ONE enabled a 2.8-fold increased AUC (compared to bulk drug) in Wistar rats [97], while Soluplus[®] formulations showed an about 5-fold increased AUC compared to the pure drug in beagle dogs. However, inter-species differences might play an important role hereby and prohibit a direct comparison. Therefore, a side-by-side comparison may be included in further studies. For itraconazole, Yi et al. observed an AUC of $9,400 \pm 2.5 \text{ ng} \times \text{h} \times \text{ml}^{-1}$ after oral application of the commercialized itraconazole-HP β CD solution (Sporanox[®] oral solution) in a dose of 7.5 mg/kg to fasted beagle dogs [89]. Although this AUC is about 4-fold higher compared to the AUC of the Soluplus[®] solid solution, a future direct comparison under identical experimental conditions may further elucidate if the commercial product is really superior to the Soluplus[®] solid solution.

4.5. Conclusion

Soluplus[®] effectively enhanced the absorption of itraconazole, danazol and fenofibrate through the intestinal barrier if applied as solid solution. This could be shown in the Caco-2 *in vitro* system as well as in beagle dogs *in vivo*. For fenofibrate additionally the physical mixture of the test compound with Soluplus[®] was able to increase absorption and bioavailability *in vivo* and *in vitro*. The current work underlines the potential of the Caco-2 monolayer model as an excellent predictive tool for intestinal absorption behavior, not only for pure drugs but also for more complex drug-exipient formulations e.g. as solid solutions. As demonstrated for fenofibrate, we were able to distinguish *in vitro* between drugs for which the use of a solid solution is effective and drugs for which a physical mixture is sufficient to achieve a good oral bioavailability in accordance to *in vivo* tests in beagle dogs. However, for a better understanding of the absorption behavior *in vivo* and *in vitro*, further studies investigating the mechanism of drug liberation and transport in the presence of Soluplus[®] are needed.

5. Inhibition of P-glycoprotein and/or trypsin by Soluplus[®]

Parts of this chapter will be published as journal article :

Inhibition of P-glycoprotein by Soluplus[®] Michael Linn, Dejan Djuric, Karl Kolter, Claus-Michael Lehr, Eva-Maria Collnot

Pharmaceutical Research in submission

Abstract

Purpose. To investigate whether polyvinyl caprolactam-polyvinyl acetate-polyethylene glycol graft copolymer (Soluplus[®]), a novel solubility enhancer, inhibits the human efflux transporter P-glycoprotein (P-gp). Additionally, Soluplus[®] was tested for a possible inhibition of the digestive protease trypsin.

Methods. Inhibition of P-gp was investigated by two methods. First, bi-directional transport experiments across Caco-2 monolayers, grown on commercial Transwell filters, were performed. Rhodamine 123 (RHO) and digoxin (DIG) were used as P-gp substrates. Second, we investigated the uptake of the fluorescent P-gp substrates rhodamine 123 and LDS 751 into P-gp transfected MDCK II cells and compared with uptake into non-P-gp containing wild type cells. A possible trypsin inhibition was evaluated by investigating the cleavage of the marker substrate N- α -benzoyl arginine ethyl ester (BAEE) in Soluplus[®] solutions.

Results. For both tested substrates the basolateral to apical transport was strongly decreased by increasing Soluplus[®] concentrations. Apical to basolateral diffusion was also

reduced by the excipient, as a result of binding of the substrates to Soluplus[®], prohibiting the calculation of efflux ratios. Uptake experiments into MDCK II cells allowed the determination of net efflux of the unbound substrate fraction. In the presence of higher concentrations of Soluplus[®] an increased net uptake into MDCK-MDR1 cells was observed, further proving P-gp inhibition by Soluplus[®]. Only a slight inhibition of trypsin was found at a concentration of 10 % Soluplus[®].

Conclusions. It was shown that Soluplus[®] inhibits P-gp mediated efflux with an EC₅₀ around 3–7 mg/ml. In the design of novel Soluplus[®] containing formulations the likelihood of reaching these concentrations *in vivo* has to be considered. No interference of Soluplus[®] with the protease trypsin was found.

5.1. Introduction

P-glycoprotein (P-gp) is a 170 kDa transmembraneous protein of the large superfamily of ATP-binding cassette (ABC) transporters [13, 20]. As it plays an important role in multidrug resistance it is also known as multidrug resistance protein 1 (MDR1). P-gp is an active transporter which mediates the efflux of several drugs under consumption of ATP. Human P-gp is strongly expressed in all major epithelia such as kidney, liver, capillary endothelium and the intestinal epithelium [22]. It is responsible for the efflux of drugs at the blood-brain barrier and even more important: the intestinal barrier [23, 24]. Thus, P-gp is able to hinder the resorption of drugs, resulting in a reduced oral bioavailability [25]. Due to its broad substrate specificity, it transports drugs of diverse classes, such as several chemotherapeutics, antibiotics, antifungals, glucocorticoids, HIV-1 protease inhibitors and cardiac glycosides.

As a not much smaller group of xenobiotics is able to inhibit or induce human P-gp, this efflux transporter bears a high potential for drug-drug and also drug-excipient interactions [27, 28]. Well-described interactions are those of the cardiac glycoside digoxin with the drugs verapamil or ketoconazole and with the natural products of St. John's wort or grapefruit [123, 124, 125].

Besides drugs and natural products, excipients are potential inhibitors of human P-gp. MDR1 inhibition was shown for surfactants, natural and synthetic polymers [29, 30, 31]. Drug-excipient interactions do not only bear the risk of adverse side effect, but may also be desired to enhance bioavailability of P-gp substrates [126, 127, 128, 129]. In this context, the non-ionic surfactant Vitamin E TPGS was used in the formulation of the HIV-1 protease inhibitor and P-gp substrate amprenavir and commercialized as Agenerase® oral solution [32].

In the present study a possible P-gp inhibition by a novel solubility enhancer (Soluplus®) was investigated. Soluplus® (polyvinyl caprolactam-polyvinyl acetate-polyethylene glycol graft copolymer) is a surfactant and allows an effective solubility enhancement of poorly aqueous soluble drugs, both by its surface active properties and by its ability to form solid solutions (see Chapter 4). Thereby, it was shown that Soluplus® increases the oral bioavailability of lipophilic drugs, such as itraconazole or fenofibrate (see Chapter 4; [84]). As many poorly soluble drugs are at the same time P-gp substrates, an inhibition of this transporter by Soluplus® may also affect drug resorption through the intestinal barrier. To determine a possible interaction of this novel excipient with MDR1, two cell culture models were used. First transport of the two P-gp model substrates rhodamine 123 (RHO) and digoxin (DIG) was measured in the well-characterized Caco-2 cell line, a widely used model of the intestinal barrier [65, 130]. As Caco-2 cells extensively express P-gp, this model is accepted for the investigation of active efflux across the cell monolayer by bi-directional transport experiments [131, 132]. Secondly, Madin Darby canine kidney (MDCK II) cells were used. While the wild type hardly expresses P-gp, it is possible to transfect this cell line with MDR1 [133, 134, 135]. Therefore, it is possible to assess the passive permeability of a drug in the parent cells in the absence or presence of Soluplus® and then determine active P-gp mediated efflux as the difference in drug uptake between wild type and transfected cells.

Another active protein that might reduce the bioavailability of orally applied drugs is the serine protease trypsin. Trypsin is produced in the pancreas and secreted into the duode-

num. It is active there and hydrolyzes peptides into amino acids. Therefore, trypsin is one main barrier for the oral application of peptide drugs, such as insulin [136, 137]. Several compounds were shown to have trypsin inhibiting activity, such as Bowman-Birk inhibitor [138, 139], soybean ingredients or flavonoids [140]. Some excipients were also shown to inhibit trypsin, e.g. poly(acrylate) derivatives [141]. Therefore, the novel solubilizing excipient Soluplus® was tested if it can act as potential trypsin inhibitor and if it hence may be applied for peptide drug delivery.

5.2. Materials and Methods

5.2.1. Chemicals

Soluplus® was provided by BASF SE (Ludwigshafen, Germany). Fetal bovine serum was from PAN-Biotech GmbH (Aidenbach, Germany). Dulbecco's modified Eagle's medium and non-essential amino acids were from PAA Laboratories GmbH (Pasching, Austria). Permeable filter inserts of type Transwell 3460 were supplied by Corning Incorporated Life Science (Lowell MA, USA). ³[H]-Digoxin (40 Ci/mmol) and Ultima Gold scintillation fluid were obtained from Perkin Elmer (Rodgau, Germany). Bovine serum albumin, digoxin, rhodamine 123, LDS751, Hoechst 33342 and all other chemicals were purchased from Sigma-Aldrich (St. Louis, MO, USA).

5.2.2. Cell culture

Caco-2 cells of clone C2BBE1 from American Type Culture Collection (Manassas, CA, USA) were grown under conditions at 37 °C in an atmosphere of 5 % CO₂ and 80 % relative humidity. Dulbecco's modified Eagle's medium supplemented with 10 % fetal bovine serum and 1 % non-essential amino acids was used as cell culture medium. Medium was changed every 2–3 days. Cells were passaged every week at a confluency of approx. 90 %. For transport experiments, cells of passage 64–77 were seeded at a density of 66,000 cells/cm² on Transwell filter inserts (0.4 µm pore size, 1.12 cm²). After 21 days in culture, cells

were used for transport experiments if the transepithelial electrical resistance (TEER) was above $500 \Omega \times \text{cm}^2$.

P-gp expressing MDCK II cells (MDCK-MDR1) and the respective maternal wild type cell line (MDCK-wt) were kindly provided by Prof. Schinkel (Netherlands Cancer Institute, Amsterdam, Netherlands). Both cell lines were cultured as described above for Caco-2 cells. The cell culture medium consisted of DMEM + 10 % FBS without addition of non-essential amino acids. For uptake experiments cells were seeded at a density of 20,000 cells per well in 96-well cell culture plates and grown to confluency for 7 days. Cells were used 4–7 passages after receiving from Prof. Schinkel.

5.2.3. Bi-directional transport experiments

Krebs Ringer buffer (KRB) was used as assay buffer. KRB contains 114.2 mM NaCl, 3.0 mM KCl, 4.0 mM d-glucose, 1.4 mM CaCl_2 , 2.6 mM MgCl_2 , and 10.0 mM HEPES. By addition of NaOH the buffer was adjusted to a final pH of 7.4. For digoxin transport studies additionally 1 % BSA was added to avoid adhesion to plastic material.

In this assay the transport of the P-gp substrates RHO and DIG across the Caco-2 monolayer was investigated in both possible directions: apical to basolateral (AB) transport and basolateral to apical (BA) transport. After washing twice with prewarmed KRB, the monolayers were pre-incubated under cell culture conditions for 1.0 h with prewarmed assay buffer with or without Soluplus® in the respective concentration to be tested. Buffer containing Soluplus® was only applied on apical side. As positive control a solution of Cyclosporine A (10 μM) was used and as well applied on the apical side of the system. After pre-incubation, solutions of 10 μM RHO or 1 μM DIG (spiked by 0.1 nM ^3H -DIG) in KRB were applied on the respective donor side. The system was agitated at 100 ± 20 rpm throughout the experiment on an orbital shaker in a cell culture incubator. At regular timepoints up to 240 minutes samples of 100 μl (RHO) or 200 μl (DIG) were drawn at regular timepoints from the receiver compartment and the volume lost by sampling was replaced with fresh pre-warmed buffer.

RHO was quantified by measuring the fluorescence at an excitation wavelength of 485 nm with an emission wavelength of 530 nm, using a 96well plate reader (Tecan infinite 200, Tecan Group Ltd, Männedorf, Switzerland). To avoid bias by signal quenching separate calibration curves were used for each tested Soluplus® concentration.

Samples of DIG were diluted by 2.0 ml of scintillation fluid and afterwards radioactivity was measured by liquid scintillation counting in a TriCarb 2100TR analyzer (Packard Bio-Science, Meriden, CT, USA).

The apparent permeability was calculated by the formula:

$$P_{app} = \frac{dc}{dt} \times \frac{1}{c_0} \times \frac{1}{A} \quad (5.1)$$

whereas dc/dt indicates the slope of the linear permeation curve, c_0 indicates the initial substrate concentration and A the area of the cell monolayer.

5.2.4. Dialysis

To investigate the binding of the model substrate RHO to Soluplus® equilibrium dialysis was performed using a DIANORM® apparatus (identical to DIALYZER by Harvard Apparatus, Holliston, MA, USA). The donor chambers of the system were filled with 2 ml of a solution of 10 μ M RHO and Soluplus® in KRB. The acceptor sides were filled with an equal volume of pure KRB. A cellulose membrane (Harvard Apparatus, Holliston, MA, USA) with a molecular cutoff of 10 kDa separated the two chambers. After one hour dialysis at a rotation speed of 20rpm, the chambers were emptied and RHO was quantified by fluorometric measurements as described above. Additionally, the experiment was performed with an inversed setup. Therefore, Soluplus® solutions functioned as acceptor media and a 10 μ M RHO solution in KRB without Soluplus® acted as donor. As indicator for drug binding the ratio of RHO between donor and acceptor was calculated (D/A ratio).

5.2.5. MDCK II uptake assay

For uptake experiments MDCK II cells, of wild type or transfected with MDR1 respectively, were washed twice with pre-warmed KRB. Afterwards 200 μl of a substrate solution (RHO: 25 μM , LDS751: 50 μM) with or without Soluplus® in KRB was added to each well and cells were maintained at 37 °C in an incubator. Cells were agitated at a speed of 100 ± 20 rpm on an orbital shaker. After two hours incubation time cells were washed three times with ice-cold KRB to stop active transport. Afterwards cells were lysed by a 200 μl of a solution of 1 % Triton X in KRB and total fluorescence in the lysate was measured. RHO was quantified as discussed above while LDS 751 was excited at 543 nm and measured at 712 nm, the detection wavelength for LDS 751 bound to cellular DNA.

The amount of substrate that was pumped out of the cells by P-gp was calculated by the formula:

$$Amount_{effluxed} = n_{WT} - n_{MDR1} \quad (5.2)$$

where n_{WT} indicates the quantity of substrate taken up in wild type cells, whereas n_{MDR1} represents the respective amount in MDR1 transfected cells.

5.2.6. Trypsin inhibition assay

For evaluating the effect of Soluplus®, the cleavage of the marker substrate N- α -benzoyl-L-arginine ethyl ester (BAEE) to N- α -benzoyl-L-arginine (BA) was studied (Figure 5.1). As buffer for this assay served a solution of 50 mM MES/KOH pH 6.7, supplied with 250 mM mannitol (assay buffer). A solution 1.5 mM BAEE \pm Soluplus® was incubated with 30 IU trypsin at 37 °C for 40 min. After the incubation time hydrolysis was stopped by the addition of 1 M hydrochloric acid. As positive control a solution of soybean trypsin inhibitor in assay buffer was used.

The amount of BA was analyzed by HPLC, injecting a sample volume of 20 μl on a reversed phase column [LiChroCART 125-4 LiChrospher 100 RP18 (5 μM) by Merck KGaA (Darmstadt, Germany)]. As mobile phase a mixture of 86 % 10 mM ammonium acetate pH 4.2

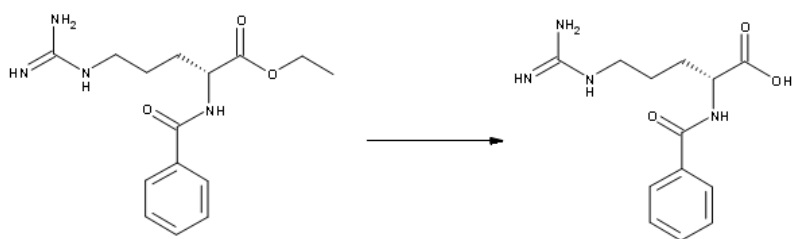


Figure 5.1.: Trypsin hydrolyzes N- α -benzoyl-L-arginine ethyl ester (BAEE) to N- α -benzoyl-L-arginine (BA)

and 14 % methanol was used. BA was detected absorptiometric at a detection wavelength of 253 nm. The detected amount of formed BA was related to the amount found for the negative control (assay buffer).

5.3. Results

5.3.1. Caco-2 transport assay

To examine, whether P-gp is inhibited by Soluplus[®] the transport of the P-gp substrates RHO and DIG across Caco-2 monolayers was determined. To allow for comparison between different experiment with slight variations in P-gp expression and thus transport rates data for apparent permeability (P_{app} values) was normalized to the respective control (KRB w/o inhibitor).

Application of Soluplus[®] on apical side lead to a reduced secretory transport of RHO from basolateral to apical side (Figure 5.2 A). P-gp mediated basolateral to apical transport was reduced to 54.3 ± 3.6 % by an excipient concentration of 25 mg/ml. As shown in Figure 5.3 A, basolateral to apical transport was also reduced in a concentration dependent manner with an onset at a Soluplus[®] concentration of 1 mg/ml. An EC_{50} value of 3.14 ± 1.13 mg/ml was calculated by a four parameter logistic fit of the curve. The positive control using 10 μ M CysA as a potent P-gp inhibitor reduced BA transport even further to a level of 31.9 % compared to control.

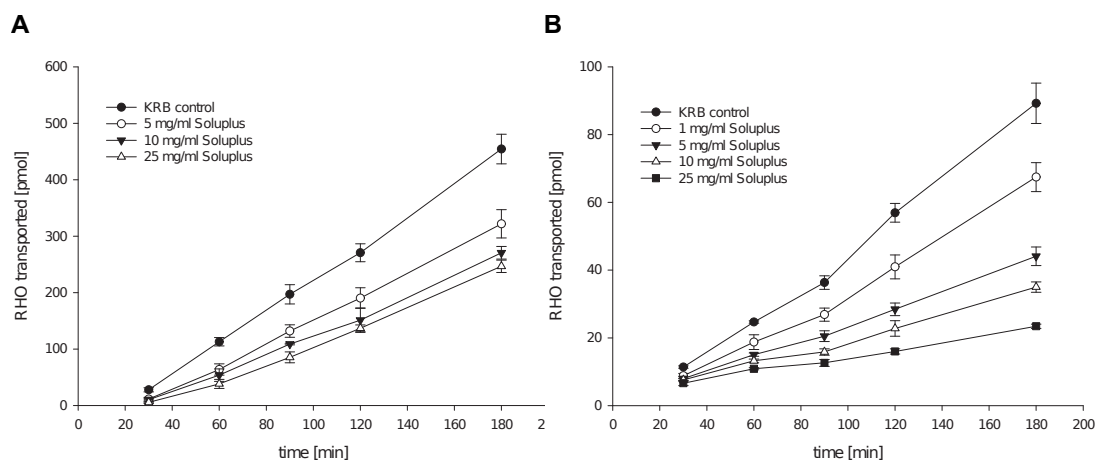


Figure 5.2.: Rhodamine 123 transport across Caco-2 monolayers. A: Active basolateral to apical transport. B: Passive apical to basolateral transport (n=3; mean \pm SD)

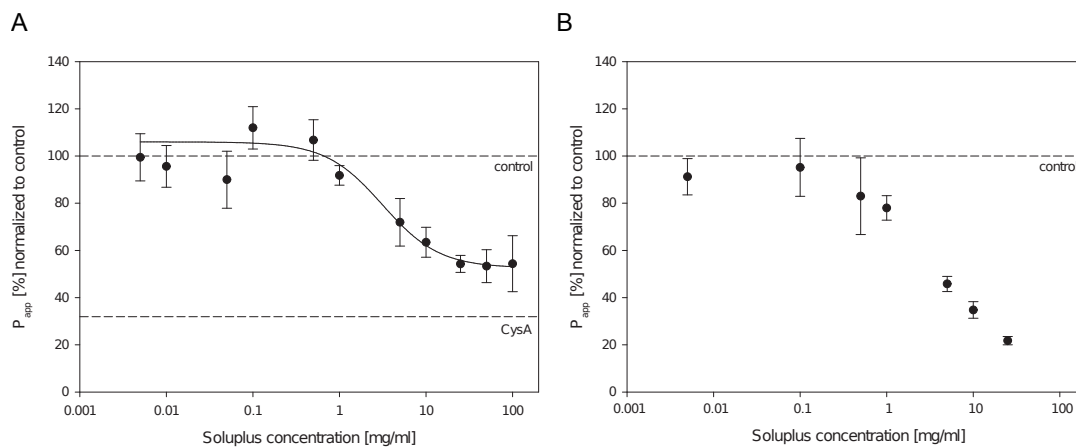


Figure 5.3.: RHO transport across Caco-2 cells. P_{app} values normalized to the respective control. A: Basolateral to apical. Fitted curve: $R^2=0.9105$. B: Apical to basolateral transport. (n=3-9; mean \pm SD)

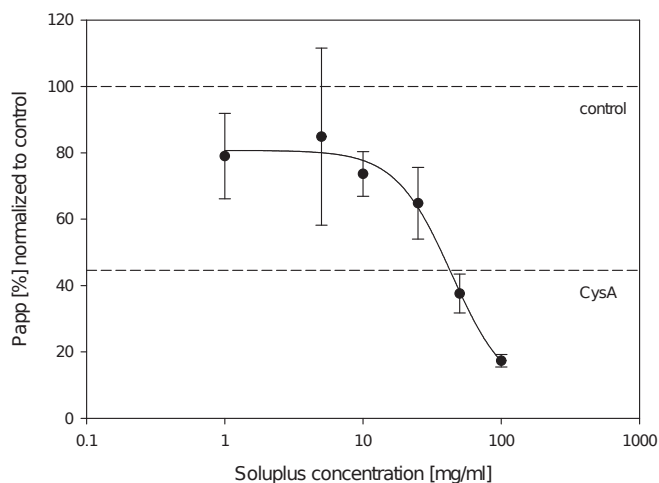


Figure 5.4.: Digoxin transport across Caco-2 cells. P_{app} values for active basolateral to apical transport are normalized to the respective control. Fitted curve: $R^2=0.9871$. (n=3-9; mean \pm SD)

RHO transport from apical to basolateral side also showed a concentration dependent decrease by apical application of Soluplus[®] (Figure 5.2 B). At a concentration of 25 mg/ml, apparent permeability of RHO was reduced to 48.3 ± 8.3 % of the control (Figure 5.3 B). In contrast, by application of CysA to the apical side, AB transport was increased to 175 % of the control.

As both AB and BA transport of RHO were reduced in the presence of Soluplus[®], efflux ratio remained mainly unchanged at all tested concentrations, while CysA control showed an efflux ratio of 1.42. As in this experiment Soluplus[®] and the substrate were applied in the same compartment, an interaction of Soluplus[®] and RHO can be assumed. If no interaction takes place, an increased AB transport would be expected for P-gp inhibitors.

Transport of DIG showed similar behavior. By increasing Soluplus[®] concentration, the apparent permeability of active basolateral to apical transport was reduced (Figure 5.4). By an excipient concentration of 100 mg/ml the permeability was reduced to 17.3 ± 1.9 % of the inhibitor-free control. As for RHO, the reduction in DIG permeability was concentration dependent, however, EC_{50} value calculated was shifted to higher Soluplus[®] con-

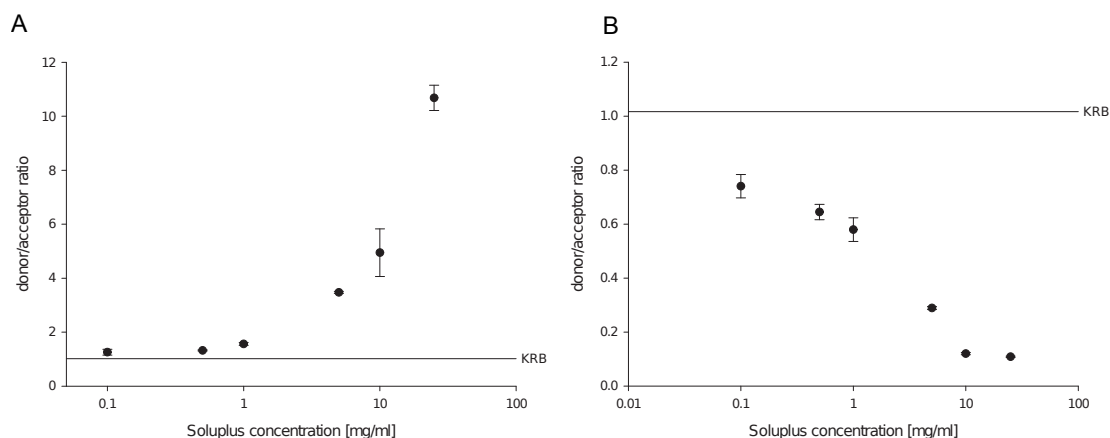


Figure 5.5.: Equilibrium dialysis of Soluplus[®]/RHO formulations. A: "Standard" setup, Soluplus[®] and RHO on donor side. B: "Inversed" setup, Soluplus[®] applied to acceptor side (n=5; mean \pm SD)

centrations ($EC_{50} = 43.68 \pm 11.96$ mg/ml).

5.3.2. Dialysis

Equilibrium dialysis was performed to investigate a possible binding of Soluplus[®] to RHO, thereby explaining the reduced A to B transport in Caco-2 experiments. Indeed, if RHO and Soluplus[®] were applied in the same compartment, RHO was retained from diffusion to the acceptor compartment. As shown in Figure 5.5 A, increasing Soluplus[®] concentrations lead to higher donor/acceptor ratios. At an excipient concentration of 25 mg/ml, the concentration of RHO in the donor compartment was 10.7-fold higher than in the acceptor compartment. As the control without Soluplus[®] showed a ratio of about 1, it was proven that equilibrium was reached after the used dialysis time.

Dialysis with an inversed setup showed that Soluplus[®], if applied on acceptor side, pulled RHO to this side. This pull-effect additionally affirms the binding of RHO to Soluplus[®] with a donor/acceptor ratio of 0.11 at 25 mg/ml Soluplus[®] (Figure 5.5 B).

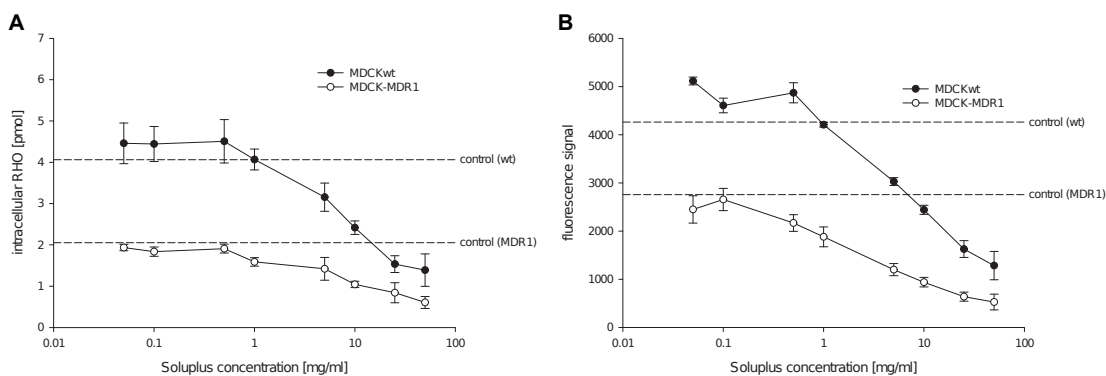


Figure 5.6.: Soluplus[®] concentration dependent uptake of RHO (A) and LDS 751 (B) into MDCK-wt and MDCK-MDR1 cells.(n=5–6; mean \pm SD)

5.3.3. Uptake into MDCK II cells

The uptake of RHO and LDS751 into MDR1-transfected and wild type MDCK II cells was tested. As shown in Figure 5.6, both P-gp substrates showed a Soluplus[®] concentration dependent decreased uptake into both cell lines. For both tested substrates the uptake into wild type cells was significantly higher compared to MDR1 transfected cells, as expected by P-gp efflux activity.

To determine the P-gp activity, the effluxed amount (Equation 5.2) was calculated as the difference between amount absorbed into wild type cells and transfectants. Hence, any possible reduction in free drug concentration in the presence of Soluplus[®] due to binding to the excipient was taken into account. For both RHO and LDS 751 the net effluxed amount was decreased by increasing Soluplus[®] concentration (Figure 5.7). For Soluplus[®] concentrations between 0.01 and 1 mg/ml (RHO) or 0.01 and 5 mg/ml (LDS751) an increased efflux was observed. Positive control experiments using 20 μ M CysA as inhibitor demonstrated a 3-fold (RHO) and 1.5-fold (LDS751) increased uptake of RHO/LDS751 into the wild type cells. In MDCK II-MDR1 cells the uptake was increased by 8.6-fold and 2.3-fold for RHO and LDS 751 in the positive control, respectively.

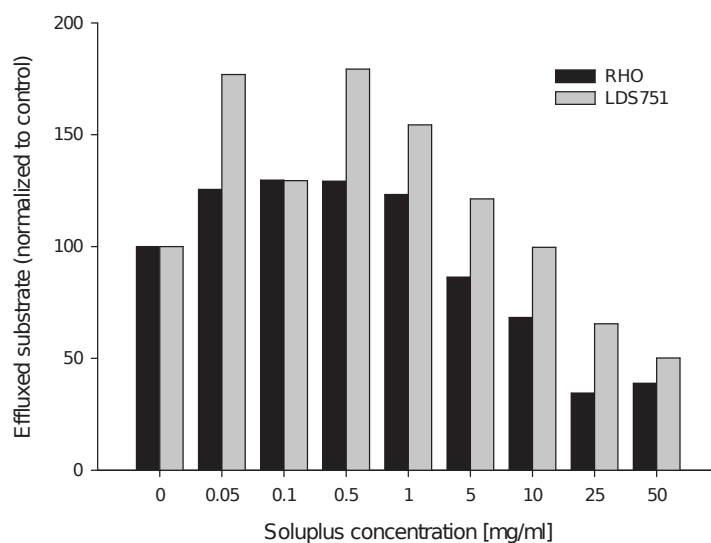


Figure 5.7.: Effluxed amount of P-gp substrates RHO and LDS 751 from MDCK II cells, normalized to the respective control (n=5–6; mean values).

5.3.4. Trypsin inhibition

As shown in Figure 5.8, only a very slight inhibition of trypsin by Soluplus® could be detected. A slight concentration dependent decrease of the metabolized amount of BAEE was found. However, at a Soluplus® concentration of 10 % still 87.8 % of the control value for BA could be found. For lower concentrations, a trypsin activity of more than 90 % was detected. Therefore, it can be assumed that Soluplus® affects trypsin only on a low level.

5.4. Discussion

In recent years, it was shown that many polymeric pharmaceutical excipients inhibit human P-gp. The interaction of an excipient with human efflux transporters bears risks of drug-formulation interactions but at the same time offers chances to enhance bioavailability of substrates in a local and controlled manner. Therefore, it is evident that a novel compound, such as Soluplus®, should be evaluated for a possible P-gp inhibition. In this work, it was shown that the novel solubilizer Soluplus®, in high concentrations, inhibits

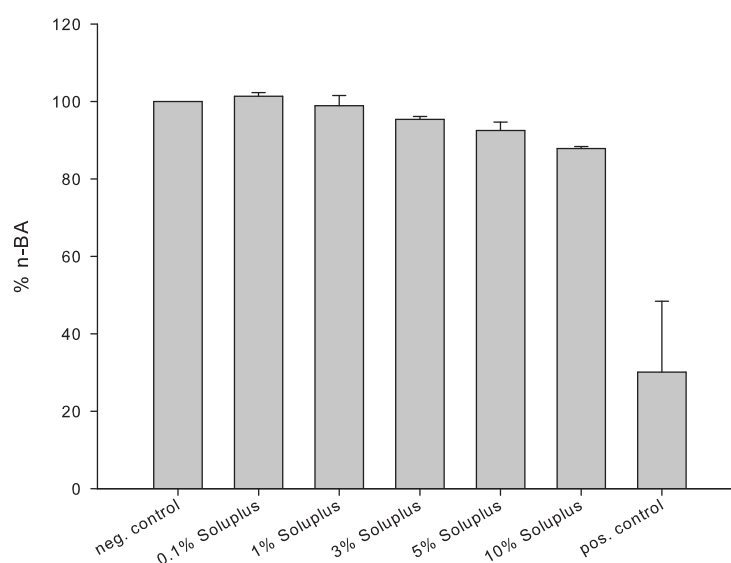


Figure 5.8.: Formation of N- α -benzoyl-L-arginine under the influence of Soluplus®. Only slight trypsin inhibition can be detected (n=3-5; mean \pm SD)

human P-glycoprotein:

Bi-directional transport experiments across Caco-2 cells showed a decreased P_{app} by increasing Soluplus® concentrations in both transport directions (AB and BA) for two different P-gp model substrates, RHO and DIG. Many studies regarding P-gp inhibition in the Caco-2 model are using the efflux ratio, calculated by the formula

$$Effluxratio(ER) = \frac{P_{app}(BA)}{P_{app}(AB)} \quad (5.3)$$

, as measure for P-gp activity [142, 143]. When calculating efflux ratios for both substances in our study no significant change in dependence of Soluplus® concentration is observed. One might therefore conclude that there is no modulation of P-gp activity afforded by Soluplus®. However, using the efflux ratio to assess P-gp inhibition might be often misleading, e.g. for substrates with a high passive permeability [144, 145, 146] or if the AB transport is too low for reliable calculations [147]. In our experiment to distinct phenomena account for the respective reduction in transport. For apical to basolateral transport the observed

reduction is associated to a binding of the model drug to the polymeric excipient, as both compounds are placed in the same compartment for this experimental setup. Such a binding of moderately to highly lipophilic compounds was previously observed for BCS class II drugs itraconazole, danazol and fenofibrate (see Chapter 4 & 6). For RHO, we could show the binding to Soluplus® in equilibrium dialysis experiments: Donor/acceptor ratios up to 10.7 were observed at the concentrations used in the transport studies. The entrapment in the drug-excipient complex limits the free drug amount available for diffusion and reduces the flux across the monolayer. A similar effect was recognized by Zuo et al. (2000) in the case of hydroxypropyl- β -cyclodextrin, which forms highly stable complexes with flutamide, hindering its diffusion across Caco-2 cells in higher concentrations [122]. In contrast, if placed in the opposite compartment to RHO, Soluplus® exhibits a pull effect in equilibrium dialysis studies. Thus, a higher drug flux across the monolayer would be expected in the presence of Soluplus® on the apical side, if RHO or DIG transport was only mediated by passive diffusion. Instead, the opposite effect is observed and the reduction of BA transport may therefore be associated to P-gp efflux inhibition.

To test this hypothesis, uptake experiments were conducted in MDCK II cells, comparing accumulation in the cells in wild type cells with low inherent efflux activity and in transfectants overexpressing human P-gp. This setup allows the calculation of net efflux mediated by P-gp, as both cell lines should have similar passive permeability for the model substrates and thus hindering effect of Soluplus®-drug complex formation can be accounted for by subtracting this amount of drug diffused. It has to be noted, that the incubation of MDCK wild type cells with CysA as positive control also increased the fluorescent model compounds uptake. Therefore, a certain efflux activity can be assumed for the wild type cells, likely due to canine efflux transporters with overlapping substrate specificity to human P-gp. The incubation of wild type MDCK II cells with Soluplus® also resulted in an increased uptake into these cells at low Soluplus® concentrations. Thus, an elevated efflux was calculated for these Soluplus® levels. However, at high Soluplus® concentrations the inhibition of human P-gp in MDCK II-MDR1 cells becomes evident.

An EC₅₀ value of 6.91 ± 2.2 mg/ml was calculated for RHO which is in the same order as calculated for RHO efflux inhibition in Caco-2 BA transport experiments (3.15 mg/ml). For digoxin, the inhibition curve is shifted to higher concentrations resulting in a 13.8-fold increased EC₅₀ value. A possible reason for this difference might be an induction of MDR1 in Caco-2 cells during the incubation time by the used substrate [148, 149] or the presence of distinct binding sites for different P-gp substrates with distinct inhibition kinetics [150, 151]. Another reason might be the efflux pathway of RHO which requires a saturable influx through the basolateral membrane to be effluxed by P-gp [152]. Furthermore, multidrug related protein 2 (MRP2), which is also present in Caco-2 cells, is known to efflux RHO and DIG [153, 154, 155]. Therefore, an interaction of Soluplus® with MRP2, might play a role in the observed differences between the two substrates.

In conclusion, for both test systems a reduced MDR1 activity in the presence of higher concentrations of Soluplus® was shown. However, an exact calculation of an EC₅₀ value was not possible, due to differences in the test systems and between the used substrates. Also an extension of the study to even higher Soluplus® concentrations to establish a better fit of the inhibition curve for digoxin was not possible, as Soluplus® solubility is limited to 100 mg/ml.

In comparison to other P-gp modulating excipients, the potency of Soluplus® is moderate. EC₅₀ values for Vitamin E TPGS, Pluronic F68 or Pluronic P85 were found to be one to two orders of magnitude lower compared to Soluplus® [31, 156]. It is questionable, if the necessary inhibitory concentrations observed in this study would be reached in the human intestine with actual Soluplus® containing formulations. Assuming an EC₅₀ value of 3.15 mg/ml (RHO, Caco-2), the corresponding dose, orally applied with 250 ml water, would be 787.5 mg. This amount of a single excipient is not likely to be formulated in a single oral dose as drug and co-excipients would be present even in the preparation of solid solution based pellet formulations. However, as this dose might be reached by concomitant application of more than one tablet, a potential for drug-excipient interactions can't be completely disregarded. Even though, the excipient is not only distributed to the

ingested volume, but also to liquids secreted into the human intestine. Taken into account that totally about 6 litres of fluids are secreted per day, the dose needed for an effect on human P-gp would be many fold higher [4].

An inhibition of the protease trypsin was only found for very high Soluplus® concentrations. A concentration of 10 % or more Soluplus® is usually not likely to be reached *in vivo*. Therefore, Soluplus® is probably no possible candidate for enhancing the oral bioavailability of peptide drugs. However, by these results also adverse side effects of trypsin inhibitors, such as a disturbed digestion of nutritive proteins or an increased protease secretion as feed-back regulation can be excluded [157, 137].

5.5. Conclusion

The novel solubility enhancer Soluplus® was tested for its inhibitory potential on human P-glycoprotein and trypsin. Our studies clearly prove an effect of the excipient on P-gp by increasing concentrations. As Soluplus® binds to the used substrates, an assessment of P-gp activity by regarding absorptive (AB) transport or calculating an efflux ratio for the bi-directional transport was not possible. However, the binding did not affect basolateral to apical transport which was reduced solely due to P-gp inhibition. Testing in the MDCK II model also allowed calculation of net efflux and determination of dose response curves for P-gp modulation by Soluplus®.

Since calculation of EC₅₀ values was dependent on the used system and on the used substrate, the effect of Soluplus® on a specific substrate can only roughly be predicted. Thus, a possible interaction should be assessed in the development of formulations of P-gp substrates with this excipient.

The mechanism of inhibition of P-glycoprotein by Soluplus® remains unclear. Among others, membrane fluidization, ATPase inhibition or down regulation of the MDR1 gene are possible causes for P-gp inhibition by excipients and might be addressed in further investigations.

No significant effect on the protease trypsin could be determined. However, investigations

on a possible peptidase inhibition may be expanded to α -chymotrypsin or carboxypeptidases in further studies.

6. Optimization of Soluplus[®] formulations

- Drug binding to Soluplus[®] and its effect on *in vitro* performance of Soluplus[®]

Parts of this chapter are planned for a future publication as journal article.

Abstract

The applicability of Caco-2 monolayers as predictive tool for the *in vivo* absorption of Soluplus[®] formulated drugs was previously demonstrated (see Chapter 4). Therefore, Caco-2 transport experiments were used for an optimization of Soluplus[®]/drug formulations. As shown by dialysis experiments, drugs may be entrapped in Soluplus[®] micelles and hence hindered in their transport across the cells. For further investigation of this phenomenon, the influence of changes in the Soluplus[®]/drug ratio on the transport across Caco-2 cells was tested. Besides binding between drug and excipient, also the solubilization capacity of Soluplus[®] plays an important role for this optimization. By increasing the drug concentration in an extrudate, the drug will appear not only in amorphous state but also crystalline. Also the concentration of Soluplus[®] after dissolution is reduced in such high drug loaded extrudates which may lead to a diminished solubilization of the drug.

Caco-2 transport experiments showed an optimal excipient/drug ratio for the drug flux of the tested drugs danazol, itraconazole and fenofibrate. The more or less sharp optimum is dependent on the respective drug and was found between ratios of 0.01–0.5 [n/n]. For higher ratios the transport was decreased, probably due to binding of drug and excipient. The decreased transport for ratios below the optimum may be explained by two factors: a) slower dissolution of the partially crystalline extrudates and b) reduced solubilization due to the reduced Soluplus[®] concentration.

6.1. Introduction

Poorly soluble APIs are today one of the most important challenges for pharmaceutical technology. Especially in solid oral dosage forms, their characteristically poor dissolution rate in the gastro-intestinal fluids hinders these drugs from absorption through the intestinal mucosa. According to the equation of Noyes-Whitney (Equation 3.1), a lower particle size results in a higher dissolution rate. This leads to the development of formulations with reduced particle sizes, such as micronized powders or nanoparticles. Also novel formulation techniques as spray drying, cogrinding or the use of supercritical fluids for micronization were used. The maximal reduction of particle size is reached if the drug is molecularly dispersed. Molecular dispersion of a drug may be reached by embedding the API in small polymer particles or by adsorption to small (porous) particles. The main drawback of this formulation approaches is their typically low yield. Accordingly these methods are challenging to scale-up and therefore also time and cost intense.

Another approach to molecularly dispersed solid forms is the production of solid solutions. In a solid solution, the API is molecularly dispersed and entrapped in a polymer matrix. This design leads to increased dissolution rates, as the particle size is reduced to the minimum. Solid solutions are stable upon crystallization if the drug shows a sufficient solubility in the polymer (see Chapter 3.3). If the concentration of the drug in a solid solution is exceeded, a glass suspension is formed (see Table 3.5). While a biphasic amorphous system still may show superior dissolution rates, a crystalline drug in a solid dispersion is

similar to a physical mixture of crystalline drug and the respective polymer. Such a biphasic amorphous solid solution is kinetically unstable and is vulnerable to crystallization by storage, milling or other process steps.

In the present study, the absorption behavior of Soluplus[®] formulations was investigated by use of the Caco-2 cell culture model. Transport experiments across Caco-2 monolayers are a widely accepted tool to estimate intestinal drug absorption (see also Chapter 3.5). As described above, the Caco-2 model is applicable to formulations with the novel excipient Soluplus[®] and allows good predictions of their *in vivo* absorption behavior (see Chapter 4).

Previously, a many fold increase of drug absorption *in vivo* and *in vitro* was proven if these drugs were applied as solid solution with Soluplus[®]. Furthermore, it was shown that these drugs bind to the excipient which may lead to a reduced absorption. Therefore, a decrease or increase of the Soluplus[®] concentration in a solid solution may lead to increased or decreased binding and consequently to an altered drug absorption.

In this study the effect of changes in the ratio between drug and excipient was investigated. Starting from solid solutions containing 15 % (danazol/itraconazole) or 20 % (fenofibrate), which were used for animal experiments, the drug part was adjusted to values between 0.5–70 %. For lower drug parts (higher Soluplus[®]/drug ratio) this was realized by addition of Soluplus[®] to the respective solid solution. For higher drug parts (lower ratio) hot melt extrudates were produced. As described above, the molecular dispersity of the API is not guaranteed in such high loaded extrudates.

The interplay between binding, crystallization and solubilization leads to an optimal Soluplus[®]/drug ratio for each API. It was shown that increased ratios cause decreased drug fluxes as result of binding. On the other hand, ratios below the optimum lead to reduced drug fluxes upon dissolution problems. Although these results were not yet validated in animal experiments, our data underscores the value of the Caco-2 model as versatile tool. It is not only useful for simple permeability testing, but also for optimization of more complex formulations, such as solid dispersions. So, if these results once can be confirmed *in vivo*, the potency of this model also for optimization purposes will be further supported.

	% API [w/w]	Temperature [°C]	Powder feed rate [kg/h]	rpm
Danazol	5, 15, 25, 35, 45, 60	140	0.9	200
Fenofibrate	10, 20, 30, 40, 60	95	0.7	200
Itraconazole	15, 30, 45, 60, 70	150	1	200

Table 6.1.: Melt extrusion parameters for production of the used solid dispersions

6.2. Materials and Methods

6.2.1. Chemicals

Soluplus[®] was obtained from BASF SE (Ludwigshafen, Germany). Itraconazole and danazol were purchased from Selectchemie AG (Zurich, Switzerland). Non-essential amino acids (NEAA) and Dulbecco's modified Eagle's medium (DMEM) were provided by PAA Laboratories GmbH (Pasching, Austria). PAN-Biotech GmbH (Aidenbach, Germany) delivered fetal bovine serum. Vitamin E TPGS was from Eastman Chemical Company (Kingsport, TN, USA). Transwell permeable filters (type 3460, 0.4 µm pore size, polycarbonate) were supplied by Corning Inc. Life Science (Lowell, MA, USA). Fenofibrate and all other chemicals were from Sigma-Aldrich (St. Louis, MO, USA).

6.2.2. Extrudates

Solid dispersions of Soluplus[®] and the drugs danazol, fenofibrate and itraconazole were produced by hot melt extrusion at BASF SE. All extrudates were manufactured by a ThermoFisher Polylab twin-screw extruder (ThermoFisher Scientific Inc., Watham, MA, USA). An overview of the used extrudates and their extrusion parameters is given in Table 6.1. All extrudates were milled by an impact mill (Clatronic KSW 3306, coffee grinder) before use.

6.2.3. Caco-2 cell culture

Caco-2 cells (of clone C2BBE1) were purchased from American Type Culture Collection (Manassas, CA, USA). DMEM, supplied by 10 % FBS and 1 % NEAA was used as cell culture

medium. Medium was replaced every 2–3 days. Cells were subcultivated at a confluency of 90 % once a week. For transport experiments cells of passages 63–80 were used. Therefore, 60,000 cells were seeded on Transwell permeable membrane inserts. After 21–23 days of growth and differentiation cells were used for transport experiments. Caco-2 cells were grown under conditions of 37 °C, 80 % relative humidity and an atmosphere of 5 % CO₂. As qualification criteria for transport studies experiments served the transepithelial electrical resistance (TEER): Only monolayers providing TEER values above 500 Ohm x cm² were used for transport experiments.







6.2.4. Caco-2 transport experiments

Krebs Ringer buffer (KRB) was used as transport medium (TM). This buffer includes 114.2 mM NaCl, 3.0 mM KCl, 4.0 mM d-glucose, 1.4 mM CaCl₂, 2.6 mM MgCl₂ and 10.0 mM HEPES. By addition of NaOH the pH was equilibrated to a value of 7.4. As the tested drugs are not sufficiently soluble in TM, 0.2 % Vitamin E TPGS (danazol, fenofibrate) or 1 % HPβCD (itraconazole) was added to the receiver compartment to maintain sink conditions.






The respective formulations (solid solutions & physical mixtures) of the drugs were dissolved in KRB for one hour before application to the cells. Therefore, the formulations were weighed in for a final drug concentration of 0.5 mg/ml (danazol/itraconazole) or 1 mg/ml (fenofibrate), representing a single oral dose dispersed in 200 ml ingested liquid. To simulate the dissolution in the GI, these dispersions were stirred on a magnetic stirrer. The used formulations for each drug are summarized in Table 6.2.

ID	mass ratio (SP/drug)	molar ratio (SP/drug)	molar ratio (drug/SP)	Final SP conc. [%]	Remarks	Picture
Danazol						
0D	0	0	n.d.	0	no Soluplus®	
PMd1	0.10	2.86×10^{-4}	3496.7	0.005		
PMd2	0.20	5.72×10^{-4}	1748.36	0.01		
PMd3	1.00	2.86×10^{-3}	349.67	0.05		
PMd4	2.00	5.72×10^{-3}	174.84	0.1		

CHAPTER 6. OPTIMIZATION OF SOLUPLUS[®] FORMULATIONS

ID	mass ratio (SP/drug)	molar ratio (SP/drug)	molar ratio (drug/SP)	Final SP conc. [%]	Remarks	Picture
PMd5	5.67	0.016	62.44	0.28		
PMd6	20	0.057	17.48	1		
PMd7	40	0.114	8.74	2		
PMd8	60	0.172	5.83	3		
PMd9	100	0.286	3.5	5		
PMd10	200	0.572	1.75	10		
SDd1	0.67	1.91×10^{-3}	524.51	0.033	60 % danazol extrudate	
SDd2	1.22	3.50×10^{-3}	286.09	0.061	45 % danazol extrudate	
SDd3	1.86	5.31×10^{-3}	188.29	0.093	35 % danazol extrudate	
SDd4	3.00	8.58×10^{-3}	116.56	0.15	25 % danazol extrudate	
SDd5*	5.67	0.016	62.44	0.28	15 % danazol extrudate	
SDd6	10	0.029	34.97	0.5	spiked	
SDd7	19	0.054	18.40	0.95	5 % danazol extrudate	
SDd8	20	0.057	17.48	1	spiked	
SDd9	40	0.114	8.74	2	spiked	
SDd10	60	0.172	5.83	3	spiked	
SDd11	100	0.286	3.50	5	spiked	
SDd12	200	0.572	1.75	10	spiked	

CHAPTER 6. OPTIMIZATION OF SOLUPLUS® FORMULATIONS

ID	mass ratio (SP/drug)	molar ratio (SP/drug)	molar ratio (drug/SP)	Final SP conc. [%]	Remarks	Picture
Fenofibrate						
OF	0	0	n.d.	0	no Soluplus®	
PMf1	0.01	3.06×10^{-5}	32702	0.001		
PMf2	0.1	3.06×10^{-4}	3270.2	0.01		
PMf3	0.5	1.53×10^{-3}	654.1	0.05		
PMf4	1.5	4.59×10^{-3}	218.0	0.15		
PMf5	2.33	7.14×10^{-3}	140.15	0.233		
PMf6	4	0.012	81.76	0.4		
PMf7	10	0.031	32.70	1		
PMf8	30	0.092	10.90	3		
PMf9	50	0.153	6.54	5		
PMf10	100	0.306	3.27	10		
SDf1	0.67	2.04×10^{-3}	490.54	0.067	60 % feno extrudate	
SDf2	1.5	4.59×10^{-3}	218.0	0.15	40 % feno extrudate	
SDf3	2.33	7.14×10^{-3}	140.15	0.233	30 % feno extrudate	
SDf4*	4	0.012	81.76	0.4	20 % feno extrudate	
SDf5	9	0.028	36.34	0.9	10 % feno extrudate	
SDf6	10	0.031	32.70	1	spiked	
SDf7	30	0.092	10.90	3	spiked	
SDf8	50	0.153	6.54	5	spiked	
SDf9	100	0.306	3.27	10	spiked	






ID	mass ratio (SP/drug)	molar ratio (SP/drug)	molar ratio (drug/SP)	Final SP conc. [%]	Remarks	Picture
Itraconazole						
SDi1	0.43	2.56×10^{-3}	390.19	0.021	70 % itra extrudate	
SDi2	0.67	3.99×10^{-3}	250.86	0.033	60 % itra extrudate	
SDi3	1.22	7.31×10^{-3}	136.82	0.061	45 % itra extrudate	
SDi4	3.33	0.020	50.16	0.167	30 % itra extrudate	
SDi5*	5.67	0.034	29.86	0.28	15 % itra extrudate	
SDi6	20	0.120	8.36	1	spiked	
SDi7	40	0.239	4.18	2	spiked	
SDi8	100	0.598	1.67	5	spiked	
SDi9	200	1.196	0.84	10	spiked	

Table 6.2.: Soluplus[®](SP)/drug formulations used for Caco-2 transport experiments: PM indicates physical mixtures, SD indicates solid dispersions; formulations labeled by “spiked” are mixtures of the respective solid solution (marked by *) and additional Soluplus[®].

For transport experiments Caco-2 monolayers were washed twice with TM, followed by 1.0 h pre-incubation time. On the apical side of the Transwell system 500 μ l of the respective sample was applied, while the basolateral compartment was filled with 1500 μ l of the respective acceptor medium (KRB + TPGS/HP β CD). Transport from apical to basolateral side was studied over 4 hours under cell culture conditions. During incubation cells were agitated on an orbital shaker (100 \pm 20 rpm) and samples of 200 μ l volume were drawn

from the basolateral compartment at 30, 60, 90, 120 and 180 minutes. The removed sample volume was replaced by the same volume of fresh prewarmed TM (+ TPGS/HP β CD).

For each well the drug flux was calculated by the formula:

$$Flux = \frac{dc}{dt} \times \frac{1}{A} \quad (6.1)$$

Hereby dc/dt indicates the slope of the linear permeation curve and A the surface of the monolayer.

As control experiment for the influence of drug binding to Soluplus[®], transport experiments using the low permeability marker fluorescein sodium were conducted. Therefore, 10 μ M solutions of fluorescein sodium in KRB, containing different amounts of Soluplus[®], were prepared. Those solutions were applied on the apical side of the Transwell system and transport across Caco-2 monolayers was studied over 4 hours (conditions as above). Fluorescein sodium was detected fluorometric at a wavelength of 480 nm/530 nm (emission/excitation) on a 96well plate reader type Tecan infinite 200 (Tecan Group Ltd, Männedorf, Switzerland). For fluorescein sodium the apparent permeability (P_{app}) was calculated by the formula:

$$P_{app} = \frac{dc}{dt} \times \frac{1}{c_0} \times \frac{1}{A} \quad (6.2)$$

Whereas dc/dt represents the slope of the permeation curve, c_0 the initial donor concentration and A the cell surface.

6.2.5. HPLC analysis

All samples were diluted by the same volume of either acetonitrile (fenofibrate, itraconazole) or methanol (danazol).

The mobile phase for analysis of danazol consisted of methanol:water:phosphate buffer pH 6.8 [80:17:3 (v/v/v)]. Samples of 50 μ l were injected on a reversed phase column [LiChroCART 125-4 LiChrospher 100 RP18 (5 μ M) by Merck KGaA (Darmstadt, Germany)]. UV/Vis absorptiometry was used for detection at a wavelength of 288 nm.

A mixture of water (acidified to pH 2.5 by phosphoric acid) and acetonitrile at a ratio of 70:30 (v/v) was used for quantification of fenofibrate and its metabolite fenofibric acid. Both compounds were quantified absorptiometric at a wavelength of 286 nm. 50 µl of each sample were injected on a reversed phase column (RP18 as above).

Itraconazole was injected at a sample volume of 80 µl on a reversed phase column (RP18 as above) and eluted by a mixture of acetonitrile, water and phosphate buffer pH 6.8 [70:27:3 (v/v/v)]. Samples were analyzed by UV/Vis absorptiometry at a detection wavelength of 263 nm. Additional data on the used HPLC analytics can be found in Appendix C.

6.2.6. Equilibrium dialysis

Equilibrium dialysis was performed to confirm the binding of Soluplus[®] to fluorescein sodium. Therefore, fluorescein/Soluplus[®] solutions (as for transport experiments) were dialyzed for 4 hours at 37 °C versus pure KRB.

Experiments were performed by a dialysis system consisting of two chambers with a volume of 2 ml each. Chambers were separated by a cellulose membrane providing a molecular cutoff of 10 kDa (Harvard Apparatus, Holliston, MA, USA). Dialysis chambers were rotated by a DIANORM apparatus (identical to DIALYZER by Harvard Apparatus, Holliston, MA, USA).

Results are expressed as ratio between donor and acceptor (D/A ratio), indicating the binding strength between exception and fluorescein.

6.2.7. Differential scanning calorimetry (DSC)

Differential scanning calorimetry was performed to distinguish between (partially) crystalline and amorphous solid dispersions. A sample of 3–7 mg was weighed into a hermetic aluminium container and analyzed at a heating rate of 10 °C/min by a TA Instruments Q100 DSC (TA Instruments, New Castle, DE, USA). The heat flow [Watts per gramm] was measured and plotted versus the temperature. Changes in heat flow are indicating exothermic or endothermic processes.

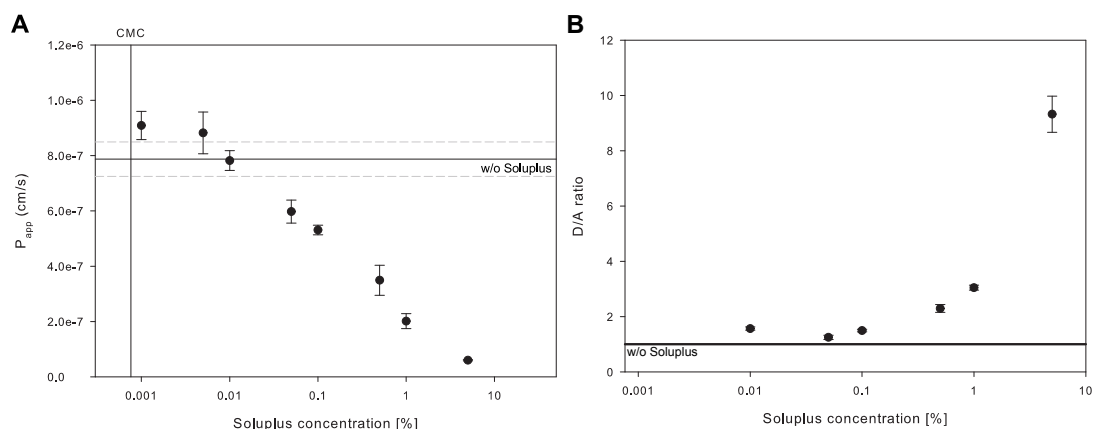


Figure 6.1.: A: Fluorescein sodium transport across Caco-2 monolayers (n=3; mean \pm SD). B: Equilibrium dialysis of Soluplus[®]/fluorescein mixtures, donor/acceptor ratios vs. Soluplus[®] concentration (n=5; mean \pm SD)

6.3. Results

6.3.1. Fluorescein sodium (control)

Transport experiments with fluorescein sodium showed a concentration dependent decrease of P_{app} values by increasing Soluplus[®] concentration (Figure 6.1 A). While the control experiment (without Soluplus[®]) established a P_{app} of 7.8×10^{-7} cm/s, a strong decrease of the apparent permeability was detected by addition of the excipient. An addition of 5 % Soluplus[®] decreased the P_{app} more than 10-fold to a value of 6.0×10^{-8} cm/s. To confirm the hypothesis that this decrease is due to binding of the substrate to Soluplus[®], equilibrium dialysis was performed.

As shown in Figure 6.1 B, Soluplus[®] was able to retain fluorescein sodium in the donor compartment, expressed in donor/acceptor ratios > 1 . By increasing Soluplus[®] concentration, the binding strength increased. While for low concentrations almost an equilibrium was reached ($D/A = 1$), the binding strength increased up to a donor/acceptor ratio of 9.3 for a 5 % Soluplus[®] solution.

A concentration dependent binding of Soluplus[®] to fluorescein sodium was proven by equilibrium dialysis. Therefore, the decreased apparent permeability in Caco-2 transport experiments is most probably due to this binding.

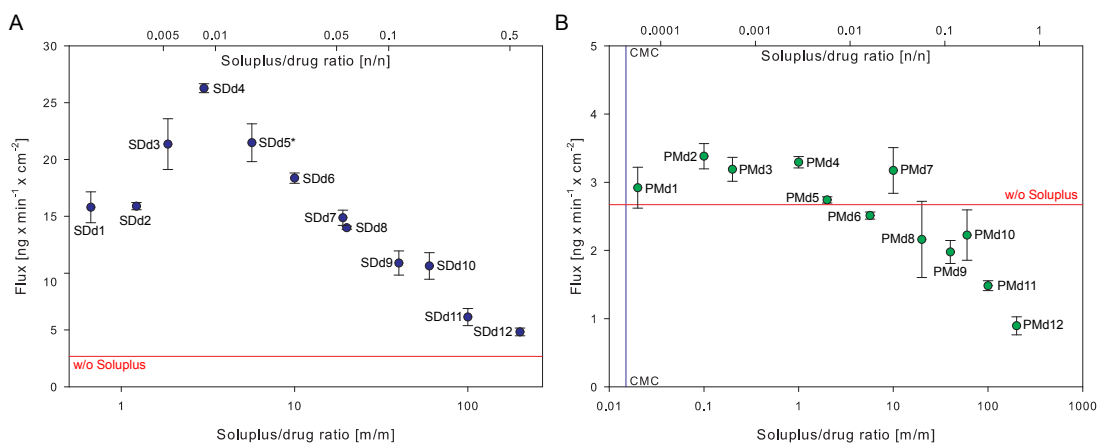


Figure 6.2.: Dependency of danazol flux on Soluplus[®]/drug ratio ($n=3-9$; mean \pm SD). A: solid dispersions; B: physical mixtures. Labels refer to Table 6.2, page 72.

6.3.2. Danazol

Solid dispersions

The drug flux of danazol across Caco-2 monolayers was dependent on the Soluplus[®]/danazol ratio of the respective formulation. As demonstrated in Figure 6.2 A the highest flux was established by the extrudate containing 25 % danazol. While this formulation showed a flux of $26.27 \text{ ng} \times \text{min}^{-1} \times \text{cm}^{-2}$, the flux decreased by increasing Soluplus[®]/drug ratio to a value of $4.83 \text{ ng} \times \text{min}^{-1} \times \text{cm}^{-2}$ for a mass ratio of 200. On the other hand, the drug flux decreased as well for decreasing Soluplus[®]/drug ratios. For the extrudate containing 60 % danazol the flux was reduced to $15.79 \text{ ng} \times \text{min}^{-1} \times \text{cm}^{-2}$.

Differential scanning calorimetry of the used extrudates proved the existence of crystalline drug in the extrudates containing 35 %, 45 % and 60 % danazol by the presence of melting peaks in the respective DSC thermograms (Figure 6.3). However, the melting peaks were not as exposed as for the pure drug, indicating a coexistence of amorphous and crystalline parts in the extrudates. Also the exothermic disintegration peaks of both danazol and Soluplus[®] [62] at temperatures above 250°C complicated a more exact analysis of the DSC data. An estimation of the crystallinity of an extrudate can also be done by optical investigation: while real solid solutions appear clear, partially crystalline extrudates are turbid (Table 6.2).

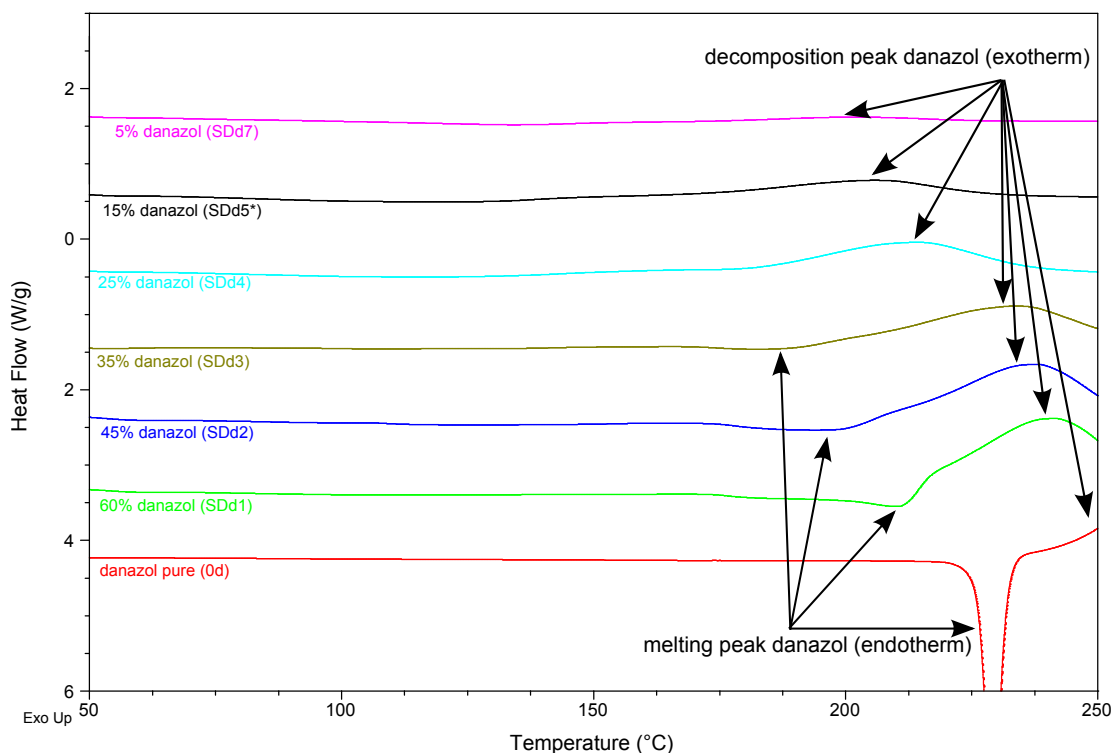


Figure 6.3.: DSC of the used danazol hot melt extrudates (Exotherm up). Melting peaks of extrudates are shifted to lower temperatures, probably due to the formation of polymorphs and/or eutectics.

Physical mixtures

As shown in previous experiments, the *in vivo* and *in vitro* absorption of physical mixtures of crystalline danazol and Soluplus[®] is comparable to the absorption of the pure drug (see Chapter 4.3.1). However, an effect of the excipient/drug ratio was also detectable for the physical mixture (Figure 6.2 B). Especially for high Soluplus[®]/drug ratios a decreased drug flux was detected. While the formulation with a ratio of 5.67 (= 15 % danazol) established a flux of $2.63 \text{ ng} \times \text{min}^{-1} \times \text{cm}^{-2}$, the flux decreased to a value of $0.90 \text{ ng} \times \text{min}^{-1} \times \text{cm}^{-2}$ for a ratio of 200. Contrarily, by decreasing ratio the flux was slightly increased compared to the pure drug ($2.67 \text{ ng} \times \text{min}^{-1} \times \text{cm}^{-2}$). However, if the total Soluplus[®] concentration reached its CMC, the flux was obviously comparable to the flux of the pure drug.

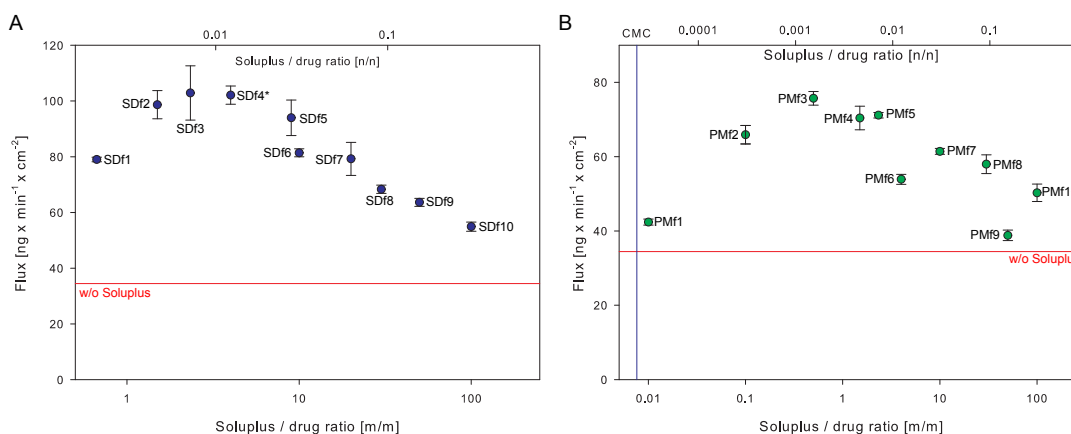


Figure 6.4.: Dependency of fenofibrate flux on Soluplus[®]/drug ratio (n=3–6; mean \pm SD). A: solid dispersions; B: physical mixtures. Labels refer to Table 6.2, page 72.

6.3.3. Fenofibrate

The prodrug fenofibrate is metabolized to its active form fenofibric acid during transport across Caco-2 cells. Therefore, all results are related to this metabolite.

Solid dispersions

As for danazol, the drug flux was dependent on the ratio between excipient and fenofibrate (Figure 6.4). The optimum is less exposed as for danazol and located at a ratio of 2.33 (Table 6.2-SDf3), enabling a flux of $102.83 \text{ ng} \times \text{min}^{-1} \times \text{cm}^{-2}$. For higher ratios the drug flux decreased to a value of $54.9 \text{ ng} \times \text{min}^{-1} \times \text{cm}^{-2}$ for a ratio of 100. Both tested formulations below the optimum (Table 6.2-SDf1 & SDf2) showed lower fluxes with $98.65 \text{ ng} \times \text{min}^{-1} \times \text{cm}^{-2}$ and $79.00 \text{ ng} \times \text{min}^{-1} \times \text{cm}^{-2}$, respectively. Compared to danazol, the optimum is less exposed and a certain range for a high flux could be determined for Soluplus[®]/drug ratios between 1.5 and 9 (m/m).

The DSC thermograms of the used extrudates offer clear melting peaks of crystalline drug for the extrudates, containing 40 % and 60 % fenofibrate (Figure 6.5). Also for the extrudate with 30 % fenofibrate, which established the maximal flux, a certain crystallinity can be assumed. However, the overlay between the T_g of Soluplus[®] ($\sim 0^\circ\text{C}$; Figure 6.6) and

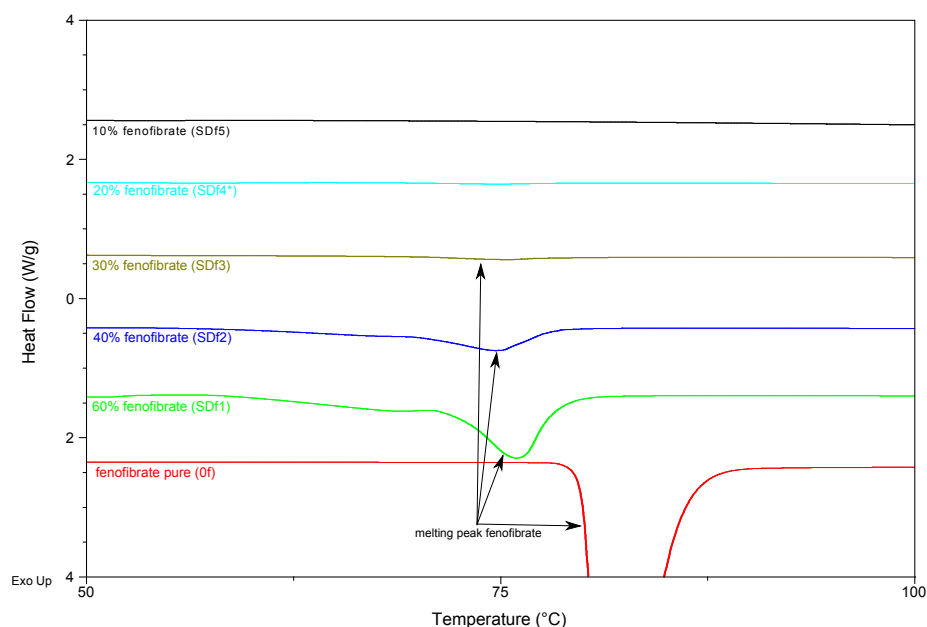


Figure 6.5.: DSC of the used fenofibrate hot melt extrudates (Exotherm up). Melting peaks of extrudates are shifted to lower temperatures, probably due to the formation of polymorphs and/or eutectics.

the melting peak of fenofibrate (m.p. 80.5 °C) hinders an exact determination of the crystalline parts. For all extrudates, no melting peaks of the metabolite fenofibric acid (m.p. 179–183 °C) was found. Optical examination of the extrudates confirmed the DSC data, as the high loaded extrudates appeared turbid, the 30 % extrudate mostly clear and the lower loaded extrudates entirely clear (Table 6.2).

Physical mixtures

Previous *in vitro* and *in vivo* studies showed that Soluplus[®] enhances the absorption of fenofibrate not only in a solid solution, but also in a physical mixture of drug and excipient (Chapter 4.3.2).

Also for the physical mixture, the drug flux was dependent on the Soluplus[®]/drug ratio. A maximal flux was reached for a ratio of 0.5 (m/m) with $75.71 \text{ ng} \times \text{min}^{-1} \times \text{cm}^{-2}$. As well as for the solid solution, the flux decreased for both lower and higher ratios. Obviously, the flux was decreased to the same level as for the pure drug if the total Soluplus[®] con-

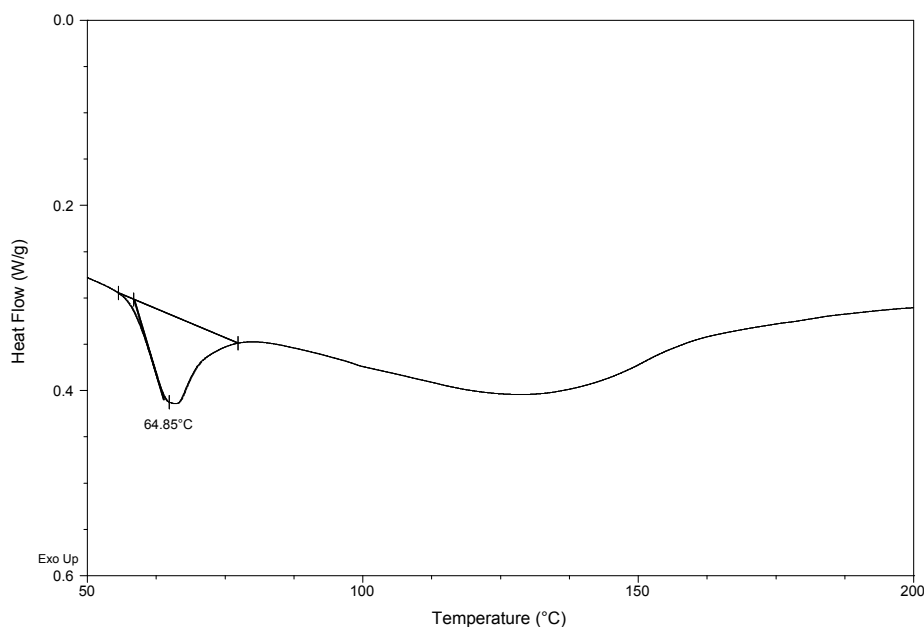


Figure 6.6.: DSC thermogramm of Soluplus[®] (Exotherm up). T_g is slightly shifted to lower temperature.

centration in the medium reached its CMC (Figure 6.4). Interestingly, the drug fluxes of formulations PMf3 ($75.71 \text{ ng} \times \text{min}^{-1} \times \text{cm}^{-2}$) and Sdf1 ($79.00 \text{ ng} \times \text{min}^{-1} \times \text{cm}^{-2}$) were similar which indicates that fenofibrate is mostly present in the crystalline form in the solid dispersion and therefore behaved similar to a physical mixture (Figure 6.7).

6.3.4. Itraconazole

For itraconazole, the absorption *in vitro* and *in vivo* for the physical mixture and for the pure drug remained very low (Chapter 4.3.3). Therefore, no experiments using the physical mixture and the bulk drug were conducted in this study.

For solid dispersions with itraconazole a clear dependence of the drug flux across Caco-2 monolayers on the Soluplus[®]/drug ratio was detected (Figure 6.8). A maximal flux was determined for a mass ratio of 20 ($17.54 \text{ ng} \times \text{min}^{-1} \times \text{cm}^{-2}$). However, a broad range of ratios can be considered as optimal: ratios between 3.33 and 40 lead to similar flux values. In contrast, by exceeding a ratio of 40, the flux strongly decreased, down to a flux of 6.39 ng

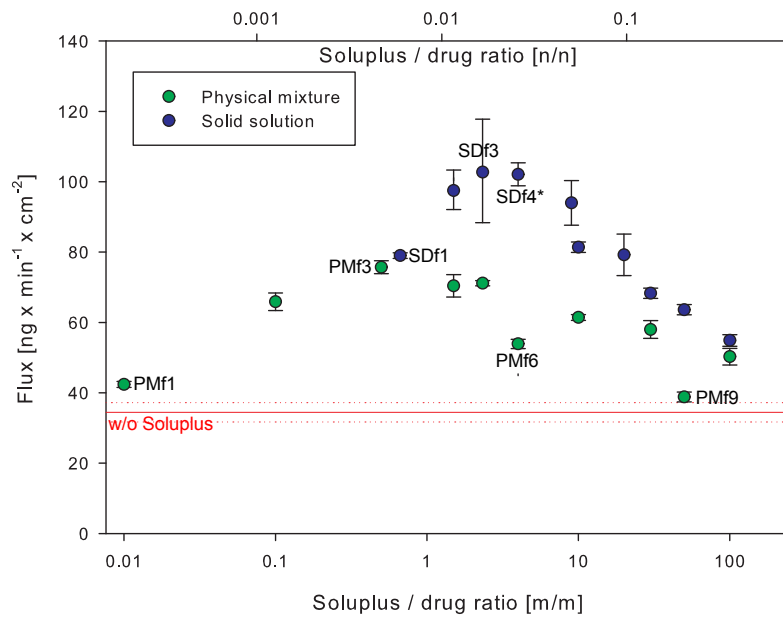


Figure 6.7.: Comparison between solid dispersions and physical mixtures of Soluplus[®]/fenofibrate. Drug fluxes of the metabolite fenofibric acid (n=3–6; mean \pm SD). Labels refer to Table 6.2, page 72.

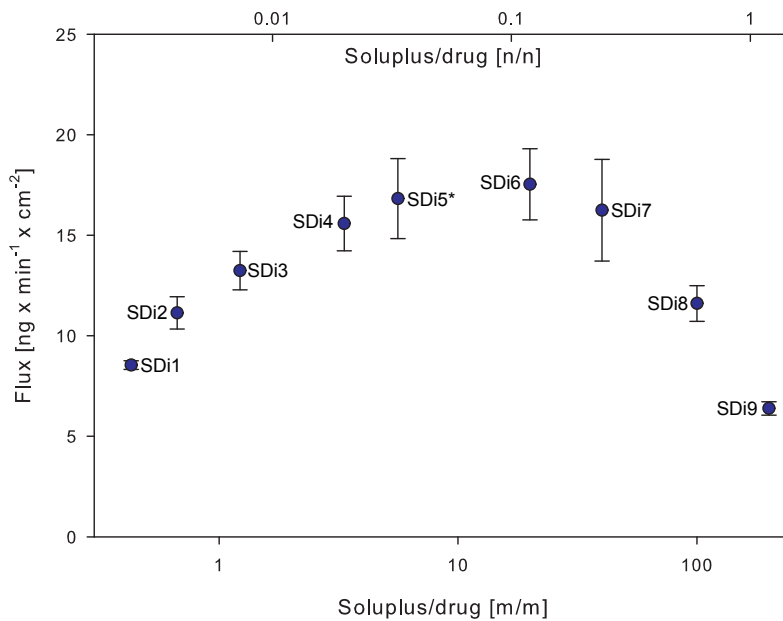


Figure 6.8.: Dependency of itraconazole flux on Soluplus[®]/drug ratio (n=3–6; mean \pm SD). Labels refer to Table 6.2, page 72.

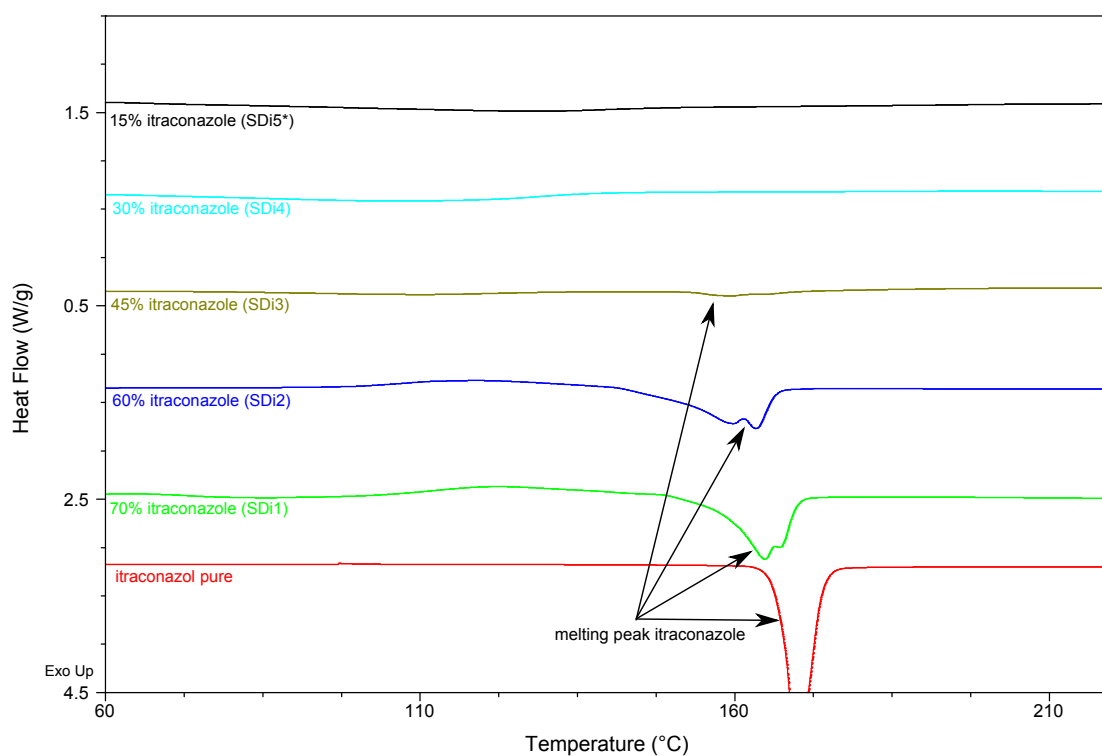


Figure 6.9.: DSC of the used itraconazole hot melt extrudates (Exotherm up). Melting peaks of extrudates are shifted to lower temperatures and doubled, probably due to the formation of polymorphs and/or eutectics.

$\times \text{min}^{-1} \times \text{cm}^{-2}$ for a ratio of 200. Also for decreasing ratios a decreased itraconazole flux was detected. For the extrudate containing 70 % itraconazole (Table 6.2-SDi1), the flux is reduced to a value of $8.54 \text{ ng} \times \text{min}^{-1} \times \text{cm}^{-2}$.

DSC data of the used solid dispersions demonstrated crystalline drug parts in extrudates containing 45 % itraconazole or more (Figure 6.9). This is in concordance with an optical investigation of the extrudates. As those high loaded dispersions showed strong turbidity compared to the extrudates with less than 45 % drug. However, the strong transport of the highest loaded extrudate (SDi1), compared to the pure drug and the physical mixture, indicates the presence of fast dissolving amorphous parts. Double melting peaks in the DSC thermograms were most probably due to the formation of different polymorphs of the drug through hot melt extrusion.

6.4. Discussion

Transport experiments across Caco-2 monolayers demonstrated an optimal Soluplus[®]/drug ratio for the absorption of danazol, fenofibrate and itraconazole solid dispersions (Figure 6.11 A). Also for physical mixtures of danazol and fenofibrate with Soluplus[®] an optimal ratio of drug and excipient could be determined.

The decreased drug flux of Soluplus[®]/drug ratios below the optimum may be explained by the appearance of crystalline drug in these extrudates. As shown by DSC and/or optical investigation, the existence of crystalline drug leads to reduced drug flux across the cell monolayer. This behavior can most probably be explained by the slow dissolution of these solid dispersions. *Real* solid solutions (see Table 3.5) show a rapid dissolution, due to the molecularly dispersed drug and therefore minimal particle size of the drug. In contrast, for solid dispersions (cf. Table 3.5) the drug is not molecularly dispersed and hence not present in the optimal particle size. Especially if the drug is present in its crystalline form, the dissolution is hindered as the lattice energy has to be overcome for a successful solubilization. Although the solubility enhancer Soluplus[®] is present, the slower dissolution of crystalline drugs leads to reduced transport, as the time scale for solubilization of the drug is limited by the duration of the experiment which tries to mimic the *in vivo* time window available for drug dissolution and absorption in the gut and small intestine. Besides slower dissolution of these high loaded extrudates, the lower Soluplus[®] concentration available for solubilization decreases the free and dissolved drug amount thus the drug flux: In this series of experiments the drug concentration was fixed to 0.5 mg/ml (danazol & itraconazole) or 1.0 mg/ml (fenofibrate), the final Soluplus[®] concentration in the transport medium is consequently reduced for low Soluplus[®]/drug ratios. As shown in Table 6.2, the final Soluplus[®] concentration is reduced to 0.021–0.33 % for the lowest Soluplus[®]/drug ratios. According to equation 3.2, the solubility of the respective drug is reduced at low surfactant concentrations. This also results in a decreased transport for low Soluplus[®]/drug ratios in physical mixtures of drug and excipient. However, as the curves for physical mixture and solid dispersion offer differing excipient/drug ratios for

the maximal flux, it can be assumed that both, the slower dissolution due to crystalline drug and decreased solubilization due to low Soluplus[®] concentrations, play a role for the reduced flux. The predominance of the high loaded extrudates versus the physical mixtures is most probably due to the coexistence of solubilized molecularly dispersed, amorphous not solubilized and crystalline drug in the used extrudates.

For Soluplus[®]/drug ratios above the optimum, the drug flux decreased for all three tested drugs. As shown by Caco-2 transport and equilibrium dialysis experiments using fluorescein sodium as dye, Soluplus[®] shows a concentration dependent binding to this marker substrate. Also for the used drugs a certain binding between drug and excipient could be determined by equilibrium dialysis (see Chapter 4.3.4). Therefore, the decreased flux is most probably due to this binding behavior. The total Soluplus[®] concentration seems not to play a role in this case, as formulations with different total Soluplus[®] (and drug) concentrations, but with the same drug/excipient ratios showed a similar drug flux: For example, a 7-fold higher initial weight in sample SDd5* leads to a flux of $20.87 \pm 0.93 \text{ ng} \times \text{min}^{-1} \times \text{cm}^{-2}$ (SDd5*: $21.48 \pm 1.67 \text{ ng} \times \text{min}^{-1} \times \text{cm}^{-2}$). The observed binding between drug and excipient is likely dependent on the lipophilicity of the respective drug: equilibrium dialysis of different drugs and fluorescence dyes showed a logP dependent increase of the binding, quantified by increasing donor/acceptor ratios (Figure 6.10). Hereby, fenofibrate and its metabolite fenofibric acid seem to be outliers. This is also in concordance with the differing behavior of fenofibrate *in vivo* and *in vitro* (see Chapter 4.3.2). The slope of the terminal decrease is also dependent on the drug and coincides with the order of the binding strength: itraconazole > danazol > fenofibrate (Figure 6.11 B & Figure 6.10). Decreased transport by a surplus of a solubilizing excipient is not a new phenomenon. For instance it was shown for formulations of HP β CD with flutamide, that a stable excipient/drug complex may hinder the transport across Caco-2 cells [122]. However, the advantage of an enhanced aqueous solubility overcompensates the reduced drug flux, as most of the tested formulations showed a significantly higher absorption than the pure crystalline drug.

The excipient/drug ratio for establishing a maximal flux is dependent on the used drug

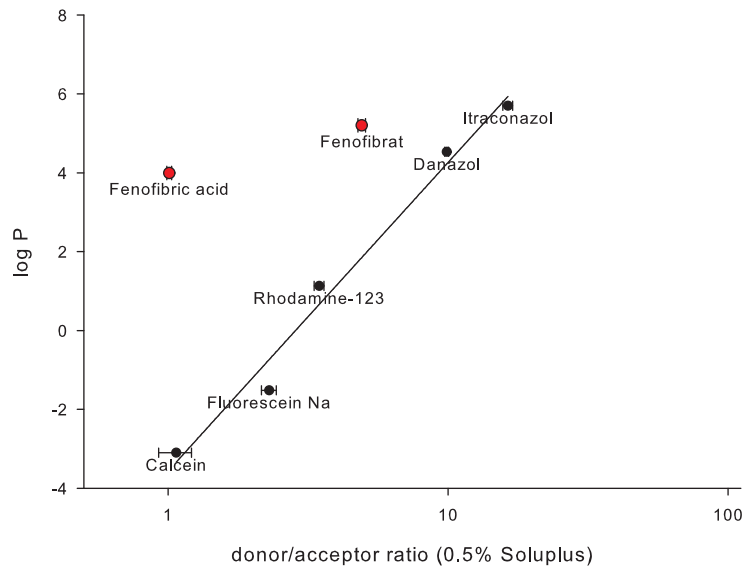


Figure 6.10.: D/A ratios of equilibrium dialysis (at a Soluplus[®] concentration of 0.5 %) correlates to logP values of the respective drug (Logarithmic fit $R^2=0.9819$). Except for the marked outliers fenofibrate and fenofibric acid.

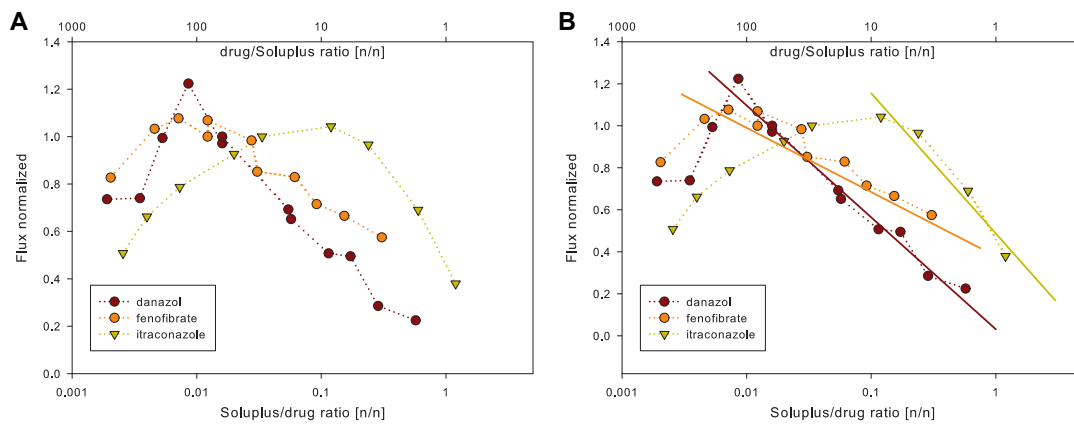


Figure 6.11.: A: Excipient/drug ratio versus drug flux. Y-axis is normalized to the respective “Standard formulation” (marked by * in Table 6.2). B: Logarithmic fit of the terminal decrease added to Graph A. $R^2=0.9495$, 0.9510 and 0.9795 for itraconazole, fenofibrate and danazol, respectively.

(Figure 6.11 A). These maxima are composed of solubilization and binding of the drug with Soluplus[®]. The highest flux is established if just enough Soluplus[®] is apparent for a successful formation of a stable solid solution. If a surplus of the excipient is present, the flux decreases as result of binding. Therefore, the composition of the Soluplus[®]/drug complex is of further interest for a better understanding of this behavior.

Since the respective drug is bond by the formed Soluplus[®] micelles, the micelle size was studied by dynamic light scattering (see Appendix A). While no or only low difference between drug-loaded and unloaded micelles could be determined, the total Soluplus[®] concentration affects the micelle size. Especially at high Soluplus[®] concentrations, which were also present in this study, the micelles seem to be differentially shaped or aggregating. Also the possible formation of rod-like or layered structures may change the release of API from the micelles. Another factor that may affect the stability of the micelle/drug complex is the pH, the presence of salts, and/or additional micelles. DLS showed no effect of the pH on micelle size, but the osmolarity of the used solvent lead to changes in micelle size.

Especially for a transfer to the *in vivo* situation this might play a role. The intestinal fluids are complexly composed and micelles formed by bile salts and phospholipids are present. Therefore, the formation of mixed micelles with Soluplus[®] or a changeover of solubilized drug from Soluplus[®] micelles to *natural micelles* might affect the drug absorption.

While for danazol and fenofibrate the optimal ratio is located at the respective ratio of the highest loaded extrudate without crystalline drug (as determined by DSC and optical investigation). The optimum for itraconazole is shifted to higher ratios. A possible reason for this shift is an interaction with the efflux transporter P-gp. As itraconazole is substrate and inhibitor of this protein and Soluplus[®] is also suspected to inhibit P-gp (Chapter 5), P-gp inhibition might compensate the reduced absorption provided by the formation of a stable complex.

6.5. Conclusion and Outlook

For solid dispersions of Soluplus[®] with danazol, fenofibrate and itraconazole an optimum for drug transport across Caco-2 cells was found. This optimum is the result of three (itraconazole: four) effects:

1. In high loaded extrudates drug crystals are present which do not dissolve rapidly in the used timescale
2. The final Soluplus[®] concentration must be high enough for a successful solubilization of the drug
3. The formation of stable drug/excipient complexes leads to a reduced absorption for high Soluplus[®]/drug ratios
4. For itraconazole an interference with inhibition of active efflux by P-gp might interfere with the optimum formed by 1.–3.

Based on the results of this Caco-2 experiments a *rule of thumb* for the formulation of poorly soluble drugs with Soluplus[®] may be formulated: “Use only as much Soluplus[®] as needed for a stable amorphous extrudate”. The stability is hereby expanded on the whole manufacturing process, including possible steps of milling, pelletizing or compaction of the extrudates.

The exact structure and mechanism of the stable complexes of drug and excipient is not fully understood and might be an aim of further investigations, using techniques as molecular modeling or analytical ultracentrifugation. First results from analytical ultracentrifugation with itraconazole loaded Soluplus[®] proved the existence of compact micellar structures, containing the drug (see Appendix A for details).

Also the behavior of Soluplus[®] micelles *in vivo* might be of interest for further studies. As described above, the composition of the intestinal fluids may affect the observed binding effects. However, a confirmation of the results from Caco-2 monolayers by animal studies would be an excellent validation for the power of this tool as surrogate for intestinal drug absorption.

7. Summary and Outlook

Many new active pharmaceutical ingredients offer a poor oral bioavailability as consequence of their poor aqueous solubility. One approach to overcome this solubility hurdle is the use of hot melt extrusion to produce rapidly dissolving solid solutions. However, a supersaturation formed by the dissolution of such an extrudate is not stable unless a solubilizing agent stabilizes this solution. The novel polymer Soluplus[®] was specifically designed to combine these two properties in one molecule: solubilization and the feasibility to form solid solutions. The efficacy of such an excipient might be tested in classical dissolution tests, but these tests can only give a rough estimate of the *in vivo* situation. Hence, animal studies are still considered as the gold standard for testing the efficacy of novel formulation approaches for poorly soluble drugs.

The Caco-2 cell culture model is widely accepted for the estimation of intestinal drug permeability and also as alternative for animal experiments. The aim of replacing and reducing animal studies by such *in vitro* models as proposed by the so-called 3R concept has not only ethical aspects, but also economic reasons. The work presented in this thesis proved the applicability of the Caco-2 model for more complex drug delivery systems, such as hot melt extrudates. The Caco-2 model was also used for an optimization of Soluplus[®] solid solutions with regards to drug excipient ratios. Additionally, the effect of the novel polymer Soluplus[®] on P-glycoprotein and trypsin as possible targets of drug-excipient interactions was studied.

In the first part of this thesis, formulations of Soluplus[®] with the poorly soluble drugs danazol, fenofibrate and itraconazole were tested for their transport behavior across Caco-2 cells. Data from these *in vitro* permeation experiments were correlated to *in vivo* data

from previously performed animal studies. As solid drug formulations cannot be applied directly on the cell surface, a dissolution step has to be included beforehand. While *in vivo* the dissolution of the solid form mostly occurs throughout the gastric passage, in our studies the formulations were dissolved outside the cell culture system before application. Our studies showed an excellent correlation between the drug flux across Caco-2 monolayers and the AUC of animal plasma curves for all three drugs. Especially the absorption enhancing effect of the solid solutions could exactly be modeled. Furthermore, we were able to confirm the efficacy of a physical mixture of fenofibrate and Soluplus[®]. Fenofibrate was the only tested drug compound for which the physical mixture demonstrated a superior bioavailability compared to the pure drug. This singularity could be confirmed in the Caco-2 model, further proving the value of the *in vitro* model as surrogate for intestinal drug absorption of Soluplus[®] formulations.

As second part of this work the effect of Soluplus[®] on the efflux transporter P-glycoprotein was studied. This transporter protein may reduce the intestinal absorption of certain drugs and is also the target of possible drug/excipient interactions. As many solubilizers were shown to inhibit P-glycoprotein, the novel solubilizer Soluplus[®] was also tested for a possible interaction. Cell culture assays using Caco-2 and MDCK-II cells proved the potential of Soluplus[®] to inhibit the efflux transporter. The effective concentration of Soluplus[®] was comparably high and in the range of polyethylene glycols which are commonly classified as unproblematic excipients. Therefore, the *in vivo* relevancy of this inhibition may be called into question.

The Caco-2 model was also used for an optimization of Soluplus[®] formulations. Since it was shown by dialysis experiments that Soluplus[®] has the potential to retain drugs in a complex by binding, the effect of increased or decreased Soluplus[®] (per drug) concentrations on the transport of danazol, fenofibrate and itraconazole was tested. Our transport studies showed that this binding leads to a strongly decreased permeation of all tested drugs by increasing Soluplus[®]/drug ratios. Therefore, the popular lore *more is better* is certainly not applicable to formulations containing Soluplus[®]. However, Soluplus[®]/drug

ratio can only be reduced to a certain point: If the excipient/drug ratio gets too low, a stable solid solution cannot be formed. In this case, the amount of Soluplus[®] in the respective extrudate is not sufficient to solubilize the drug, hence the extrudate is partially crystalline. Accordingly, the drug flux decreases as result of the reduced dissolution of such a partially crystalline formulation. For all tested drugs a more or less sharply expressed optimum for the drug flux across Caco-2 cells was found. This optimum seems to be the result of interplay between the effects of drug dissolution, solubilization and binding between drug and excipient.

In all three parts of this work an unspecific binding between Soluplus[®] and the respective drug or P-gp substrate occurred and somehow affected the experimental outcome. Therefore, a deeper investigation into this behavior should be considered. Dialysis experiments showed that the strength of this binding is dependent on the compound and also correlates mostly to the respective drug logP. Once again the outlier fenofibrate is remarkable as the substance also showed some singularities *in vivo* and in Caco-2 transport. As Soluplus[®] gathers its solubilizing properties from the formation of micelles, these micelles were further investigated by DLS measurements. While the micelle size was sensitive to temperature changes, the enclosed drug molecules seemed not to affect the micellar size. A certain effect of the used medium and its osmolarity on the micellar structures could be determined.

This dependency on the used media leads to the question how these micelles behave in *in vivo* liquids. If the micellar structure changes by alterations of the media, a different binding behavior between drug and excipient may be assumed. Accordingly, the use of more biorelevant transport media might be considered in further studies. Fasted or fed state simulated intestinal fluid (FaSSIF/FeSSIF) are more complex biosimilar media for dissolution tests, providing mixed micelles of bile salts and phospholipids [158]. Due to their high osmolarity these media cannot be directly used in cell culture, but adaptations from this fluids were developed for application on cells [159, 160, 161].

Another point, which may influence the behavior of Soluplus[®] formulations *in vivo*, is the

difference in the dissolution process compared to the Caco-2 model. While in our experiments the dissolution step was performed by simple and delimited stirring in transport buffer, the real situation is even more complex. *In vivo* the pH may change during the dissolution as it gradually increases during GI passage. One approach to simulate this effect is the use of an acid dissolution medium to simulate the gastric passage and dissolution which is subsequently equilibrated to a cell-compatible pH [106]. Also the dissolution *in vivo* is not limited to a certain time window as in our experiments and absorption and dissolution occur at the same time. To simulate this behavior the use of a combined dissolution/permeation system might be useful. Hereby a flow-through dissolution cell is combined with a permeation model such as Caco-2 cells [97, 162]. Such a system may lead to even better correlations to the *in vivo* behavior and may further elucidate the mechanism of bioavailability enhancement by Soluplus®. However, also our more simple approach to simulate the dissolution step leads to excellent correlations with the *in vivo* behavior of the tested formulations. Therefore, those more complex and hence more error-prone systems might be considered as unnecessary. According to the principle of *Occam's razor* the simple method is to be favored over too complex systems.

8. Zusammenfassung und Ausblick

Viele neue Arzneistoffe sind aufgrund ihrer schlechten Wasserlöslichkeit nur in geringem Maße oral bioverfügbar. Ein Forschungsansatz zur Überwindung dieser Hürde ist das Schmelzextrusionsverfahren zur Herstellung schnellauflösender fester Lösungen. Durch die Auflösung eines derartigen Extrudats entsteht eine Übersättigung, welche ohne Zusatz eines Löslichkeitsverbesserers nicht stabil ist. Der neue polymere Hilfsstoff Soluplus[®] wurde entwickelt, um diese zwei Funktionen in einem Molekül zu vereinen: Löslichkeitsverbesserung sowie die Nutzbarkeit zur Herstellung fester Lösungen. Die Wirksamkeit eines solchen Hilfsstoffes kann mit klassischen Dissolutionstests geprüft werden, allerdings können diese Experimente nur eine vage Vorhersage für die *in vivo* Situation geben. Daher gelten Tierversuche immer noch als Goldstandard zur Wirksamkeitsbestimmung neuer Formulierungen für schwerlösliche Arzneistoffe.

Das Caco-2 Zellkulturmodell ist zum Einen ein weitverbreitetes und akzeptiertes Modell zur Abschätzung der Arzneistoffaufnahme über die Darmwand und zum Anderen auch eine akzeptierte Tierversuchersatzmethode. Das Ziel durch derartige Modelle Tierversuche zu reduzieren, zu verfeinern und zu ersetzen (reduce, refine, replace = 3R-Konzept) hat nicht nur ethische Gründe, sondern ist auch durch ökonomische Aspekte zu begründen. Die in dieser Dissertation vorgestellte Arbeit konnte die Nutzbarkeit des Caco-2 Modells auch für komplexe Formulierungen wie Schmelzextrudate aufzeigen. Des Weiteren wurde das Caco-2 Modell genutzt, um feste Lösungen von Arzneistoffen mit Soluplus[®] zu optimieren. Zusätzlich wurde der Effekt von Soluplus[®] auf P-glykoprotein und Trypsin untersucht, welches mögliche Wirkstätten von Arzneistoff-Hilfsstoff-Interaktionen sind. Im ersten Teil dieser Arbeit wurde das Transportverhalten der schwerlöslichen Arznei-

stoffe Danazol, Fenofibrat und Itraconazol, in Formulierungen mit Soluplus[®], über Caco-2 Zellen untersucht. Die Daten aus dieser *in vitro* Untersuchung wurden mit *in vivo* Daten von zuvor durchgeführten Tierversuchen verglichen. Da feste Arzneistoffformulierungen nicht direkt auf die Zellen appliziert werden können, muss zuvor eine Auflösung stattfinden. Während *in vivo* die Auflösung des Arzneistoffs hauptsächlich während der Magenpassage stattfindet, so wurde in unseren Experimenten die Dissolution der Formulierungen außerhalb des Zellkultursystems vorgenommen. Eine sehr gute Korrelation zwischen dem Arzneistoffflux über Caco-2 Zellen und der AUC der Plasmakurven aus dem Tierversuch konnte für die drei getesteten Arzneistoffe gefunden werden. Insbesondere die Absorptionsverbesserung durch die festen Lösungen konnte sehr gut vorhergesagt werden. Zusätzlich wurde die Effektivität einer physikalischen Mischung aus Fenofibrat und Soluplus[®] im Zellmodell bestätigt. Ausschließlich für Fenofibrat war die physikalische Mischung der Reinsubstanz hinsichtlich der Bioverfügbarkeit überlegen. Diese Besonderheit konnte im Caco-2-Modell bestätigt werden, was einen weiteren Beweis für die Mächtigkeit dieses Testsystems als Modell für die intestinale Arzneistoffaufnahme aus Soluplus[®]-Formulierungen darstellt.

Im zweiten Teil dieser Arbeit wurde die Wirkung von Soluplus[®] auf den Effluxtransporter P-Glykoprotein untersucht. Dieses Transporterprotein ist in der Lage die intestinale Aufnahme diverser Arzneistoffe zu verringern. Außerdem ist P-Glykoprotein eine Zielstruktur möglicher Arzneistoff/Hilfsstoff-Interaktionen. Da bereits für einige Löslichkeitsverbesserer eine P-gp-Inhibition bewiesen werden konnte, wurde auch der neue Solubilizer Soluplus[®] auf eine mögliche Interaktion mit diesem Transporter untersucht. In Zellkulturversuchen mit Caco-2 und MDCK-II Zellen konnte gezeigt werden, dass Soluplus[®] den P-gp vermittelten Efflux hemmen kann. Die wirksame Konzentration von Soluplus[®] war allerdings vergleichsweise hoch und befindet sich in etwa auf dem Niveau der Polyethylenglykole, welche üblicherweise als unproblematisch hinsichtlich P-gp-Hemmung angesehen werden. Aus diesem Grunde darf die Relevanz dieses Inhibitionsverhaltens für die *in-vivo*-Situation in Frage gestellt werden.

Im dritten Teil dieser Arbeit wurde das Caco-2 Modell zur Optimierung von Soluplus[®]-Formulierungen eingesetzt. Durch Gleichgewichtsdialyse wurde gezeigt, dass Soluplus[®] Arzneistoffe in einem Komplex binden kann und dadurch vom epithelialen Transport zurückhalten könnte. Daher wurde die Auswirkung einer erhöhten bzw. verringerten Soluplus[®]-Konzentration (pro Arzneistoff) auf den Transport über Caco-2 Zellen untersucht. In Transportversuchen konnte gezeigt werden, dass diese Bindung mit steigendem Soluplus[®]/Arzneistoff-Verhältnis zu einer stark verringerten Permeation führt. Aus diesem Grund ist die sprichwörtliche Empfehlung *viel hilft viel* nicht auf Arzneistoffformulierungen mit Soluplus[®] anzuwenden. Die Menge an Soluplus[®] pro Arzneistoff kann allerdings auch nur bis zu einem bestimmten Punkt reduziert werden: Wird das Hilfsstoff/Arzneistoff-Verhältnis zu klein, so kann keine stabile feste Lösung gebildet werden. In diesem Falle reicht die Soluplus[®]-Menge im Extrudat nicht aus, um eine ausreichende Löslichkeit des Arzneistoffes zu gewährleisten, daher ist das jeweilige Extrudat zumindest teilweise kristallin. Wegen der verringerten Dissolutionsrate einer solch teilkristallinen Formulierung verringert sich der Arzneistoffflux dementsprechend. Für alle drei Arzneistoffe konnte ein mehr oder weniger scharf ausgeprägtes Optimum für den Transport über Caco-2 Zellen gefunden werden. Dieses Optimum ergibt sich aus dem Zusammenspiel der Effekte Dissolutionsrate, Solubilisierung und Bindung zwischen Arzneistoff und Hilfsstoff.

In sämtlichen Teilen dieser Arbeit trat eine unspezifische Bindung zwischen Soluplus[®] und dem jeweiligen Arzneistoff bzw. P-gp-Substrat auf und hatte auch Auswirkungen auf das experimentelle Ergebnis. Aus diesem Grunde sollte eine weitere Untersuchung dieses Verhaltens in Betracht gezogen werden. Mittels Gleichgewichtsdialyse konnte gezeigt werden, dass die Bindungsstärke substanzabhängig ist und weitestgehend mit dem logP der jeweiligen Substanz korreliert. Beachtenswert ist hierbei wiederum der Ausreißer Fenofibrat, welcher auch im Tierversuch und in den Caco-2-Transportversuchen ein abweichendes Verhalten zeigte. Da Soluplus[®] die Arzneistoffe durch Mizellbildung solubilisiert, wurden diese Mizellen mittels dynamischer Lichtstreuung weiter charakterisiert. Die Mizellgröße ist temperaturabhängig, die eingeschlossenen Arzneistoffmoleküle beeinflusst

ten die Mizellgröße jedoch nicht. Ein Effekt des verwendeten Mediums und dessen Osmolarität auf die mizellaren Strukturen konnte gezeigt werden.

Diese Abhängigkeit vom verwendeten Medium wirft die Frage auf, wie sich diese Mizellen in den realen Körperflüssigkeiten verhalten. Da eine Veränderung des Mediums zu veränderten Mizellgrößen führt, so kann auch ein verändertes Bindungsverhalten zwischen Arzneistoff und Soluplus[®] vermutet werden. Dementsprechend sollte die Verwendung bio-relevanterer Transportmedien für zukünftige Studien in Betracht gezogen werden. Die simulierten Intestinalflüssigkeiten FaSSIF und FeSSIF (fasted/fed state simulated intestinal fluid) sind komplexe Medien, welche den realen Verdauungssäften im Dissolutionsverhalten ähneln. Unter anderem enthalten diese Medien Mischmizellen aus Gallensalzen und Phospholipiden [158]. Aufgrund ihrer hohen Osmolarität können diese Medien nicht direkt auf Zellen angewendet werden, allerdings können diese Medien zur Anwendung auf Zellen angepasst werden [159, 160, 161].

Ein weiterer Punkt welcher das Verhalten von Soluplus[®]-Formulierungen *in vivo* beeinflussen kann sind die Unterschiede in der Dissolution im Vergleich zum Caco-2 Modell. In unserem Versuch wurde die Auflösung der Arzneistoffe durch einfaches Rühren im Transportmedium über einen begrenzten Zeitraum durchgeführt. Die reale Situation ist sehr viel komplexer: Unter anderem verändert sich der pH während der Dissolution durch den pH-Gradienten im Gastrointestinaltrakt. Eine Möglichkeit diesen Effekt zu simulieren wäre die Verwendung eines sauren Dissolutionsmediums, um die Auflösung während der Magenpassage zu simulieren. Anschließend kann der pH dieses Mediums auf ein zellkompatibles Niveau angehoben werden [106]. Auch die Dissolution ist in der Realität nicht auf einen bestimmten Zeitraum beschränkt wie in unseren Versuchen, vielmehr können Dissolution und Arzneistoffabsorption gleichzeitig stattfinden. Um dies zu simulieren könnte in zukünftigen Versuchen ein kombiniertes Dissolutions- und Permeationssystem eingesetzt werden. Hierbei wird eine Durchflussdissolutionszelle mit einem Permeationsmodell, wie zum Beispiel Caco-2-Zellen kombiniert [97, 162]. Solch ein System könnte zu noch besseren Korrelationen des *in vivo* Verhaltens führen und könnte den Mechanismus der Bio-

verfügbarkeitsverbesserung durch Soluplus[®] noch weiter ergründen. Andererseits zeigte auch unsere recht einfache Simulation der Arzneiformauflösung sehr gute Korrelationen zur Absorption der jeweiligen Formulierungen im Tierversuch. Daher könnten diese komplexeren und damit einhergehend auch fehleranfälligeren System auch als nicht notwendig angesehen werden. Dem Prinzip von *Ockhams Rasiermesser* folgend, ist der einfachere Ansatz stets den komplexeren Systemen zu bevorzugen.

Der nächste Schritt für eine Validierung des verwendeten Caco-2 Modells als Tierversuchersatzmethode für die Absorption von Soluplus[®]-Formulierungen wäre eine Bestätigung der Daten aus dem Optimierungsansatz im Tierversuch. Falls *in vivo* Studien die Ergebnisse aus dem Caco-2 Modell bestätigen werden, könnte dieses Modell routinemäßig zur Optimierung von Soluplus[®]-Formulierungen eingesetzt werden. Dadurch könnten die Formulierungen so optimiert werden, dass eine maximal Absorption erreicht wird, was letztendlich zu einer verringerten Dosis und dadurch auch verringerten Nebenwirkungen führen könnte. Auch das höhere Ziel Tierversuche einzusparen könnte erreicht werden, wenn Caco-2 Zellen routinemäßig zur Vorhersage der intestinalen Absorption von festen Lösungen mit Soluplus[®] eingesetzt würden.

9. Bibliography

- [1] Rudolf Voigt. *Pharmazeutische Technologie*. Deutscher Apotheker Verlag, 10th edition, 2006.
- [2] Schreiner T, Schaefer UF, and Loth H. Immediate drug release from solid oral dosage forms. *Journal of Pharmaceutical Sciences*, 94(1):120–133, 2005.
- [3] Noyes A and Whitney W. The rate of solution of solid substances in their own solutions. *Journal of the American Chemical Society*, 19(12):930–934, 1897.
- [4] Dressman J, Amidon GL, Reppas C, and Shah VP. Dissolution testing as a prognostic tool for oral drug absorption: Immediate release dosage forms. *Pharmaceutical Research*, 15(1):11–22, 1998.
- [5] Gerhard Thews, Ernst Mutschler, and Peter Vaupel. *Anatomie Physiologie Pathophysiologie des Menschen*. Wissenschaftliche Verlagsgesellschaft, 5th edition, 1999.
- [6] Cummings JH, Pomare EW, Branch WJ, Naylor CPE, and Macfarlane GT. Short chain fatty acids in human large intestine, portal, hepatic and venous blood. *Gut*, 28(10):1221–1227, 1987.
- [7] Amidon GL, Lennernäs H, Shah VP, and Crison JR. A theoretical basis for a biopharmaceutic drug classification: The correlation of in vitro drug product dissolution and in vivo bioavailability. *Pharmaceutical Research*, 12(3):413–420, 1995.
- [8] US Food and Drug Administration. Guidance for Industry - Waiver of In Vivo Bioavailability and Bioequivalence Studies for Immediate-Release Solid Oral Dosage Forms Based on a Biopharmaceutics Classification System. 2000.
- [9] Dressman J and Reppas C. In vitro-in vivo correlations for lipophilic, poorly water-soluble drugs. *European Journal of Pharmaceutical Sciences*, 11(SUPPL. 2):S73–S80, 2000.
- [10] Lipinski CA, Lombardo F, Dominy BW, and Feeney PJ. Experimental and computational approaches to estimate solubility and permeability in drug discovery and development settings. *Advanced Drug Delivery Reviews*, 23(1-3):3–25, 1997.
- [11] Artursson P, Ungell AL, and Lofroth JE. Selective paracellular permeability in two models of intestinal absorption: Cultured monolayers of human intestinal epithelial cells and rat intestinal segments. *Pharmaceutical Research*, 10(8):1123–1129, 1993.
- [12] DuBuske LM. The role of P-glycoprotein and organic anion-transporting polypeptides in drug interactions. *Drug Safety*, 28(9):789–801, 2005.

- [13] Dean M, Rzhetsky A, and Allikmets R. The Human ATP-Binding Cassette (ABC) Transporter Superfamily. *Genome Research*, 11(7):1156–1166, 2001.
- [14] Hyde SC, Emsley P, Hartshorn MJ, Mimmack MM, Gileadi U, Pearce SR, Gallagher MP, Gill DR, Hubbard RE, and Higgins CF. Structural model of ATP-binding proteins associated with cystic fibrosis, multidrug resistance and bacterial transport. *Nature*, 346(6282):362–365, 1990.
- [15] Leslie EM, Deeley RG, and Cole SPC. Multidrug resistance proteins: Role of P-glycoprotein, MRP1, MRP2, and BCRP (ABCG2) in tissue defense. *Toxicology and Applied Pharmacology*, 204(3):216–237, 2005.
- [16] Gottesman MM, Fojo T, and Bates SE. Multidrug resistance in cancer: Role of ATP-dependent transporters. *Nature Reviews Cancer*, 2(1):48–58, 2002.
- [17] Leonard GD, Fojo T, and Bates SE. The role of ABC transporters in clinical practice. *The Oncologist*, 8(5):411–424, 2003.
- [18] Staud F and Pavek P. Breast cancer resistance protein (BCRP/ABCG2). *International Journal of Biochemistry and Cell Biology*, 37(4):720–725, 2005.
- [19] Juliano RL and Ling V. A surface glycoprotein modulating drug permeability in Chinese hamster ovary cell mutants. *Biochimica et Biophysica Acta (BBA) - Biomembranes*, 455(1):152–162, 1976.
- [20] Higgins CF. ABC Transporters: From microorganisms to man. *Annual Review of Cell Biology*, 8:67–113, 1992.
- [21] Aller SG, Yu J, Ward A, Weng Y, Chittaboina S, Zhuo R, Harrell PM, Trinh YT, Zhang Q, Urbatsch IL, and Chang G. Structure of P-glycoprotein reveals a molecular basis for poly-specific drug binding. *Science*, 323(5922):1718–1722, 2009.
- [22] Thiebaut F, Tsuruo T, Hamada H, Gottesman MM, Pastan I, and Willingham MC. Cellular localization of the multidrug-resistance gene product P-glycoprotein in normal human tissues. *Proceedings of the National Academy of Sciences of the United States of America*, 84(21):7735–7738, 1987.
- [23] Tamai I and Tsuji A. Drug delivery through the blood-brain barrier. *Advanced Drug Delivery Reviews*, 19(3):401–424, 1996.
- [24] Tsuji A and Tamai I. Carrier-mediated intestinal transport of drugs. *Pharmaceutical Research*, 13(7):963–977, 1996.
- [25] Wachter VJ, Salphati L, and Benet LZ. Active secretion and enterocytic drug metabolism barriers to drug absorption. *Advanced Drug Delivery Reviews*, 20(1):99–112, 1996.
- [26] Zagermann-Muncke P. Wenn Arzneistoffe Transportproteine beeinflussen. *Pharmazeutische Zeitung online*, 2011.

- [27] Werle M. Polymeric and low molecular mass efflux pump inhibitors for oral drug delivery. *Journal of Pharmaceutical Sciences*, 97(1):60–70, 2008.
- [28] Zhou S, Lim LY, and Chowbay B. Herbal Modulation of P-Glycoprotein. *Drug Metabolism Reviews*, 36(1):57–104, 2004.
- [29] Nerurkar MM, Burton PS, and Borchardt RT. The use of surfactants to enhance the permeability of peptides through caco-2 cells by inhibition of an apically polarized efflux system. *Pharmaceutical Research*, 13(4):528–534, 1996.
- [30] Rege BD, Kao JPY, and Polli JE. Effects of nonionic surfactants on membrane transporters in Caco-2 cell monolayers. *European Journal of Pharmaceutical Sciences*, 16(4–5):237–246, 2002.
- [31] Werle M. Natural and synthetic polymers as inhibitors of drug efflux pumps. *Pharmaceutical Research*, 25(3):500–511, 2008.
- [32] Varma MV, Perumal OP, and Panchagnula R. Functional role of P-glycoprotein in limiting peroral drug absorption: optimizing drug delivery. *Current Opinion in Chemical Biology*, 10(4):367–373, 2006.
- [33] Huttunen KM, Raunio H, and Rautio J. Prodrugs—from serendipity to rational design. *Pharmacological Reviews*, 63(3):750–771, 2011.
- [34] Csóka K, Dhar S, Fridborg H, Larsson R, and Nygren P. Differential activity of Cremophor EL and paclitaxel in patients' tumor cells and human carcinoma cell lines in vitro. *Cancer*, 79(6):1225–1233, 1997.
- [35] Bardelmeijer HA, Ouwehand M, Beijnen JH, Schellens JHM, and Van Tellingen O. Efficacy of novel P-glycoprotein inhibitors to increase the oral uptake of paclitaxel in mice. *Investigational New Drugs*, 22(3):219–229, 2004.
- [36] Yalkowsky SH. *Solubility and solubilization in aqueous media*. American Chemical Society, 1999.
- [37] Jain A, Ran Y, and Yalkowsky SH. Effect of pH-sodium lauryl sulfate combination on solubilization of PG-300995 (an anti-HIV agent): A technical note. *AAPS PharmSciTech*, 5(3), 2004.
- [38] Torchilin V. Structure and design of polymeric surfactant-based drug delivery systems. *Journal of Controlled Release*, 73(2–3):137–172, 2001.
- [39] Gaucher G, Satturwar P, Jones MC, Furtos A, and Leroux JC. Polymeric micelles for oral drug delivery. *European Journal of Pharmaceutics and Biopharmaceutics*, 76(2):147–158, 2010.
- [40] van Hasselt PM, Janssens GEPJ, Slot TK, van der Ham M, Minderhoud TC, Talelli M, Akkermans LM, Rijcken CJF, and van Nostrum CF. The influence of bile acids on the oral bioavailability of vitamin K encapsulated in polymeric micelles. *Journal of Controlled Release*, 133(2):161–168, 2009.

- [41] Mathot F, van Beijsterveldt L, Pr eat V, Brewster M, and Ari en A. Intestinal uptake and biodistribution of novel polymeric micelles after oral administration. *Journal of Controlled Release*, 111(1-2):47-55, 2006.
- [42] Bromberg L. Polymeric micelles in oral chemotherapy. *Journal of Controlled Release*, 128(2):99-112, 2008.
- [43] Strickley RG. Solubilizing Excipients in Oral and Injectable Formulations. *Pharmaceutical Research*, 21(2):201-230, 2004.
- [44] Jones MC and Leroux JC. Polymeric micelles - A new generation of colloidal drug carriers. *European Journal of Pharmaceutics and Biopharmaceutics*, 48(2):101-111, 1999.
- [45] BASF SE. Soluplus - Technical Information. Technical report, 2010.
- [46] Chiou W and Riegelman S. Pharmaceutical applications of solid dispersion systems. *Journal of Pharmaceutical Sciences*, 60(9):1281-1302, 1971.
- [47] Maegerlein M. Solid dispersions of poorly water soluble substances - a challenge for analytical development. *Innovative Drug Delivery Technologien zur Verbesserung der Bioverf ugbarkeit APV- Kurs Ludwigshafen (2005)*, 2005.
- [48] Leuner C and Dressman J. Improving drug solubility for oral delivery using solid dispersions. *European Journal of Pharmaceutics and Biopharmaceutics*, 50(1):47-60, 2000.
- [49] Tachibana T and Nakamura A. A methode for preparing an aqueous colloidal dispersion of organic materials by using water-soluble polymers: Dispersion of B-carotene by polyvinylpyrrolidone. *Kolloid-Zeitschrift & Zeitschrift f ur Polymere*, 203(2):130-133, 1965.
- [50] Betageri GV and Makarla KR. Enhancement of dissolution of glyburide by solid dispersion and lyophilization techniques. *International Journal of Pharmaceutics*, 126(1-2):155-160, 1995.
- [51] Lo WY and Law SL. Dissolution behavior of griseofulvin solid dispersions using polyethylene glycol, talc, and their combination as dispersion carriers. *Drug Development and Industrial Pharmacy*, 22(3):231-236, 1996.
- [52] Sekiguchi K and Obi N. Studies on absorption of eutectic mixture. I. A comparison of the behavior of eutectic mixture of sulfathiazole and that of ordinary sulfathiazole in man. *Chemical and Pharmaceutical Bulletin*, 9:866-872, 1961.
- [53] Sekiguchi K, Obi N, and Ueda Y. Studies on absorption of eutectic mixture. II. Absorption of fused conglomerates of chloramphenicol and urea in rabbits. *Chemical & pharmaceutical bulletin*, 12:134-144, 1964.
- [54] Chiou WL and Riegelman S. Preparation and dissolution characteristics of several fast-release solid dispersions of griseofulvin. *Journal of Pharmaceutical Sciences*, (12):1505-1510.

- [55] Kanig JL. Properties of fused mannitol in compressed tablets. *Journal of Pharmaceutical Sciences*, 53:188–192, 1964.
- [56] Zhu Y, Shah NH, Malick AW, Infeld MH, and McGinity JW. Solid-state plasticization of an acrylic polymer with chlorpheniramine maleate and triethyl citrate. *International Journal of Pharmaceutics*, 241(2):301–310, 2002.
- [57] Ghebremeskel AN, Vemavarapu C, and Lodaya M. Use of surfactants as plasticizers in preparing solid dispersions of poorly soluble API: Selection of polymer-surfactant combinations using solubility parameters and testing the processability. *International Journal of Pharmaceutics*, 328(2):119–129, 2007.
- [58] Crowley MM, Zhang F, Repka MA, Thumma S, Upadhye SB, Battu SK, McGinity JW, and Martin C. Pharmaceutical applications of hot-melt extrusion: Part I. *Drug Development and Industrial Pharmacy*, 33(9):909–926, 2007.
- [59] el Egaakey MA, Soliva M, and Speiser P. Hot extruded dosage forms. I. Technology and dissolution kinetics of polymeric matrices. *Pharmaceutica Acta Helveticae*, 46(1):31–52, 1971.
- [60] Repka MA, Battu SK, Upadhye SB, Thumma S, Crowley MM, Zhang F, Martin C, and McGinity JW. Pharmaceutical applications of hot-melt extrusion: Part II. *Drug Development and Industrial Pharmacy*, 33(10):1043–1057, 2007.
- [61] Breitenbach J. Melt extrusion: from process to drug delivery technology. *European Journal of Pharmaceutics and Biopharmaceutics*, 54(2):107–117, 2001.
- [62] Kolter K, Karl M, Nalawade S, and Rottmann N. Hot-Melt Extrusion with BASF Pharma Polymers - Extrusion Compendium, 2010.
- [63] Forster A, Hempenstall J, Tucker I, and Rades T. Selection of excipients for melt extrusion with two poorly water-soluble drugs by solubility parameter calculation and thermal analysis. *International Journal of Pharmaceutics*, 226(1–2):147–161, 2001.
- [64] Forster A, Hempenstall J, and Rades T. Characterization of glass solutions of poorly water-soluble drugs produced by melt extrusion with hydrophilic amorphous polymers. *Journal of Pharmacy and Pharmacology*, 53(3):303–315, 2001.
- [65] Hidalgo IJ, Raub TJ, and Borchardt RT. Characterization of the human colon carcinoma cell line (Caco-2) as a model system for intestinal epithelial permeability. *Gastroenterology*, 96(3):736–749, 1989.
- [66] Artursson P. Epithelial transport of drugs in cell culture. I: A model for studying the passive diffusion of drugs over intestinal absorptive (Caco-2) cells. *Journal of Pharmaceutical Sciences*, 79(6):476–482, 1990.
- [67] Yee S. In vitro permeability across Caco-2 cells (colonic) can predict in vivo (small intestinal) absorption in man - Fact or myth. *Pharmaceutical Research*, 14(6):763–766, 1997.

- [68] Bailey CA, Bryla P, and Malick AW. The use of the intestinal epithelial cell culture model, Caco-2, in pharmaceutical development. *Advanced Drug Delivery Reviews*, 22(1-2):85-103, 1996.
- [69] Sambruy Y, Ferruzza S, Ranaldi G, and De Angelis I. Intestinal cell culture models: Applications in toxicology and pharmacology. *Cell Biology and Toxicology*, 17(4-5):301-317, 2001.
- [70] Custodio JM, Wu CY, and Benet LZ. Predicting drug disposition, absorption / elimination / transporter interplay and the role of food on drug absorption. *Advanced Drug Delivery Reviews*, 60(6):717-733, 2008.
- [71] Rubas W, Jezyk N, and Grass GM. Comparison of the permeability characteristics of a human colonic epithelial (Caco-2) cell line to colon of rabbit, monkey, and dog intestine and human drug absorption. *Pharmaceutical Research*, 10(1):113-118, 1993.
- [72] Lennernäs H, Palm K, Fagerholm U, and Artursson P. Comparison between active and passive drug transport in human intestinal epithelial (Caco-2) cells in vitro and human jejunum in vivo. *International Journal of Pharmaceutics*, 127(1):103-107, 1996.
- [73] Pinto M, Leon SR, and Appay MD. Enterocyte-like differentiation and polarization of the human colon carcinoma cell line Caco-2 in culture. *Biology of the Cell*, 47(3):323-330, 1983.
- [74] Artursson P, Palm K, and Luthman K. Caco-2 monolayers in experimental and theoretical predictions of drug transport. *Advanced Drug Delivery Reviews*, 46(1-3):27-43, 2001.
- [75] Hilgendorf C, Ahlin G, Seithel A, Artursson P, Ungell AL, and Karlsson J. Expression of thirty-six drug transporter genes in human intestine, liver, kidney, and organotypic cell lines. *Drug Metabolism and Disposition*, 35(8):1333-1340, 2007.
- [76] Sun H, Chow ECY, Liu S, Du Y, and Pang KS. The Caco-2 cell monolayer: Usefulness and limitations. *Expert Opinion on Drug Metabolism and Toxicology*, 4(4):395-411, 2008.
- [77] Thummel KE, Brimer C, Yasuda K, Thottassery J, Senn T, Lin Y, Ishizuka H, Kharasch E, Schuetz J, and Schuetz E. Transcriptional control of intestinal cytochrome P-4503A by 1 α ,25-dihydroxy vitamin D3. *Molecular Pharmacology*, 60(6):1399-1406, 2001.
- [78] Brimer C, Dalton JT, Zhu Z, Schuetz J, Yasuda K, Vanin E, Relling MV, Lu Y, and Schuetz EG. Creation of polarized cells coexpressing CYP3A4, NADPH cytochrome P450 reductase and MDR1/P-glycoprotein. *Pharmaceutical Research*, 17(7):803-810, 2000.
- [79] MacAdam A. The effect of gastro-intestinal mucus on drug absorption. *Advanced Drug Delivery Reviews*, 11(3):201-220, 1993.

- [80] Hou SYE, Cowles VE, and Berner B. Gastric retentive dosage forms: A review. *Critical Reviews in Therapeutic Drug Carrier Systems*, 20(6):461–497, 2003.
- [81] Nollevaux G, Devillé C, El Moualij B, Zorzi W, Deloyer P, Schneider YJ, Peulen O, and Dandrifosse G. Development of a serum-free co-culture of human intestinal epithelium cell-lines (Caco-2/HT29-5M21). *BMC Cell Biology*, 7, 2006.
- [82] Mahler GJ, Shuler ML, and Glahn RP. Characterization of Caco-2 and HT29-MTX cocultures in an in vitro digestion/cell culture model used to predict iron bioavailability. *Journal of Nutritional Biochemistry*, 20(7):494–502, 2009.
- [83] Hilgendorf C, Spahn-Langguth H, Regardh CG, Lipka E, Amidon GL, and Langguth P. Caco-2 versus Caco-2/HT29-MTX co-cultured cell lines: Permeabilities via diffusion, inside- and outside-directed carrier-mediated transport. *Journal of Pharmaceutical Sciences*, 89(1):63–75, 2000.
- [84] Hardung H, Djuric D, and Ali S. Combining HME & solubilization: Soluplus® - The solid solution. *Drug Delivery Technology*, 10(3):20–27, 2010.
- [85] Hong JY, Kim JK, Song YK, Park JS, and Kim CK. A new self-emulsifying formulation of itraconazole with improved dissolution and oral absorption. *Journal of Controlled Release*, 110(2):332–338, 2006.
- [86] Rabinow BE. Nanosuspensions in drug delivery. *Nature Reviews Drug Discovery*, 3(9):785–796, 2004.
- [87] Vogt M, Kunath K, and Dressman J. Dissolution improvement of four poorly water soluble drugs by cogrinding with commonly used excipients. *European Journal of Pharmaceutics and Biopharmaceutics*, 68(2):330–337, 2008.
- [88] Meng X, Chen Y, Chowdhury SR, Yang D, and Mitra S. Stabilizing dispersions of hydrophobic drug molecules using cellulose ethers during anti-solvent synthesis of micro-particulates. *Colloids and Surfaces B-Biointerfaces*, 70(1):7–14, 2009.
- [89] Yi Y, Yoon H, Kim B, Shim M, Kim SO, Hwang SJ, and Seo M. A mixed polymeric micellar formulation of itraconazole: Characteristics, toxicity and pharmacokinetics. *Journal of Controlled Release*, 117(1):59–67, 2007.
- [90] Peeters J, Neeskens P, Tollenaere JP, Van Remoortere P, and Brewster M. Characterization of the interaction of 2-hydroxypropyl-beta-cyclodextrin with itraconazole at pH 2, 4, and 7. *Journal of Pharmaceutical Sciences*, 91(6):1414–1422, 2002.
- [91] Buckett WM, Saleh A, Tulandi T, and Tan SL. Endometriosis: Critical assessment of current therapies. *Current Obstetrics and Gynaecology*, 8(4):204–208, 1998.
- [92] Liversidge GG and Cundy KC. Particle size reduction for improvement of oral bioavailability of hydrophobic drugs: I. Absolute oral bioavailability of nanocrystalline danazol in beagle dogs. *International Journal of Pharmaceutics*, 125(1):91–97, 1995.

- [93] Hu J, Johnston KP, and Williams III RO. Rapid dissolving high potency danazol powders produced by spray freezing into liquid process. *International Journal of Pharmaceutics*, 271(1-2):145-154, 2004.
- [94] Overhoff KA, Engstrom JD, Chen B, Scherzer BD, Milner TE, Johnston KP, and Williams III RO. Novel ultra-rapid freezing particle engineering process for enhancement of dissolution rates of poorly water-soluble drugs. *European Journal of Pharmaceutics and Biopharmaceutics*, 65(1):57-67, 2007.
- [95] Sant V, Smith D, and Leroux JC. Enhancement of oral bioavailability of poorly water-soluble drugs by poly(ethylene glycol)-block-poly(alkyl acrylate-co-methacrylic acid) self-assemblies. *Journal of Controlled Release*, 104(2):289-300, 2005.
- [96] Vogt M, Kunath K, and Dressman J. Dissolution enhancement of fenofibrate by micronization, cogrinding and spray-drying: Comparison with commercial preparations. *European Journal of Pharmaceutics and Biopharmaceutics*, 68(2):283-288, 2008.
- [97] Buch P, Langguth P, Kataoka M, and Yamashita S. IVIVC in oral absorption for fenofibrate immediate release tablets using a dissolution/permeation system. *Journal of Pharmaceutical Sciences*, 98(6):2001-2009, 2009.
- [98] Jaruratanasirikul S and Sriwiriyan S. Effect of omeprazole on the pharmacokinetics of itraconazole. *European Journal of Clinical Pharmacology*, 54(2):159-161, 1998.
- [99] Six K, Berghmans H, Leuner C, Dressman J, Van Werde K, Mullens J, Benoist L, Thimon M, Meublart L, Verreck G, Peeters J, Brewster M, and Van den Mooter G. Characterization of Solid Dispersions of Itraconazole and Hydroxypropylmethylcellulose Prepared by Melt Extrusion, Part II. *Pharmaceutical Research*, 20(7):1047-1054, 2003.
- [100] Miller DA, DiNunzio JC, Yang W, McGinity JW, and Williams III RO. Targeted intestinal delivery of supersaturated itraconazole for improved oral absorption. *Pharmaceutical Research*, 25(6):1450-1459, 2008.
- [101] Buchanan CM, Buchanan NL, Edgar KJ, Klein S, Little JL, Ramsey MG, Ruble KM, Wacher VJ, and Wempe MF. Pharmacokinetics of itraconazole after intravenous and oral dosing of itraconazole-cyclodextrin formulations. *Journal of Pharmaceutical Sciences*, 96(11):3100-3116, 2007.
- [102] Yamashita S, Furubayashi T, Kataoka M, Sakane T, Sezaki H, and Tokuda H. Optimized conditions for prediction of intestinal drug permeability using Caco-2 cells. *European Journal of Pharmaceutical Sciences*, 10(3):195-204, 2000.
- [103] Collnot EM, Baldes C, Wempe MF, Hyatt J, Navarro L, Edgar KJ, Schaefer UF, and Lehr CM. Influence of vitamin E TPGS poly(ethylene glycol) chain length on apical efflux transporters in Caco-2 cell monolayers. *Journal of Controlled Release*, 111(1-2):35-40, 2006.

- [104] Thanou MM, Verhoef JC, Romeijn SG, Nagelkerke JF, Merkus FWHM, and Junginger HE. Effects of N-trimethyl chitosan chloride, a novel absorption enhancer, on Caco-2 intestinal epithelia and the ciliary beat frequency of chicken embryo trachea. *International Journal of Pharmaceutics*, 185(1):73–82, 1999.
- [105] Komura H and Iwaki M. Pitfalls in high throughput screening for drug absorption optimization in drug discovery. *Current Analytical Chemistry*, 3(4):302–309, 2007.
- [106] Mellaerts R, Mols R, Kayaert PJ, Annaert P, Van Humbeeck J, Van den Mooter G, Martens JA, and Augustijns P. Ordered mesoporous silica induces pH-independent supersaturation of the basic low solubility compound itraconazole resulting in enhanced transepithelial transport. *International Journal of Pharmaceutics*, 357(1–2):169–79, 2008.
- [107] Brodie RR, Chasseaud LF, and Elson FF. Antilipidemic drugs. Part IV: The metabolic fate of the hypolipidemic agent isopropyl [4' (p chlorobenzoyl) 2 phenoxy 2 methyl] propionate (LF 178) in rats, dogs and man. *Arzneimittel-Forschung / Drug Research*, 26(5):896–901, 1976.
- [108] Weil A, Caldwell J, and Strolin-Benedetti M. The metabolism and disposition of fenofibrate in rat, guinea pig, and dog. *Drug Metabolism and Disposition*, 16(2):302–309, 1988.
- [109] Takahashi Y, Kondo H, Yasuda T, Watanabe T, Kobayashi SI, and Yokohama S. Common solubilizers to estimate the Caco-2 transport of poorly water-soluble drugs. *International Journal of Pharmaceutics*, 246(1–2):85–94, 2002.
- [110] Chu K and Yalkowsky SH. An interesting relationship between drug absorption and melting point. *International Journal of Pharmaceutics*, 373(1–2):24–40, 2009.
- [111] Balfour J, McTavish D, and Heel R. Fenofibrate: A Review of its Pharmacodynamic and Pharmacokinetic Properties and Therapeutic Use in Dyslipidaemia. *Drugs*, 40(2), 1990.
- [112] Sauron R, Wilkins M, Jessent V, Dubois A, Maillot C, and Weil A. Absence of a food effect with a 145 mg nanoparticle fenofibrate tablet formulation. *International Journal of Clinical Pharmacology and Therapeutics*, 44(2):64–70, 2006.
- [113] Charman WN, Rogge MC, Boddy AW, and Berger BM. Effect of food and a monoglyceride emulsion formulation on danazol bioavailability. *Journal of Clinical Pharmacology*, 33(4):381–386, 1993.
- [114] De Beule K and Van Gestel J. Pharmacology of itraconazole. *Drugs*, 61(SUPPL. 1):27–37, 2001.
- [115] Schmidt LE and Dalhoff K. Food-drug interactions. *Drugs*, 62(10):1481–1502, 2002.
- [116] Chapman M. Pharmacology of fenofibrate. *American Journal of Medicine*, 83(5, Supplement 2):21–25, 1987.

- [117] Dintaman JM and Silverman JA. Inhibition of P-glycoprotein by D-alpha-tocopheryl polyethylene glycol 1000 succinate (TPGS). *Pharmaceutical Research*, 16(10):1550–1556, 1999.
- [118] Balayssac D, Authier N, Cayre A, and Coudore F. Does inhibition of P-glycoprotein lead to drug-drug interactions? *Toxicology Letters*, 156(3):319–329, 2005.
- [119] Oda M, Saitoh H, Kobayashi M, and Aungst BJ. β -Cyclodextrin as a suitable solubilizing agent for in situ absorption study of poorly water-soluble drugs. *International Journal of Pharmaceutics*, 280(1–2):95–102, 2004.
- [120] Shah RB, Palamakula A, and Khan MA. Cytotoxicity Evaluation of Enzyme Inhibitors and Absorption Enhancers in Caco-2 Cells for Oral Delivery of Salmon Calcitonin. *Journal of Pharmaceutical Sciences*, 93(4):1070–1082, 2004.
- [121] Johnson BM, Charman WN, and Porter CJH. An in vitro examination of the impact of polyethylene glycol 400, Pluronic P85, and vitamin E d- α -tocopheryl polyethylene glycol 1000 succinate on P-glycoprotein efflux and enterocyte-based metabolism in excised rat intestine. *AAPS PharmSci*, 4(4), 2002.
- [122] Zuo Z, Kwon G, Stevenson B, Diakur J, and Wiebe LI. Flutamide-hydroxypropyl-beta-cyclodextrin complex: formulation, physical characterization, and absorption studies using the Caco-2 in vitro model. *Journal of Pharmacy & Pharmaceutical Sciences*, 3(2):220–227, 2000.
- [123] Honda Y, Ushigome F, Koyabu N, Morimoto S, Shoyama Y, Uchiumi T, Kuwano M, Ohtani H, and Sawada Y. Effects of grapefruit juice and orange juice components on P-glycoprotein- and MRP2-mediated drug efflux. *British Journal of Pharmacology*, 143(7):856–864, 2004.
- [124] Izzo AA and Ernst E. Interactions between herbal medicines and prescribed drugs: A systematic review. *Drugs*, 61(15):2163–2175, 2001.
- [125] Jodoin J, Demeule M, and Béliveau R. Inhibition of the multidrug resistance P-glycoprotein activity by green tea polyphenols. *Biochimica et Biophysica Acta - Molecular Cell Research*, 1542(1–3):149–159, 2001.
- [126] Bansal T, Akhtar N, Jaggi M, Khar RK, and Talegaonkar S. Novel formulation approaches for optimising delivery of anticancer drugs based on P-glycoprotein modulation. *Drug Discovery Today*, 14(21–22):1067–1074, 2009.
- [127] Shono Y, Fujita T, and Yamamoto A. Improvement of intestinal absorption of drugs as P-glycoprotein substrate by various surfactants. *Proceedings of the Controlled Release Society*, (25):677–678, 1998.
- [128] Shono Y, Nishihara H, Matsuda Y, Furukawa S, Okada N, Fujita T, and Yamamoto A. Modulation of Intestinal P-Glycoprotein Function by Cremophor EL and Other Surfactants by an In Vitro Diffusion Chamber Method Using the Isolated Rat Intestinal Membranes. *Journal of Pharmaceutical Sciences*, 93(4):877–885, 2004.

- [129] Sikic BI. New approaches in cancer treatment. *Annals of Oncology*, 10(Supplement 6):S149–S153, 1999.
- [130] Prieto P, Hoffmann S, Tirelli V, Tancredi F, González I, Bermejo M, and De Angelis I. An exploratory study of two Caco-2 cell models for oral absorption: A report on their within-laboratory and between-laboratory variability, and their predictive capacity. *ATLA Alternatives to Laboratory Animals*, 38(5):367–386, 2010.
- [131] Augustijns PF, Bradshaw TP, Gan LSL, Hendren RW, and Thakker DR. Evidence for a polarized efflux system in Caco-2 cells capable of modulating cyclosporin A transport. *Biochemical and Biophysical Research Communications*, 197(2):360–365, 1993.
- [132] Hunter J, Jepson MA, Tsuruo T, Simmons NL, and Hirst BH. Functional expression of P-glycoprotein in apical membranes of human intestinal Caco-2 cells. Kinetics of vinblastine secretion and interaction with modulators. *Journal of Biological Chemistry*, 268(20):14991–14997, 1993.
- [133] Bakos E, Evers R, Szakacs G, Tusnady GE, Welker E, Szabo K, De Haas M, Van Deemter L, Borst P, Varadi A, and Sarkadi B. Functional multidrug resistance protein (MRP1) lacking the N-terminal transmembrane domain. *Journal of Biological Chemistry*, 273(48):32167–32175, 1998.
- [134] Evers R, Kool M, Smith AJ, Van Deemter L, De Haas M, and Borst P. Inhibitory effect of the reversal agents V-104, GF120918 and pluronic L61 on MDR1 Pgp-, MRP1-, MRP2-mediated transport. *British Journal of Cancer*, 83(3):366–374, 2000.
- [135] Louvard D. Apical membrane aminopeptidase appears at site of cell-cell contact in cultured kidney epithelial cells. *Proceedings of the National Academy of Sciences of the United States of America*, 77(7 II):4132–4136, 1980.
- [136] Marschütz MK, Caliceti P, and Bernkop-Schnürch A. Design and in vivo evaluation of an oral delivery system for insulin. *Pharmaceutical Research*, 17(12):1468–1474, 2000.
- [137] Bernkop-Schnürch A. The use of inhibitory agents to overcome the enzymatic barrier to perorally administered therapeutic peptides and proteins. *Journal of Controlled Release*, 52(1–2):1–16, 1998.
- [138] Morishita M, Morishita I, Takayama K, Machida Y, and Nagai T. Novel oral microspheres of insulin with protease inhibitor protecting from enzymatic degradation. *International Journal of Pharmaceutics*, 78(1):1–7, 1992.
- [139] Birk Y. The Bowman-Birk inhibitor. Trypsin- and chymotrypsin-inhibitor from soybeans. *International Journal of Peptide and Protein Research*, 25(2):113–131, 1985.
- [140] Parellada J and Guinea M. Flavonoid inhibitors of trypsin and leucine aminopeptidase: A proposed mathematical model for IC50 estimation. *Journal of Natural Products*, 58(6):823–829, 1995.

- [141] Luessen HL, Verhoef JC, Borchard G, Lehr CM, De Boer AG, and Junginger HE. Mucoadhesive polymers in peroral peptide drug delivery. II. Carbomer and polycarboxophil are potent inhibitors of the intestinal proteolytic enzyme trypsin. *Pharmaceutical Research*, 12(9):1293–1298, 1995.
- [142] Eagling VA, Profit L, and Back DJ. Inhibition of the CYP3A4-mediated metabolism and P-glycoprotein-mediated transport of the HIV-I protease inhibitor saquinavir by grapefruit juice components. *British Journal of Clinical Pharmacology*, 48(4):543–552, 1999.
- [143] Kajikawa T, Mishima HK, Murakami T, and Takano M. Role of P-glycoprotein in distribution of rhodamine 123 into aqueous humor in rabbits. *Current Eye Research*, 18(3):240–246, 1999.
- [144] Lentz KA, Polli JW, Wring SA, Humphreys JE, and Polli JE. Influence of passive permeability on apparent P-glycoprotein kinetics. *Pharmaceutical Research*, 17(12):1456–1460, 2000.
- [145] Neuhoff S, Ungell AL, Zamora I, and Artursson P. pH-dependent bidirectional transport of weakly basic drugs across Caco-2 monolayers: Implications for drug-drug interactions. *Pharmaceutical Research*, 20(8):1141–1148, 2003.
- [146] Troutman MD and Thakker DR. Efflux ratio cannot assess P-glycoprotein-mediated attenuation of absorptive transport: Asymmetric effect of P-glycoprotein on absorptive and secretory transport across Caco-2 cell monolayers. *Pharmaceutical Research*, 20(8):1200–1209, 2003.
- [147] Li J, Volpe DA, Wang Y, Zhang W, Bode C, Owen A, and Hidalgo IJ. Use of transporter knockdown caco-2 cells to investigate the in vitro efflux of statin drugs. *Drug Metabolism and Disposition*, 39(7):1196–1202, 2011.
- [148] Takara K, Tsujimoto M, Ohnishi N, and Yokoyama T. Digoxin up-regulates MDR1 in human colon carcinoma Caco-2 cells. *Biochemical and Biophysical Research Communications*, 292(1):190–194, 2002.
- [149] Takara K, Tsujimoto M, Ohnishi N, and Yokoyama T. Effects of continuous exposure to digoxin on MDR1 function and expression in Caco-2 cells. *Journal of Pharmacy and Pharmacology*, 55(5):675–681, 2003.
- [150] Pascaud C, Garrigos M, and Orlowski S. Multidrug resistance transporter P-glycoprotein has distinct but interacting binding sites for cytotoxic drugs and reversing agents. *Biochemical Journal*, 333(2):351–358, 1998.
- [151] Shapiro AB and Ling V. Positively cooperative sites for drug transport by P-glycoprotein with distinct drug specificities. *European Journal of Biochemistry*, 250(1):130–137, 1997.
- [152] Troutman MD and Thakker DR. Rhodamine 123 requires carrier-mediated influx for its activity as a P-glycoprotein substrate in Caco-2 cells. *Pharmaceutical Research*, 20(8):1192–1199, 2003.

- [153] Lowes S, Cavet ME, and Simmons NL. Evidence for a non-MDR1 component in digoxin secretion by human intestinal Caco-2 epithelial layers. *European Journal of Pharmacology*, 458(1-2):49-56, 2003.
- [154] Siissalo S, Hannukainen J, Kolehmainen J, Hirvonen J, and Kaukonen AM. A Caco-2 cell based screening method for compounds interacting with MRP2 efflux protein. *European Journal of Pharmaceutics and Biopharmaceutics*, 71(2):332-338, 2009.
- [155] Twentyman PR, Rhodes T, and Rayner S. A comparison of rhodamine 123 accumulation and efflux in cells with P-glycoprotein-mediated and MRP-associated multidrug resistance phenotypes. *European Journal of Cancer Part A: General Topics*, 30(9):1360-1369, 1994.
- [156] Huang J, Si L, Jiang L, Fan Z, Qiu J, and Li G. Effect of pluronic F68 block copolymer on P-glycoprotein transport and CYP3A4 metabolism. *International Journal of Pharmaceutics*, 356(1-2):351-353, 2008.
- [157] Reseland JE, Holm H, Jacobsen MB, Jenssen TG, and Hanssen LE. Proteinase inhibitors induce selective stimulation of human trypsin and chymotrypsin secretion. *Journal of Nutrition*, 126(3):634-642, 1996.
- [158] Galia E, Nicolaidis E, Hörter D, Löbenberg R, Reppas C, and Dressman J. Evaluation of various dissolution media for predicting In vivo performance of class I and II drugs. *Pharmaceutical Research*, 15(5):698-705, 1998.
- [159] Ingels F, Beck B, Oth M, and Augustijns P. Effect of simulated intestinal fluid on drug permeability estimation across Caco-2 monolayers. *International Journal of Pharmaceutics*, 274(1-2):221-232, 2004.
- [160] Fossati L, Dechaume R, Hardillier E, Chevillon D, Prevost C, Bolze S, and Maubon N. Use of simulated intestinal fluid for Caco-2 permeability assay of lipophilic drugs. *International Journal of Pharmaceutics*, 360(1-2):148-155, 2008.
- [161] Ingels F, Deferme S, Destexhe E, Oth M, Van Den Mooter G, and Augustijns P. Simulated intestinal fluid as transport medium in the Caco-2 cell culture model. *International Journal of Pharmaceutics*, 232(1-2):183-192, 2002.
- [162] Motz SA, Klimundová J, Schaefer UF, Balbach S, Eichinger T, Solich P, and Lehr CM. Automated measurement of permeation and dissolution of propranolol HCl tablets using sequential injection analysis. *Analytica Chimica Acta*, 581(1):174-180, 2007.
- [163] Filipe V, Hawe A, and Jiskoot W. Critical evaluation of nanoparticle tracking analysis (NTA) by NanoSight for the measurement of nanoparticles and protein aggregates. *Pharmaceutical Research*, 27(5):796-810, 2010.

A. Characterization of Soluplus[®] micelles

Introduction

As described in Chapter 6, the drug transport across Caco-2 cells is dependent on an entrapment of the respective drug in micelles formed by Soluplus[®]. For further investigations of this behavior the micelle size at different conditions was studied by dynamic light scattering (DLS). All measurements were performed using a Malvern Zetasizer Nano ZS (Malvern Instruments GmbH, Herrenberg, Germany).

Analytic ultracentrifugation was performed at BASF SE (Dr. Wendel Wohlleben, Volodymyr Boyko) on a Beckman XLI/XLA ultracentrifuge with absorption and interference optics at a rotation speed of 60,000 rpm and a temperature of 23 °C.

Temperature effects on micelle size

By increasing temperature the micelle size strongly increases until the lower crystalline solution temperature (LCST) is reached (Figure A.1). For temperatures above the LCST, the measured size slightly decreases probably to aggregation of Soluplus[®] micelles to solid particles.

Concentration effects on micelle size

Increasing Soluplus[®] concentrations have no influence on the micellar size at a temperature of 25 °C and the size is stable at around 66 nm. At 37 °C the micelle size increases with increasing concentration (Figure A.2). The polydispersity increases which is also expressed by the appearance of double-peaks in DLS size-intensity plots (Figure A.3). These double-peaks might also be an indicator for the formation of rod-like or layered structures. A beginning aggregation at this point close to the LCST of 40 °C is probable.

Effects of osmolarity on micelle size

The osmolarity of a 1 % Soluplus[®] solution was changed, by addition of either NaCl or glucose. As shown in Figure A.4, increasing concentrations of NaCl or glucose lead to shifted

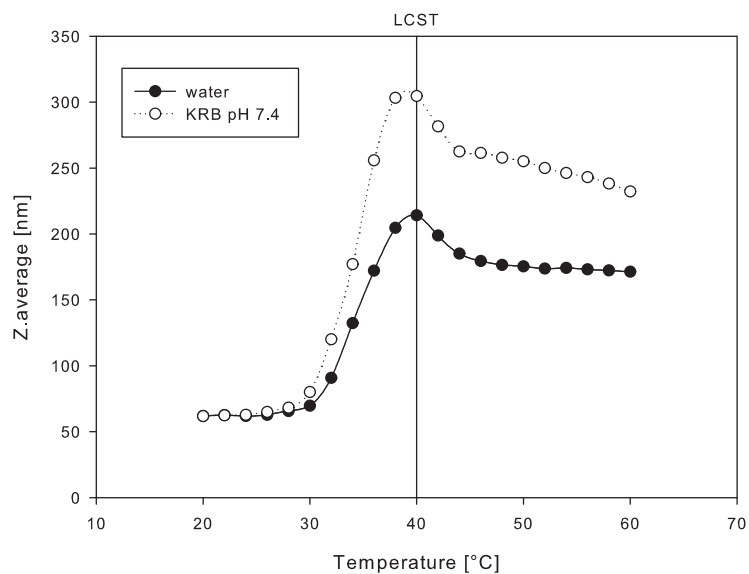


Figure A.1.: Temperature/size plot of Soluplus[®] micelles solved either in water or Krebs Ringer buffer pH 7.4 (concentration: 1 % (w/w)). Lower crystalline solution temperature (LCST) is marked by the vertical line.

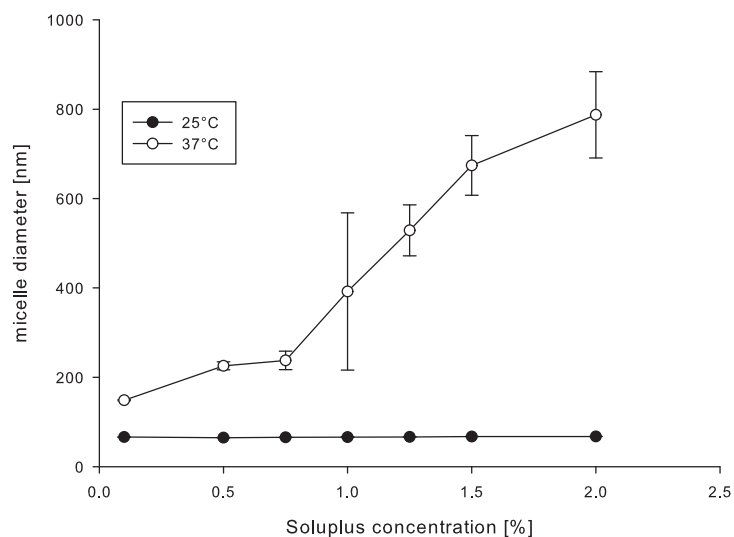


Figure A.2.: Concentration dependence of Soluplus[®] micelles at 25 °C and 37 °C.

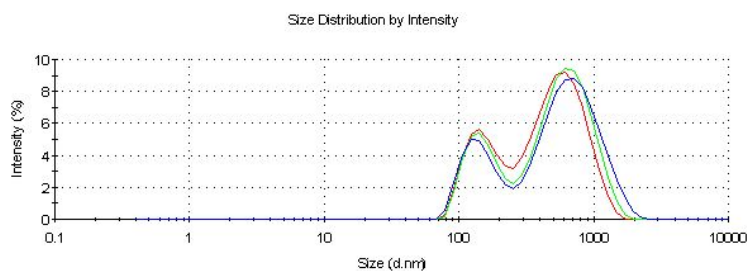


Figure A.3.: DLS size/intensity plot of 1.5 % Soluplus[®] solution (n=3).

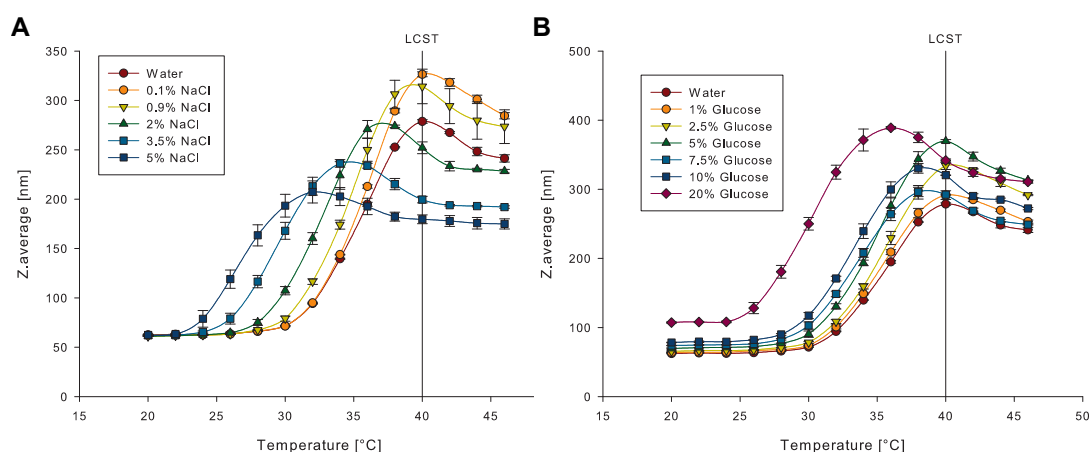


Figure A.4.: A: Addition of the ionic additive NaCl leads to shifted temperature/size curves and reduced LCST B: Addition of the non-ionic additive glucose shifts curves to lower temperatures and higher micellar sizes. n=3; mean \pm SD

temperature/size plots. For both additives, the curves are shifted to lower temperatures for increasing concentrations (Figure A.5 A). While for the non-ionic additive glucose the micelle size at 37 °C is slightly increasing, for the ionic additive sodium chloride the micelle size at body temperature decreases for hypertonic conditions (Figure A.5 B). As shown before, the maximal size is located at the LCST, therefore a shift of the LCST to lower temperatures can be assumed for high NaCl concentrations (> 2 %).

Effects of drug load on micelle size

DLS measurements showed no or only slight differences in the micellar size, whether the micelles were drug loaded or not (Figure A.6).

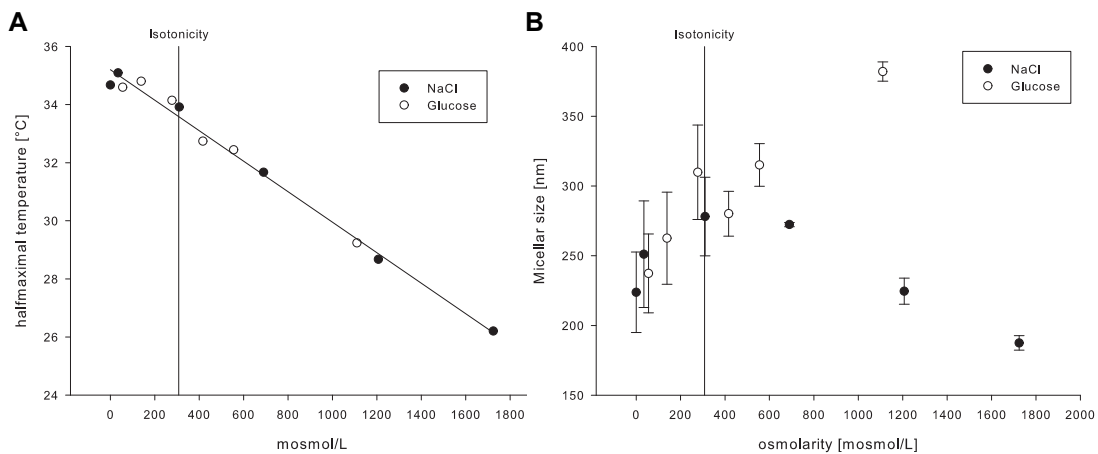


Figure A.5.: A: Half-maximal temperatures of Plot A.4 versus osmolarity. B: Micelle size at 37 °C is not only dependent on the osmolarity, but also on the used additive.

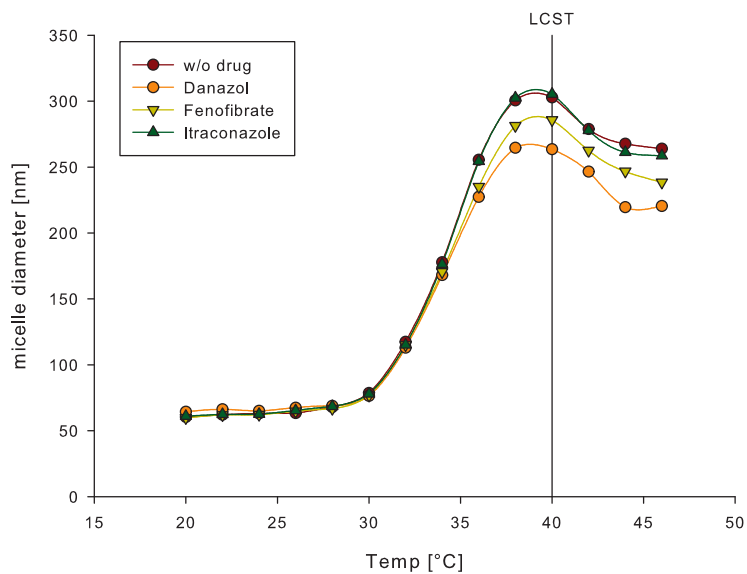


Figure A.6.: Temperature/size plot of SoluPlus[®] micelles with and without solubilized drug.

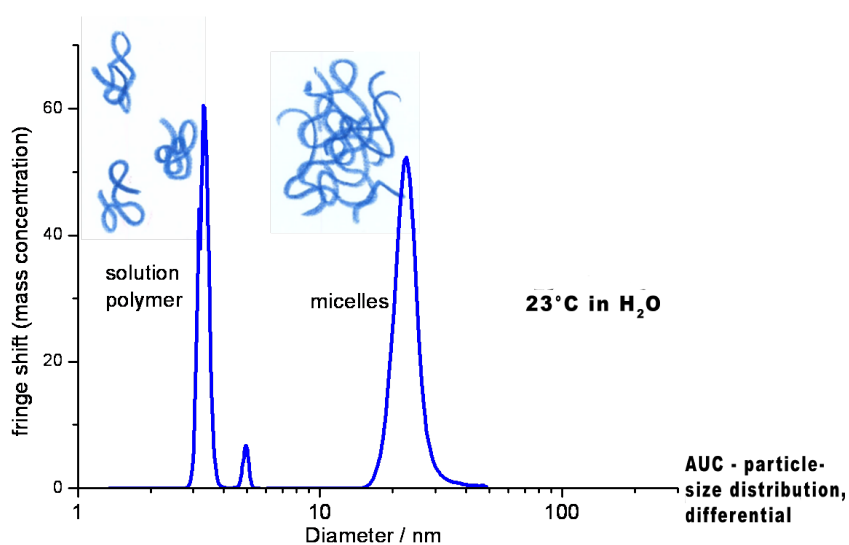


Figure A.7.: Analytical ultracentrifugation of Soluplus[®] in H₂O. Micelles and free solved polymer can be observed.

Analytical ultracentrifugation

By the time this work was written only preliminary data of the analytical ultracentrifugation (AUC) was available. However, also this preliminary data gives us hints for a better understanding how Soluplus[®] micelles act in solution.

Analytical ultracentrifugation of pure Soluplus[®] (1 %) offered two forms of the polymer in solution: First, micelles of a diameter between 20 nm and 30 nm and second, solved polymer, probably monomers, at a size of around 3 nm (Figure A.7).

Analytical ultracentrifugation of itraconazole-loaded micelles showed a changed behavior. In this experiment, a solid solution containing 15 % itraconazole was dissolved to a final Soluplus[®] concentration of 1 %. While Soluplus[®] alone showed a bimodal distribution, the distribution is trimodal by addition of itraconazole (Figure A.8). By selective UVVIS-AUC it was possible to distinguish the drug content in the centrifugation plot. According to this measurement the drug was only present in the biggest structures. Further analysis of the AUC plot showed that in this big drug-loaded structures, the ratio between excipient and API is approximately 1:1.

This first results from analytical ultracentrifugation are partially contradictorily to those from the DLS measurements (see above). However, DLS measurements are often tending for technical reasons to a monomodal distribution and to overestimate bigger structures

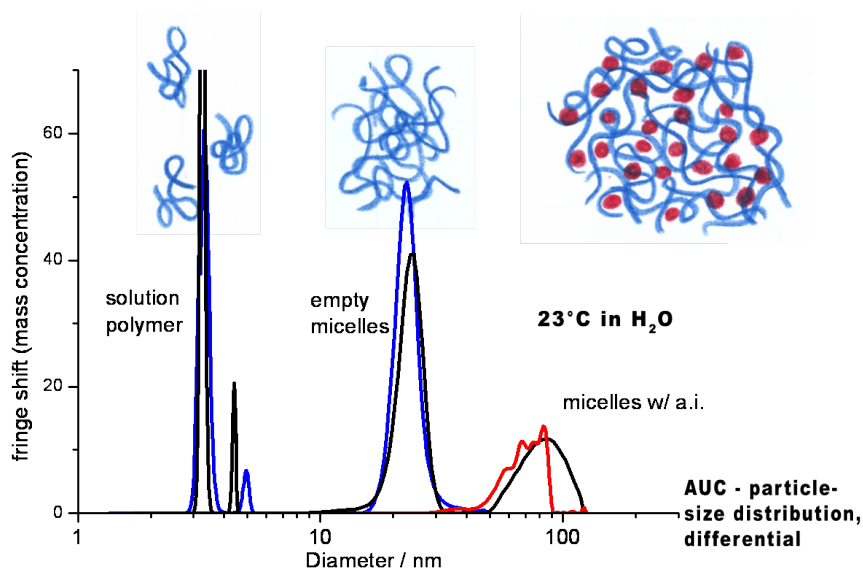


Figure A.8.: Analytical ultracentrifugation of Soluplus[®] + itraconazole. Specific UV-Absorption of itraconazole at 267 nm is only present in the biggest structures. 28 % of the solids were found in large micelles.

[163]. Therefore, these results prove the existence of micellar-bound drug in a compact structure. Ongoing experiments will further show how this structures behave at different excipient/drug ratios, temperatures and in varying media. This data will help us to a further understanding of the mechanisms how the binding between drug and Soluplus[®] occurs. Also the observed decreased transport across Caco-2 cells as result of this binding may be further elucidated.

B. TEER measurements throughout transport experiments

All measurements of the transepithelial electrical resistance (TEER) in this work were performed by a so called “chop-stick” electrode (STX-2 electrode, World Precision Instruments, Sarasota, FL, USA). Therefore, the shorter end of this electrode was inserted in the apical compartment, and the longer end into the basolateral compartment of the Transwell system without contact to the cell monolayer. The electrical resistance was read out by an electrical Volt-Ohm meter (EVOM). As shown in Figure B.1, Soluplus[®] did not affect the integrity of the cell monolayer, as the TEER values stay constantly on the level of the untreated control (KRB buffer).

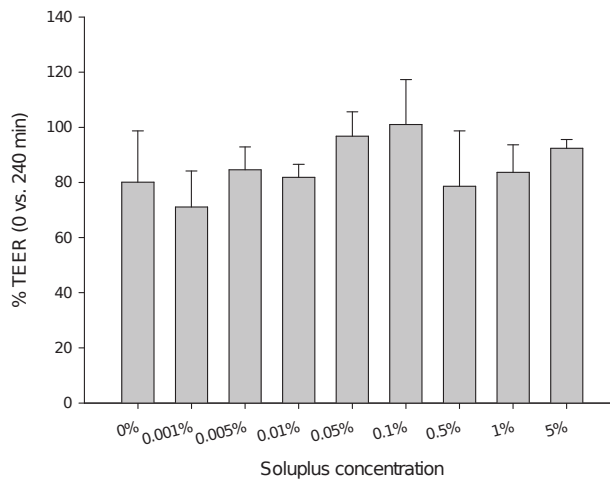


Figure B.1.: TEER values after fluoresceine sodium transport experiment with varying Soluplus[®] concentrations. Expressed as % of the pre-experimental value (n=3; mean \pm SD). Absolute TEER values were above $500 \Omega \times \text{cm}^2$ before the experiment (qualification criterium for transport experiments).

C. HPLC and LC/MS analytics

Introduction

In this appendix the analytical methods for danazol, itraconazole and fenofibrate are summarized. HPLC was used for quantification of danazol, fenofibrate, fenofibric acid and itraconazole of samples from Caco-2 transport and equilibrium dialysis of the respective drugs. LC/MS was used for the quantification of plasma samples of the animal experiments (performed at BASF SE).

HPLC

All HPLC analytics were performed on Dionex (Dionex Corporation, Sunnyville, CA, USA) machines using UV/Vis absorptiometric detection. Reversed phase columns of type LiChroCART 125-4 LiChrospher 100 RP18 (5 μ M) (Merck KGaA, Darmstadt, Germany) were used for separation. Further information is given in Table C.1. Representative chromatograms for each substance are shown in Figures C.1–C.4.

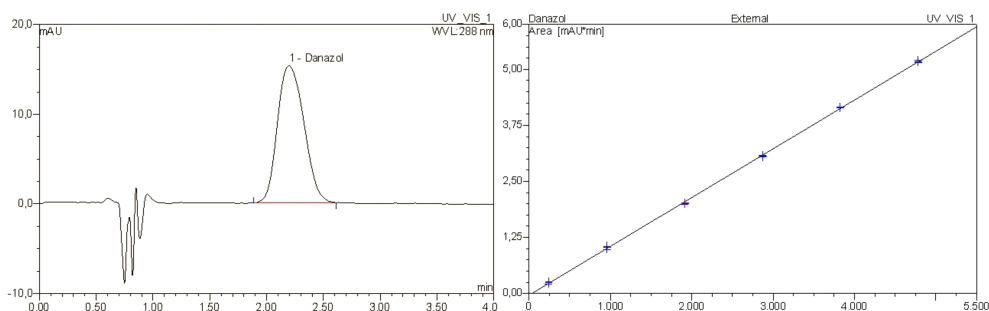


Figure C.1.: Representative chromatogram and calibration curve for danazol HPLC analytics

	Mobile phase (v:v:v)	Eluent flux	Detection wavelength	Injection volume	Retention time	Limit of detection	Limit of quantification
Danazol	methanol: water: phosphate buffer pH 6.8 (80:17:3)	1 ml/min	50 µl	288 nm	2.5 min	25.6 ng/ml	53.9 ng/ml
Fenofibrate / fenofibric acid	acetonitrile: water (70:30) acidified to pH 2.5 by orthophosphoric acid	1 ml/min	286 nm	50 µl	6.4 min (fenofibrate)	11.1 ng/ml (fenofibrate)	30.4 ng/ml (fenofibrate)
Itraconazol	acetonitrile: water: phosphate buffer pH 6.8 (70:27:3)	1 ml/min	263 nm	80 µl	2.3 min (fenofibric acid) 3.1 min	18.1 ng/ml (fenofibric acid) 6.8 ng/ml	30.2 ng/ml (fenofibric acid) 12.8 ng/ml

Table C.1.: Summary of used HPLC analytics. All HPLC analytics were performed isocratic. LOD/LOQ were determined as described in ICH guideline Q2(R1) Chapter 6.2/7.2

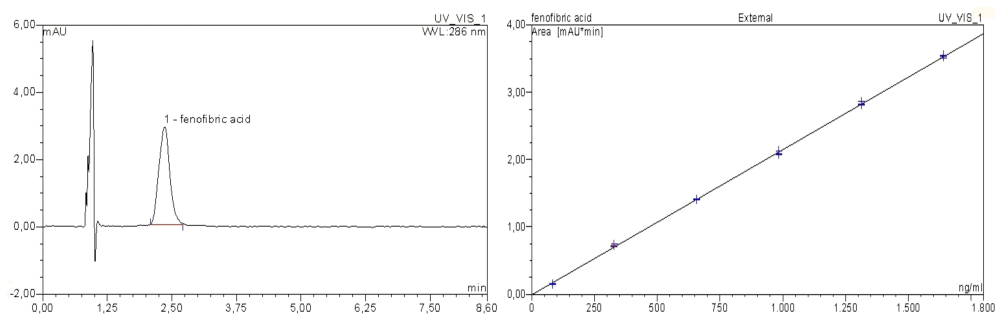


Figure C.2.: Representative HPLC chromatogram and calibration curve for the active compound fenofibric acid

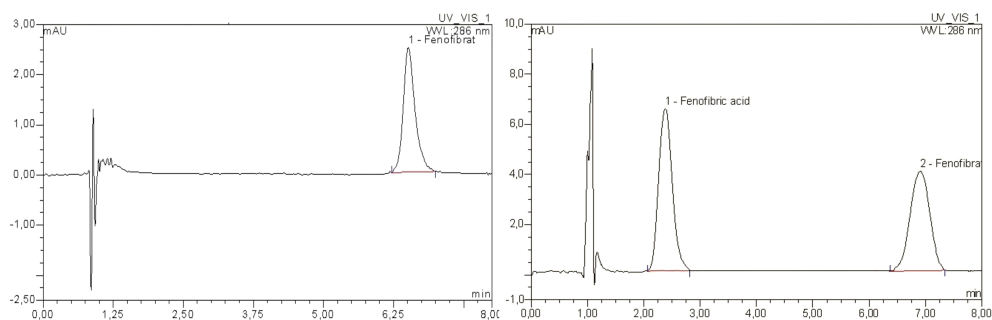


Figure C.3.: HPLC chromatogram of fenofibrate alone and in combination with fenofibric acid. Slight changes in retention time are due to analysis on different HPLC machines and slight changes in eluent composition

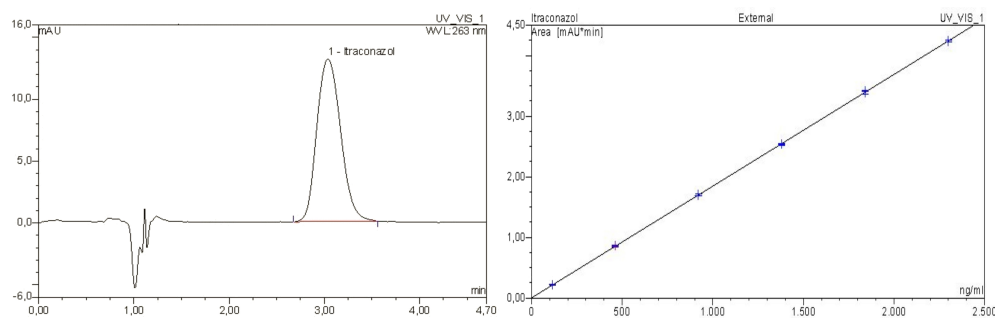


Figure C.4.: Representative chromatogram and calibration curve for itraconazole HPLC analytics

LC/MS

Bioavailability studies using beagle dogs were performed by BASF SE. The below listed LC/MS methods for drug quantification in plasma samples are summarized *as received* from BASF SE.

Danazol

LC/MS machine	ABSciex API 3000
Column	Symmetry C18 150 × 2, 1 mm, 5 µm
Eluents	A: highly deionized water B: acetonitrile
Gradient	
0 min	50 % B
10 min	100 % B
13 min	50 % B
Flow rate	0.3 ml/min
Injection volume	25 µl

Detection by MS was performed by ESI-MS positive ionization in a single reaction mode (SRM; 160 °C; 4000 V) with mass transition m/z 338 to 310, 295, and 148. The collision energy was 20 V. Quantification was based on external calibration. The limit of quantification was 10 ng/ml.

Itraconazole

LC/MS machine	WATERS 2695 Separations Module with Quattromicro™ mass detector
Column	Luna C18 50 × 2 mm, 2.5 µm
Eluents	A: highly deionized water, acidified with formic acid (1 ml/l) B: acetonitrile, acidified with formic acid (1 ml/l)
Gradient	
0 min	50 % B
2 min	95 % B
5 min	95 % B
5.1 min	50 % B
Flow rate	0.3 ml/min
Injection volume	10 µl

Detection by MS was performed by ESI-MS negative ionization in a single ion monitoring

(source temperature 120 °C; desolvation temperature 250 °C; 3200 V). Quantification was based on external calibration. The limit of quantification was 1.3 ng/ml.

Fenofibrate/Fenofibric acid

Fenofibrate only appeared as its active form fenofibric acid in animal plasma samples. Fenofibric acid was analyzed by an appropriate BASF-internal LC/MS method.

D. Abbreviations

A/D ratio	acceptor/donor ratio	HP β CD	hydroxypropyl- β -cyclodextrin
AB, A to B transport	apical to basolateral transport	HME	hot melt extrusion
ABC	ATP binding cassette	HPLC	high performance liquid chromatography
ADME	absorption, distribution, metabolism, excretion/elimination	HPMC	hydroxypropyl methyl cellulose
ADP	adenosine diphosphate	ICH	International Conference on Harmonisation
API	active pharmaceutical ingredient	itra	itraconazole
ATP	adenosine triphosphate	IVIVC	in-vitro in-vivo correlation
AUC	area under the curve	IU	international unit
AUC	analytical ultracentrifugation	KRB	Krebs Ringer buffer
BA, B to A transport	basolateral to apical transport	LADME	liberation, absorption, distribution, metabolism, excretion/elimination
BA	N- α -benzoyl-L-arginine	LC/MS	liquid chromatography/mass spectrometry
BAEE	N- α -benzoyl-L-arginine ethyl ester	LCST	lower crystalline solution temperature
BCRP	breast cancer resistance protein	LOD	limit of detection
BCS	biopharmaceutics classification system	LOQ	limit of quantification
BSA	bovine serum albumine	MCT1	monocarboxylate transporter 1
CHO	chinese hamster ovary	MDCK	Madin darby canine kidney
CMC	critical micelle concentration	MDR1	multidrug resistance protein 1
CysA	Cyclosporine A	MES	2-(N-morpholino)ethanesulfonic acid
D/A ratio	donor/acceptor ratio	m.p.	melting point
dana	danazol	MRP	multidrug resistance associated protein
DIG	digoxin	NBF	nucleotide binding fold
DLS	dynamic light scattering	NCE	new chemical entity
DMEM	Dulbecco's modified Eagle's medium	NEAA	non-essential amino acids
DSC	differential scanning calorimetry	OATP	organic anion transporting peptide
FaSSIF	fasted state simulated intestinal fluid	P-gp	P-glycoprotein
FBC	fetal bovine serum	P _{app}	apparent permeability
FCS	fetal calve serum	PM	physical mixture
FDA	US Food and drug administration	rH	relative humidity
fenof	fenofibrate	RHO	rhodamine 123
FeSSIF	fed state simulated intestinal fluid	SD	standard deviation
GI	gastro-intestinal	TEER	transepithelial electrical resistance
HEPES	4-(2-hydroxyethyl)-1-piperazine- ethanesulfonic acid	T _g	glass transition temperature
		TPGS	α -tocopheryl polyethylene glycol succinate

E. Curriculum vitae

personal information

name	Michael Linn
address	Kantstraße 34, 66125 Saarbrücken
born	3.11.1982 in Mainz
nationality	german

doctoral thesis

2008–2011	Institute for Biopharmacy and Pharmaceutical Technology, Saarland University, Saarbrücken, Germany
-----------	--

undergraduate studies

2003–2008	Pharmacy, Johannes Gutenberg University, Mainz, Germany
2005–2006	Pharmacy, University of Burgundy, Dijon, France

civil service

2002–2003	Evangelische Sozialstation Ingelheim
-----------	--------------------------------------

school

1993–2002	Sebastian-Münster-Gymnasium Ingelheim
1989–1993	Theodor-Heuss-Grundschule Ingelheim

F. Publications

Research papers

- **Michael Linn**, Eva-Maria Collnot, Dejan Djuric, Katja Hempel, Eric Fabian, Karl Kolter, Claus-Michael Lehr, Soluplus[®] as an effective absorption enhancer of poorly soluble drugs *in vitro* and *in vivo*, *European Journal of Pharmaceutical Sciences* **in press**
- **Michael Linn**, Dejan Djuric, Karl Kolter, Claus-Michael Lehr, Eva-Maria Collnot., Inhibition of P-glycoprotein by Soluplus[®], *Pharmaceutical Research* **in submission**

Poster presentations

- **Michael Linn**, Eva-Maria Collnot, Dejan Djuric, Karl Kolter, Claus-Michael Lehr., Effect of Soluplus[®] on *in vitro* and *in vivo* transport of poorly soluble drugs, *PSWC 2010 Congress for Students and Postdoctoral Fellows and FIP Pharmaceutical Sciences 2010 World Congress in Association with the AAPS Annual Meeting and Exposition, November 13–18 2010, New Orleans, USA*
- **Michael Linn**, Dejan Djuric, Karl Kolter, Claus-Michael Lehr, Eva-Maria Collnot., The effect of Soluplus[®], a novel solubilizing agent on P-gp efflux in Caco-2 cell culture model, *PSWC 2010 Congress for Students and Postdoctoral Fellows and FIP Pharmaceutical Sciences 2010 World Congress in Association with the AAPS Annual Meeting and Exposition, November 13–18 2010, New Orleans, USA*
- **Michael Linn**, Eva-Maria Collnot, Dejan Djuric, Karl Kolter, Claus-Michael Lehr., *In vitro* evaluation of the effect of Soluplus[®] on intestinal absorption of poorly soluble drugs, *DPhG-Doktorandentagung, March 30 – April 2 2010, Heringsdorf, Germany*

G. Danksagung

Ich bedanke mich herzlich bei Herrn Prof. Claus-Michael Lehr für die Überlassung des interessanten Arbeitsthemas und die Betreuung meiner Doktorarbeit. Ich danke Herrn Prof. Rolf Hartmann für die Anfertigung des Zweitgutachtens, sowie den anderen Mitgliedern der Prüfungskommission.

Einen ganz besonderen Dank spreche ich Frau Dr. Eva Collnot für die ausgezeichnete Betreuung meiner Arbeit aus. Es freut mich als erstes von Evas "Darm-Team-Schäfchen" diese Arbeit abgeben zu dürfen. Auch bei Prof. Ulrich Schäfer möchte ich mich für die Betreuung in den ersten Monaten meiner Arbeit und für Rat und Tat in der folgenden Zeit bedanken.

Ich möchte mich bei der BASF SE für die Finanzierung und Unterstützung dieser Arbeit bedanken. Auch den an dieser erfolgreichen Kooperation beteiligten Personen Frau Dr. Kathrin Meyer-Böhm, Herr Dr. Dejan Djuric und Herr Dr. Karl Kolter danke ich für die gute Zusammenarbeit herzlich.

Ich bedanke mich bei den Technikern unseres Instituts für die nicht zu unterschätzende Arbeit im Hintergrund bei der Routinezellkultur und der Gerätebetreuung.

Ein ganz großes Dankeschön geht auch an alle meine Mitdoktoranden, welche hauptverantwortlich für das, trotz der enormen Expansion in den vergangenen dreieinhalb Jahren, gute Arbeitsklima in unserem Institut sind.

Meinen Eltern möchte ich für die bestmögliche Unterstützung in allen Lebenslagen danken. Abgesehen von finanzieller und moralischer Unterstützung auch für das Korrekturlesen dieser Arbeit und besonders für die oft gehörte Frage: "Was macht deine Forschung?"

Ich bedanke mich beim Wüg fürs Korrekturlesen und werde mich revanchieren.

Mein wichtigster Dank geht an Christina dafür, dass Sie immer für mich da ist, allabendliche Telefonate und das insbesondere für das Aushalten von dreieinhalb Jahren Fernbeziehung. Diese Arbeit soll ein kleiner Baustein für eine glückliche, gemeinsame Zukunft sein.